

# JELS

ISSN 2087-2852

A large graphic at the top of the cover features a blue-to-purple gradient background. It contains several molecular models: a large green and red ball-and-stick model on the right, a smaller green and red ball-and-stick model below it, and a green and red wireframe model on the left. The background is filled with small black dots, suggesting a molecular simulation or data visualization.

## The Journal of **EXPERIMENTAL** **LIFE SCIENCE**

J.Exp. Life Sci.

Vol. 11

No. 3

pages 68-114

October 2021

**Published by :**  
**Graduate Program, Universitas Brawijaya**

[jels.ub.ac.id](http://jels.ub.ac.id)

# The Journal of **Experimental** Life Science

Discovering Living System Concept through Nano, Molecular and Cellular Biology

---

## Editorial Board

### Chief Editor

Wenny Bekti Sunarharum, STP., M.Food.St., Ph.D

### Editorial Board

Yuli Witono, S.TP., MP., Dr., Prof. - UNEJ

Pa. Raajeswari, Dr. – Avinashilingam Inst.

Tiparat Tikapunya, Dr.- Lampung Rajabhat Univ

Eddie Tan Ti Tjih, Dr. - Teknologi MARA Univ

Ms. Ni-ornChomsri, Ph.D. - ATRI

Muhaimin Rifa'i, Ph.D.Med.Sc., Prof. - UB

Swasmi Purwajanti, ST., M.Sc., Dr. - BPPT

Suciati, S.Si., MPhil., PhD., Apt - UNAIR

Mochamad Nurcholis, STP., MP., PhD - UB

Yoga Dwi Jatmiko, S.Si., M.App.Sc. Ph.D - UB

Moch. Sasmito Djati, MS., Ir., Dr., Prof. – UB

Muhamad Firdaus, MP., Dr., Ir. - UB

### Reviewers

Attabik Mukhammad Amrillah, S.Pi., M.Si. – UB

Indah Yanti, S.Si., M.Si. – UB

Moch. Sasmito Djati, MS., Ir., Dr., Prof. – UB

Irfan Mustafa, S.Si., M.Si., Ph.D – UB

Rizky Nurdiansyah, S.Si., M.Si. – UB

Andi Kurniawan, S.Pi, M.Eng, D.Sc – UB

Evi Octaviany, S.Pd., M.Si. – UB

### Editorial Assistant

Jehan Ramdani Haryati, S.Si, M.Si.

### Address

The Journal of Experimental Life Science  
Building B, 1<sup>st</sup> Floor, Postgraduate School, University of Brawijaya  
Jl. Mayor Jenderal Haryono 169, Malang, 65145  
Telp: (0341) 571260 ; Fax: (0341) 580801  
Email: [jels@ub.ac.id](mailto:jels@ub.ac.id)  
Web: <http://www.jels.ub.ac.id>





## Table of Content

<b>Analysis of Phytoplankton Structure Community, Water Quality and Cultivation Performance in <i>Litopenaeus vannamei</i> Intensive Pond Located in Tembokrejo Village, Muncar, Banyuwangi</b> (Gesang Maulana Dwi Katmoko, Yenny Risjani, Endang Dewi Masithah) .....	68-76
DOI: <a href="https://doi.org/10.21776/ub.jels.2021.011.03.01">https://doi.org/10.21776/ub.jels.2021.011.03.01</a>	
<b>Preventive Effects of Yogurt Fortified with Purple Roselle Extract Against Cardiotoxicity in Rats Exposed With 2,3,7,8-Tetrachlorodibenzo-P-Dioxin</b> (Ani Setianingrum, Iffa Fanadila, Herlina Pratiwi, Ajeng Erika Prihastuti Haskito) .....	77-83
DOI: <a href="https://doi.org/10.21776/ub.jels.2021.011.03.02">https://doi.org/10.21776/ub.jels.2021.011.03.02</a>	
<b>Phytoplankton and Its Relationship to White Leg Shrimp (<i>Litopenaeus vannamei</i>) Culture Productivity in Alasbulu, Banyuwangi</b> (Fitroh Aulani, Wuryansari Muharini Kusumawinahyu, Isnani Darti) .....	84-88
DOI: <a href="https://doi.org/10.21776/ub.jels.2021.011.03.03">https://doi.org/10.21776/ub.jels.2021.011.03.03</a>	
<b>In Silico Study to Predict the Potential of Beta Asarone, Methyl Piperonylketone, Coumaric Acid in <i>Piper crocatum</i> as Anticancer Agents</b> (Ahmed Hasan Abkar, Moch. Sasmito Djati, Widodo Widodo) .....	89-99
DOI: <a href="https://doi.org/10.21776/ub.jels.2021.011.03.04">https://doi.org/10.21776/ub.jels.2021.011.03.04</a>	
<b>Screening of Potential Biosurfactant Producing Bacteria from Tanjung Perak Port, Surabaya</b> (Marlinda Elvina Susanti, Maftuch Maftuch, Asep Awaludin Prihanto) .....	100-105
DOI: <a href="https://doi.org/10.21776/ub.jels.2021.011.03.05">https://doi.org/10.21776/ub.jels.2021.011.03.05</a>	
<b>Expression Virus-Like Particles (VLPs) at Geomembrane and Concret in Asian Pacific Shrimp Culture (<i>Litopenaeus vannamei</i>)</b> (Venny Nur Hidayah, Muhammad Musa, Yuni Kilawati) .....	106-114
DOI: <a href="https://doi.org/10.21776/ub.jels.2021.011.03.06">https://doi.org/10.21776/ub.jels.2021.011.03.06</a>	

## Analysis of Phytoplankton Structure Community, Water Quality and Cultivation Performance in *Litopenaeus vannamei* Intensive Pond Located in Tembokrejo Village, Muncar, Banyuwangi

Gesang Maulana Dwi Katmoko<sup>1\*</sup>, Yenny Risjani<sup>1</sup>, Endang Dewi Masithah<sup>2</sup>

<sup>1</sup>Study Program of Aquaculture, Faculty of Fisheries and Marine Sciences, University of Brawijaya, Malang, Indonesia

<sup>2</sup>Study Program of Aquaculture, Faculty of Fisheries and Marine Sciences, Airlangga University, Surabaya, Indonesia

### Abstract

Phytoplankton plays an important role in *Litopenaeus vannamei* cultivation. It plays a role as natural feed, water quality control, and indicator of shrimp cultivation success. The community structure of phytoplankton can be influenced by organic matter concentration in ponds. On the other hand, water quality and phytoplankton community structure also influence the productivity of shrimp cultivation. The research aimed to analyze the phytoplankton structure community, cultivation performance and the water quality in one of vananmei shrimp cultivation located in Muncar District. The research used the descriptive method. The research was conducted in two shrimp intensive system ponds in Tembokrejo Village, Muncar District, Banyuwangi, on February-March 2020. Parameters observed were composition, diversity, and density of phytoplankton, water quality parameters, and production performance in each pond. Based on the results, five phytoplankton classes was found: Bacillariophyceae (12 genera), Chlorophyceae (4 genera), Cyanophyceae (8 genera), Dinophyceae (2 genera), and Euglenophyceae (1 genus). Based on the density, *Cyclotella* and *Chlorella* were dominated in both ponds. Diversity index values on ponds 1 and ponds 2 were 1.64 and 1.71, respectively. The productivity of both ponds was 10.794 kg.ha<sup>-1</sup> and 11.698 kg.ha<sup>-1</sup>, FCR (Feed Conversion Ratio) were 0.99 and 1.18, and ADG (Average Daily Growth) on both ponds were 0.16 g.day<sup>-1</sup>. Water quality parameters in both ponds showed an optimal range for vannamei cultivation, except phosphate, which is quite high. Overall, the cultivation performance of both ponds in our research showed good results. However, cultivation performance obtained in this research was not on its best performance yet due to Infectious Myonecrosis (IMNV) infection.

**Keywords:** Cultivation performance, *Litopenaeus vannamei*, muncar, phytoplankton.

### INTRODUCTION

The cultivation performance of vannamei (*Litopenaeus vannamei*) currently increases. Based on data, vannamei cultivation contributed as much as 53% of total crustacean production in the world [1]. In addition, vannamei shrimp also has various advantages compared to other types of shrimp. The advantages comprised the fry quality of shrimp are easy to obtain, having high survival rate, can be cultivated in ponds with high stocking densities, more resistant to disease, short cultivation cycle, and has low feed conversion [2]. The species has become an object for studies to increase their immune system against vibriosis [3].

Muncar, a district in Banyuwangi Regency, is one of the main vannamei production districts located in East Java. Muncar is also the center of the fish processing industry in Indonesia. Although it has many positives impacts on improving the economy, the existence of these industries also brings a negative impact on the environment, especially the aquatic

environment. A previous study mentioned that the industry activity in Muncar produced around 14,300 m<sup>3</sup> of waste per day [4]. These wastes are organic waste which can cause pollution in the waters.

Meanwhile, shrimp ponds around these industries use seawater around the coast of Muncar as a medium for vannamei shrimp cultivation. In addition, intensification in vannamei cultivation also causes various problems. The high stocking densities and the increase of feed given lead to the increasing in organic matter content in shrimp ponds and then followed by increasing in shrimp excretion and feed residue.

The excretion and feed residue in the water can be a source of organic matter and nitrogen (N). About 80% of the nitrogen entered the pond will be wasted and suspended [5]. It will lead to nutrient enrichment or also called eutrophication. Eutrophication can affect the structure of the phytoplankton community. Eutrophication is an abnormal condition in waters characterized by high levels of nutrients contained in water that exceed normal limits. Eutrophication conditions and high water temperature due to global warming will cause Harmful Algal Blooms (HABs). In addition,

\* Correspondence address:

Gesang Maulana Dwi Katmoko

Email : gmaulana45@student.ub.ac.id

Address : Faculty of Fisheries and Marine Science,

University of Brawijaya, Veteran, Malang, 65145

nutrient content will also affect the diversity and density of phytoplankton in the waters.

Although Indonesian archipelago has the highest biodiversity of phytoplankton, like marine [6], the study related to their role in brackish water ponds is needed to be explored. Phytoplankton in shrimp pond ecosystems has an important role in supporting the success of the cultivation. Generally, phytoplankton occurs naturally in all shrimp ponds. The existence of phytoplankton provides benefits both directly and indirectly for cultivation productivity. A previous study argued that the type of phytoplankton growth in shrimp pond ecosystems affects productivity [7]. Therefore, this study aimed to analyze the phytoplankton community structure, water quality parameters, and cultivation performance in one of the vannamei cultivation ponds in Tembokrejo Village, Muncar District, Banyuwangi regency.

## MATERIAL AND METHOD

### Sample collection

The research was conducted from February to March 2020 in one of the vannamei shrimp farming locations located in Tembokrejo Village, Muncar District, Banyuwangi Regency. The number of ponds observed was two ponds (pond 1 and pond 2), which were randomly selected. The parameters observed in this study were the phytoplankton community structure consisting of the composition, diversity, and density of phytoplankton. The productivity performance parameters observed were productivity, Survival Rate (SR), Feed Conversion Ratio (FCR), and Average Daily Growth (ADG). Water quality parameters observed were temperature, water transparency (WT), dissolved oxygen, pH, nitrate, nitrite, ammonia, and phosphate.

Phytoplankton samples were sampled every day during the study at 1 PM. Sampling was carried out at four stations using a 5 L volume bucket with two repetitions at each station. The water sample was filtered using a plankton net of 25 $\mu$  size and put into a 20 mL film bottle. Then, 1% Lugol's iodine solution was added to keep the sample from being damaged. Samples were given the label as a marker and stored in a cool box for later identification at the Jatisari 2 Laboratory located in Bomo Village, Blimbingsari District, Banyuwangi Regency.

Phytoplankton samples were observed under a binocular microscope with a magnification of 400X. Phytoplankton calculations using a hemocytometer with counted with hand tally

counter. The calculation of phytoplankton densities uses the following method [6].

$$PD = \left( \frac{nA + nB + nC + nD}{4} \right) \times 10,000$$

#### Description:

PD = Phytoplankton Density

nA, nB, nC, and nD = Number of cells count in block A, B, C and D

4 = Number of block count;

10,000 = The volume of Haemocytometer Big Block

A diversity index is calculated using the Shannon-Wiener method as follows:

$$H' = \sum_{i=1}^n p_i \ln p_i$$

#### Description:

H' = the value of Diversity Index;

p<sub>i</sub> = a number of cells of type i (n<sub>i</sub>) divided by the total number of cells in the sample (N).

Cultivation performance parameters observed in both ponds included harvest tonnage (yield/pond area), survival rate (SR), feed conversion ratio (FCR), and average daily growth (ADG). The formula used to measure the SR value is based on [7]:

$$SR = \frac{N_t}{N_0} \times 100\%$$

#### Description:

SR = survival rate

N<sub>t</sub> = the total number of shrimp harvested

N<sub>0</sub> = the number of shrimp stocked.

FCR is calculated using the formula as follows [7]:

$$FCR = \left( \frac{F}{W - W_0} \right)$$

#### Description:

FCR = feed ratio converted to biomass

F = the weight of feed consumed (kg)

W<sub>t</sub> = shrimp biomass at the end cultivation (kg)

W<sub>0</sub> = the initial weight of shrimp biomass (kg)

ADG is calculated using the formula as follows [8]:

$$ADG = \frac{MBW_o - MBW_t}{t}$$

#### Description:

ADG = the average daily gain of shrimp

MBW<sub>o</sub> = the average body weight actual sampling

MBW<sub>t</sub> = the average body weight after sampling

t = the sampling period

Ponds Temperature, water transparency, pH, salinity, and dissolved oxygen were measured every day during the study. Temperature, water

transparency, DO, pH, and salinity were observed twice a day. While, Nitrate, nitrite, ammonium, and phosphate were measured every three days.

**RESULT AND DISCUSSION**

**Phytoplankton identification**

Based on the results, 27 genera were obtained from five classes of phytoplankton in both ponds. The phytoplankton genera obtained can be seen in Table 1.

Based on Table 2, it can be shown that both ponds have almost the same genera, but the second pond has more diverse phytoplankton genera. The genera of phytoplankton found in both ponds are the common phytoplankton found in shrimp ponds. The results from observations of phytoplankton from both ponds during the study were supported by previous research [7] in a vannamei shrimp (*L. vannamei*) farm in Situbondo, where the genera found were: Oocystis, Chlorella, Nannocloropsis, Chaetoceros, Nitzschia, Coscinodiscus, Cyclotella, and Ulothrix. However, the phytoplankton found in this study had a higher diversity. It can be due to the relatively high nutrient content (N and P) in our study compared to the previous study so that the diversity is also high. Another previous research explained that phytoplankton requires N and P elements in the synthesis of fat and protein [11]. These compounds could only be used directly by phytoplankton if they are in the form of nitrates and orthophosphates. The N:P ratio required by phytoplankton is generally 16:1.

**Phytoplankton composition**

The percentage of each phytoplankton class found in both ponds can be seen in Figure 1. Based on the diagram above, the three dominant classes found in both ponds are Bacillario-

phyceae, Chlorophyceae, and Cyanophyceae. Dinophyceae and Euglenophyceae were also found, but still in a low percentage. The composition of phytoplankton in pond 1 and pond 2 is relatively the same, but the diversity is different.

Bacillariophyceae is the dominant phytoplankton class among other classes. It can be influenced by the source of cultivation water. According to a previous study [12], Bacillariophyceae or diatoms are the most dominant types of phytoplankton in marine waters. Other previous research also found Diatom dominating in vannamei cultivation located in Bangladesh [13]. In addition, diatoms are a type of phytoplankton that are beneficial for the growth of vannamei shrimp because they can help form carapace in shrimp.

**Phytoplankton Density**

The phytoplankton average density observed in both ponds can be seen in Table 1. Based on the Table, *Cyclotella* from Bacillariophyceae was the highest density phytoplankton. The percentage density of a phytoplankton species in the waters should reach more than 10% of the total density, for the species can be said to dominate [5].

*Chlorella* from Chlorophyceae was the second class that dominated in both ponds. Chlorophyceae can be found dominated in water ecosystems with high light intensity [14]. The dominance of phytoplankton in shrimp ponds is strongly influenced by water quality, such as nitrogen and phosphorus. The density values of the Bacillariophyceae and Chlorophyceae classes are still quite high. Both genera are types of plankton that are beneficial to shrimp.

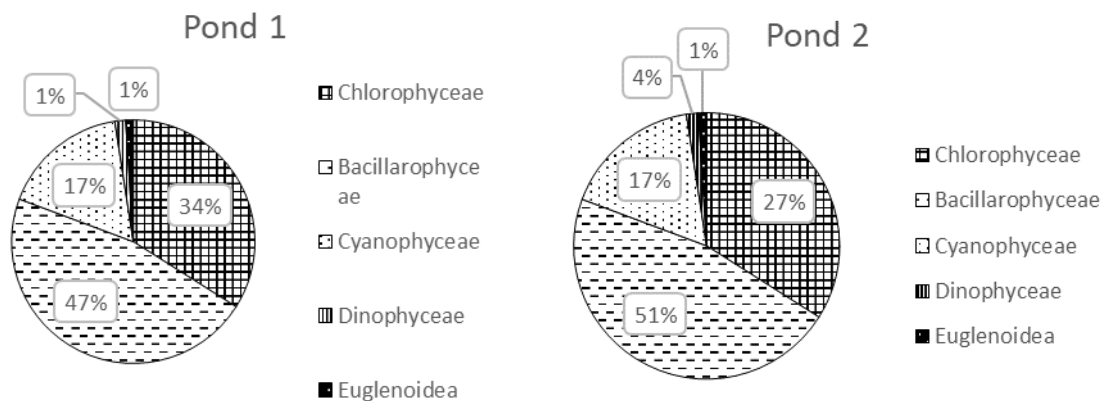


Figure 1. The percentage of phytoplankton composition in ponds



Meanwhile, the genera belonging to Cyanophyceae, Dinophyceae, and Euglenophyceae are genera that are quite harmful to cultivated organisms because they can produce toxins that are harmful to aquatic organisms. In the Cyanophyceae class, the most common genera found is *Oscillatoria*. *Oscillatoria* is a type of blue-green algae (BGA) that is commonly found in brackish waters. *Oscillatoria* is a diazotrophic group in Cyanobacteria, where this genus can fix nitrogen gas (N<sub>2</sub>) from the air so that this type of organism can live in waters that have low nitrogen levels even as long as there is phosphorus [17].

The diversity index value can be seen in Table 1. The diversity index value showed that the diversity value H' of phytoplankton genera in pond 1 and pond 2 were only slightly different. Based on the H' value, both ponds have a moderate diversity index (1<H'<3), indicating the water ponds are still of good quality to support phytoplankton growth. It was mentioned that the diversity index value H' is greater than 3, then the diversity of genera is high. If the value of diversity H' is between 1 and 3, then the diversity of genera is moderate, and if the diversity value H'

is less than 1, indicated that the water ecosystem has low genera diversity [18].

**Cultivation Performance**

**Productivity**

The cultivation performance parameters of both ponds can be seen in Table 2. The productivity in pond 2 was higher than in pond 1. It can be influenced by the amount of stocking density, feed management, water quality. The productivity of cultivation was also influenced by the length of the cultivation day. The longer cultivation day can result in higher yields. The existence of phytoplankton is also a supporting factor. Besides its role as natural food which is useful for the formation of the carapace in shrimp, several types of diatoms can produce some toxins which have a negative impact on aquatic organisms.

**Table 2.** Cultivation Performance of Both Ponds

No	Indicator	P1	P2
1	Day of Culture (DOC)	62	64
2	Productivity (kg.ha <sup>-1</sup> )	10,794	11,698
3	Survival Rate (%)	95	97
4	FCR	0.99	1.18
5	ADG (g.day <sup>-1</sup> )	0.16	0.16

**Table 1.** The Average of Phytoplankton Density of Both Ponds

Class	Genera	Pond 1	Pond 2
Chlorophyceae	<i>Chlorella</i>	31,000	28,611
	<i>Cosmarium</i>	800	833
	<i>Oocystis</i>	3,100	3,519
	<i>Gleocystis</i>	1,800	5,278
Bacillariophyceae	<i>Skeletonema</i>	7,500	7,037
	<i>Cyclotella</i>	31,400	42,222
	<i>Nitzschia</i>	1,200	1,944
	<i>Coscinodiscus</i>	6,200	11,389
	<i>Dithyllum</i>	1,900	370
	<i>Navicula</i>	1,200	2,870
	<i>Amphiphora</i>	1,000	463
	<i>Biduphia</i>	200	741
	<i>Chaetoceros</i>	2,800	22,22
	<i>Melosira</i>	1,000	185
	<i>Amphora</i>	-	1,574
	<i>Cerataulina</i>	-	3,981
Cyanophyceae	<i>Microcystis</i>	5,400	2,500
	<i>Chroococcus</i>	4,400	10,926
	<i>Oscillatoria</i>	11,700	926
	<i>Gleocapsa</i>	-	28,611
	<i>Anabaena</i>	2,900	2,778
	<i>Pseudoanabaena</i>	-	556
	<i>Anabaenopsis</i>	-	463
Dinophyceae	<i>Merismopedia</i>	-	1,944
	<i>Protoperdinium</i>	1,400	2,407
Euglenophyceae	<i>Alexandrium</i>	500	3,981
	<i>Euglena</i>	1,250	1,574
<b>Total</b>		<b>118,650</b>	<b>141,296</b>
<b>Shanon-Wierner Index</b>		<b>1.64</b>	<b>1.71</b>



The productivity on Pond 2 showed a higher value than on pond 1. The differences of these values were might due to the higher density of Bacillariophyceae and Chlorophyceae in Pond 2 than Pond 1. We argued that the availability of natural food in pond 2 was higher than in pond 1, so shrimp obtain more nutrient sources due to the phytoplankton. Bacillariophyceae and Chlorophyceae are good natural food for vannamei shrimp due to these high nutrients. Microalgae contain b-carotene and chlorophyll content increase the antioxidant pigment astaxanthin in shrimp tissue, which leads to an increase in the growth of the shrimp [19].

In contrast, when viewed from the adverse phytoplankton types, the density of *Microcystis*, *Chroococcus*, *Oscillatoria*, and *Anabaena* was found to be higher in pond 1. These types of phytoplankton can produce cyanotoxins. Cyanobacteria have an important role as the main oxygen producer in waters [20]. However, its ability to adapt causes cyanobacteria to grow rapidly. It cause various negative impacts on the waters, such as changing water color, decreasing water quality, and causing an unpleasant taste in the meat of cultivated organisms due to the production of geosmin and methyl iso-borneol (MIB), which can result in decreased quality of aquaculture products. *Oscillatoria*, as one of the many phytoplankton found, could also cause negative impacts if the density is uncontrolled. *Oscillatoria* can produce toxin compounds such as neurotoxins, anatoxins, and hepatotoxins [21].

#### Survival Rate

The survival rate in ponds 1 and 2 was 95% and 97%, respectively. The survival rate in both ponds is quite high. In previous research [22], the survival rate obtained ranges from 88-91%. When compared with the survival rate in this study, the survival value in both ponds has a higher value. It is because the harvesting in both ponds was carried out quickly before the IMNV virus spreads and increased shrimp mortality.

Phytoplankton also may affect the survival rate in shrimp ponds. The types of phytoplankton dominated were Bacillariophyceae and Chlorophyceae. These types of phytoplankton play a role as a natural food that contained high nutrients so that it can support the growth, development, and immune response of vannamei shrimp. Microalgae contain b-carotene and vitamin C compounds which can improve the health condition of shrimp [17]. Our result is supported by previous research, which showed

the pond dominated by phytoplankton *Nanocloropsis* and *Chlorella* from Chlorophyceae class and *Navicula* from the Bacillariophyceae class that showed a higher survival rate than the control pond, which was dominated by phytoplankton genera of Cyanophyceae [21]. The survival rate can also be influenced by the stocking density at the beginning of cultivation. A previous study mentioned the optimal stocking density in the intensive system of vannamei shrimp cultivation is 100 fish.m<sup>-2</sup> [20]. Based on another research, vannamei shrimp reared at a density of 100 ind.m<sup>-2</sup> showed a better survival rate and growth [22].

#### Feed Conversion Ratio (FCR)

The FCR value in ponds 1 and 2 was 0.99 and 1.18, respectively. The FCR value in both ponds was considered good. The good FCR value in shrimp culture is 1.37-1.66 [3]. The FCR value indicates the level of performance of shrimp in converting feed to yields. FCR is a comparison between the feed consumed and the biomass produced, thus the lower the FCR indicate the better performance of the shrimp in converting feed into biomass [23].

The FCR value in pond 1 was lower than pond 2, indicating the shrimp reared in pond 1 had a better performance in converting feed to yields than pond 2. It may be influenced due to the differences in stocking density in both ponds. The stocking density applied to pond 1 was lower than that of pond 2. It is consistent with the results of previous research [24], which explained that the lowest FCR value was obtained in the vannamei shrimp reared on the medium with the lowest stocking density. The lower stocking density results in a lower level of competition in feed utilization, thus the shrimp cultivated in pond 1 could more utilize the feed given. In addition, it can also be seen that the density of phytoplankton from the Dinophyceae class in pond 2 is higher than pond 1. Dinophyceae is able to produce some toxins that cause damage to the organism's cells [25]. It may be assumed that the digestive tract cells of shrimp in pond 2 had a disturbance due to these toxins, thus the absorption process of nutrients could not run optimally. Therefore, most farmers prefer their cultivation ponds to be dominated by diatoms and green algae in the phytoplankton community structure.

#### Average Daily Gain (ADG)

The average Daily Gain (ADG) value in pond 1 and pond 2 was 0.16 g.day<sup>-1</sup>. The ADG value in

both ponds is still in a good range in the cultivation of vannamei shrimp. The normal ADG value in vannamei shrimp cultivation is 0.22 g.day<sup>-1</sup> [26]. A research obtained daily growth rate values for vannamei shrimp of 0.12 - 0.17 g.day<sup>-1</sup> [27]. The growth rate of vannamei shrimp can be influenced by several factors such as the volume of water change every day, feed supply, fertilization, aeration, and the composition of the phytoplankton in the pond.

**Water Quality Parameters**

The range of average values for the water quality parameters of both ponds can be seen in Table 3. The temperature in both ponds was in optimal conditions for shrimp growth. It is supported by a previous study that stated the optimal temperature value for shrimp growth is in the range of 24-32°C [28]. Temperature can influence the metabolism rate of shrimp.

The water transparency in both ponds was classified as good for vannamei shrimp cultivation. The optimal water transparency value in shrimp ponds ranged between 30-45 cm. Pond with water transparency under 30 cm indicated the content of the suspension or phytoplankton is very dense, thus it needs to be recirculated [29].

DO in both ponds was still in a tolerable range for vannamei shrimp. The optimal DO range for shrimp culture is 3.5 - 7.5 ppm [28]. Less than 3 ppm DO content can cause shrimp stressed, thus they became susceptible to disease infection, while DO content less than 2 ppm has the potential of death in organisms, including shrimp. Oxygen levels in waters can be influenced by salinity and temperature [31]. The solubility of oxygen will be higher in low-temperature water conditions and will decrease with higher salinity.

The pH values in both ponds were in the optimal range for the growth of vannamei shrimp. The allowable pH value limit in shrimp farming is 7.5 - 8.5 [32]. However, when viewed

from the pH fluctuation occurred, the pH fluctuation in pond 2 was higher than in pond 1. The phytoplankton density may influence the pH fluctuation in the water environment. The higher density of phytoplankton, the greater the pH fluctuation occurred. However, based on the data obtained, the pH fluctuation from the beginning to the end of the observation is still in a safe range for vannamei shrimp. A sudden change in pH value of 1 unit could kill aquatic organisms [33].

The salinity in both ponds was in the optimal range. The ideal salinity range for shrimp culture is 15 to 25 ppt [34]. Lower salinity value leads to thinning the shrimp shell, while a too high salinity value leads to inhibition of the molting process [35]. Salinity has a significant role in influencing the growth rate, survival, and physiological function of shrimp.

The nitrate concentration in both ponds was in a safe range for cultivating vannamei shrimp. The tolerable nitrate concentration for vannamei shrimp cultivation in ponds is not more than 177 mg.L<sup>-1</sup> [36]. Nitrate is a form of nitrogen which not too dangerous for aquatic organisms, especially vannamei shrimp. However, too high nitrate concentration and the influence of salinity in the waters could be dangerous compounds [37]. Nitrates can be used by phytoplankton to grow and develop [38].

The nitrite concentration in both ponds is in a safe range for cultivating vannamei shrimp. Nitrite toxicity can be influenced by pH and salinity in the water ecosystem. In vannamei shrimp culture, the tolerable nitrite content is not more than 6.1 mg.L<sup>-1</sup> at 15 ppt salinity and no more than 15.2 mg.L<sup>-1</sup> at 25 ppt salinity [39]. Excess nitrite content in aquaculture ponds could cause a decrease in appetite, growth, increase oxygen consumption and nitrogen excretion, disrupt hemolymph protein concentrations and increase mortality [40].

**Table 3.** The Data of Water Quality of Both Ponds

Parameters	Pond 1		Pond 2		Optimum Range
	5 AM	3 PM	5 AM	3 PM	
DO (mg.L <sup>-1</sup> )	4.0-4.7	4.9-8.9	3.9-5.1	4.1-8.9	3.5 – 7.5 [30]
Temperature (°C)	28-31	29-33	27-31	29-32	24 – 32 [28]
pH	7.1-7.9	7.6-8.5	7.1-8.1	7.3-8.3	7.5 – 8.5 [32]
Sal (g.L <sup>-1</sup> )	18-22	18-22	19-23	18-22	15 – 25 [34]
WT (cm)	33-42	28-41	32-40	29-37	30 – 45 [29]
NO2- (mg.L <sup>-1</sup> )		0.02-2		0.02-2	< 15.2 [39]
NO3- (mg.L <sup>-1</sup> )		1-10		1-15	< 177 [36]
NH4+ (mg.L <sup>-1</sup> )		0.1-3.2		0.1-3	< 5 [3]
PO4-3 (mg.L <sup>-1</sup> )		0.5-1.5		0.25-2	0.08 – 0.28 [5]
N:P Ratio		1.3-16.5 : 1		0.6-11.6 :1	16:1 [11]

The range between the maximum and minimum phosphate values in pond 2 was higher than in pond 1. It may be related to the higher FCR value in pond 2. Higher FCR indicates that the feed given is still left and not utilized by the shrimp. The remaining feed wasted in the waters is a source of phosphate [41]. The phosphate content of both ponds is quite high. Sukadi [42] conducted observations of water quality in shrimp aquaculture ponds in Bangladesh and found a phosphate content of 0.08 - 0.28 mg.L<sup>-1</sup>.

Ammonium ranges in both ponds are still in a good range for shrimp growth. A safe level of ammonium concentration for shrimp culture is less than 5 mg.L<sup>-1</sup> [30]. The ammonium content in water can be regulated by the content of organic matter in the waters. Organic materials such as food waste, organisms, and dead organisms will break down into ammonium. Ammonium is ammonia that ionizes in water.

#### CONCLUSION

In conclusion, the phytoplankton community structure in both ponds consisted of 27 genera from five phytoplankton classes with a moderate diversity index (H'), which Chlorophyceae and Bacillariophyceae were dominated. The physical and chemical parameters of the water quality in both ponds are in the optimal range for vannamei shrimp culture. Overall, the cultivation performance of both ponds in our research showed good results.

#### ACKNOWLEDGEMENT

The author thanks to Mr. Ersan as the shrimp farm's owner, Mr. Djito as the shrimp farm technician and Alvian as the shrimp farm technical assistance whose support this research done successfully.

#### REFERENCES

- [1] Food and Agriculture Organization (FAO). 2018. The state of world fisheries and aquaculture: meeting the sustainable development goals. FAO. Rome.
- [2] Gunarto, G., H.S. Suwoyo, B.R. Tampangallo. 2012. Budidaya udang vaname pola intensif dengan sistem bioflok di tambak. *Jurnal Riset Akuakultur*. 7(3). 393–405.
- [3] Risjani, Y., N. Mutmainnah, P. Manurung, S. N. Wulan, Yunianta. 2021. Exopolysaccharide from *Porphyridium cruentum* (purpleum) is not toxic and stimulates immune response against vibriosis: the assessment using zebrafish and white shrimp *Litopenaeus vannamei*. *Mar. Drugs*. 19(3): 133.
- [4] Priambodo, G., S. Mangkoedihardjo, W. Hadi, E.S. Soedjono. 2011. Wastewater treatment strategy for fish processing industry in Kota Pantai Muncar of Indonesia. *Int. J. Acad. Res*. 3(2). 93–97.
- [5] Zafar, M., M.K. Abbasi, A. Khaliq. 2013. Effect of different phosphorus sources on the growth, yield, energy content and phosphorus utilization efficiency in maize at Rawalakot Azad Jammu and Kashmir, Pakistan. *J. Plant Nutr*. 36(12). 1915-1934.
- [6] Risjani, Y., A Witkowski, A. Kryk, Yunianta, E. Gorecka, M. Krzywda, I. Safitri, A. Sapar, P. Dabek, S. Arsad, E. Gusev, Rudiyanayah, L. Peszek, R. J Wrobel. 2021. Indonesian coral reef habitats reveal exceptionally high species richness and biodiversity of diatom assemblages. *Estuarine, Coastal and Shelf Science*. 261. 107551.
- [7] Arifin, N.B., M. Fakhri, A. Yuniarti, A.M. Hariati. 2017. Phytoplankton community at intensive cultivation system of whiteleg shrimp, *Litopenaeus vannamei* in Probolinggo, East Java. *El-Hayah*. 6(3). 79-85.
- [8] LeGresley, M., G. McDermott. 2010. Metodos microscopicos y moleculares para el analisis cuantitativo del fitoplankton. *Exchange Organizational Behavior Teaching Journal*. 110.
- [9] Effendi, I. 1997. Biologi perikanan. Yayasan Pustaka Nusantara. Yogyakarta.
- [10] Haliman, Adijaya. 2005. Pembudidayaan dan prospek pasar udang putih yang tahan penyakit : udang vannamei. Penebar Swadaya. Jakarta. 126.
- [11] Mustofa, A. 2015. Kandungan nitrat dan pospat sebagai faktor tingkat kesuburan perairan pantai. *Disprotek*. 6(1). 13–19.
- [12] Fauziah, A., D.G. Bengen, M. Kawaroe, H. Effendi, M. Kristanti. 2018. Spatio-temporal distribution of microalgae producing chlorophyll and carotenoid pigments in Bali Strait, Indonesia. *Biodiversitas*. 20(1). 61-67.
- [13] Casé, M., E.E. Leça, S.N. Leitão, E.E. SantAnna, R. Schwamborn, A.T. de Moraes Junior. 2008. Plankton community as an indicator of water quality in tropical shrimp culture ponds. *Mar. Pollut. Bull*. 56(7). 1343–1352.
- [14] Pratiwi, H., A. Damar, Sulistiono. 2018. Phytoplankton community structure in the

- Estuary of Donan River, Cilacap, Central Java, Indonesia. *Biodiversitas*. 19(6). 2104–2110.
- [15] Aliviyanti, D., S. Suharjono, C. Retnaningdyah. 2017. Cyanobacteria community dynamics and trophic status of intensive shrimp (*Litopenaeus vannamei*) farming pond in Situbondo East Java Indonesia. *J. Trop. Life Sci*. 7(3). 251–257.
- [16] Odum, E.P. 1993. Dasar-dasar ekologi, 3<sup>rd</sup> Ed. In: Samingan, T. (transl.) Gadjah Mada University Press. Yogyakarta.
- [17] Parker, R. 2002. Aquacultural Science, 2<sup>nd</sup> Ed. Delmar. New York.
- [18] Li, Y., G. Xiao, A. Mangott, M. Kent, I. Pirozzi. 2016. Nutrient efficacy of microalgae as aquafeed additives for the adult black tiger prawn, *Penaeus monodon*. *Aquac. Res*. 47(11). 3625–3635.
- [19] Saad, A., A. Atia. 2014. Review on freshwater blue-green algae (cyanobacteria): occurrence, classification and toxicology. *Biosci. Biotechnol. Res. Asia*. 11(3). 1319–1325.
- [20] Ariadi, H., M. Mahmudi, M. Fadjar. 2019. Correlation between density of vibrio bacteria with *Oscillatoria* sp. abundance on intensive *Litopenaeus vannamei* shrimp ponds. *Life Sci*. 6(2). 114–129.
- [21] Junda, M. 2018. development of intensive shrimp farming, *Litopenaeus vannamei* in land-based ponds: production and management. *J. Phys. Conf. Ser.* 1028. 1.
- [22] Lukwambe, B., L. Qiuqian, J. Wu, D. Zhang, K. Wang, Z. Zheng. 2015. The effects of commercial microbial agents (probiotics) on phytoplankton community structure in intensive white shrimp (*Litopenaeus vannamei*) aquaculture ponds. *Aquac. Int*. 23(6). 1443–1455.
- [23] Samadan, G. M., Rustadi, Djumanto, Murwantoko. 2018. Production performance of whiteleg shrimp *Litopenaeus vannamei* at different stocking densities reared in sand ponds using plastic mulch. *AAAL Bioflux*. 11(4). 1213–1221.
- [24] Ridlo, A., Subagio. 2013. Pertumbuhan, rasio konversi pakan dan kelulushidupan udang *Litopenaeus vannamei* yang diberi pakan dengan suplementasi prebiotik fos (fruktooligosakarida). *Buletin Oseanografi Marina*. 2(4). 1–8.
- [25] Sookying, D., D.A. Davis. 2011. Pond production of Pacific white shrimp (*Litopenaeus vannamei*) fed high levels of soybean meal in various combinations. *Aquac*. 319(1–2). 141–149.
- [26] Shi, F., P. McNabb, L. Rhodes, P. Holland, S. Webb, J. Adamson, A. Immers, R. Gooneratne, J. Holland. 2012. The toxic effects of three dinoflagellate species from the genus *Karenia* on invertebrate larvae and finfish. *N. Z. J. Mar. Freshwater Res*. 46(2). 149–165.
- [27] Lailiyah, U.S., S Rahardojo, M.G.E. Kristiany, M. Mulyono. 2018. Provinsi Jawa Barat productivity of vannamei shrimp cultivation (*Litopenaeus vannamei*) super intensive pond in PT. Dewi Laut Aquaculture Garut District. *Jurnal Kelautan dan Perikanan Terapan*. 1. 1–11.
- [28] Gunarto, E.A. Hendrajat. 2008. Budidaya udang vannamei, *Litopenaeus vannamei* udang vannamei, *Litopenaeus vannamei* pola semi intensif dengan aplikasi beberapa jenis probiotik komersial. *Jurnal Riset Akuakultur*. 3(3). 339–349.
- [29] Kumar, P. 2015. Survival and growth performance of pacific white shrimp *Litopenaeus vannamei* (Boone1931) under different stocking densities. *IOSR Journal of Agriculture and Veterinary Science Ver. 1*. 8. 5. 2319–2372.
- [30] Kilawati, Y., Y. Maimunah. 2015. Kualitas lingkungan tambak insentif *litopenaeus vannamei* dalam kaitannya dengan prevalensi penyakit white spot syndrome virus. *Res. J. Life Sci*. 2(1). 50–59.
- [31] Supriatna, Marsoedi, A.M. Hariati, M. Mahmudi. 2017. Dissolved oxygen models in intensive culture of whiteleg shrimp, *Litopenaeus vannamei*, in East Java, Indonesia. *AAAL Bioflux*. 10(4). 768–778.
- [32] Mainassy, M.C. 2015. Pengaruh parameter fisika dan kimia terhadap kehadiran ikan lampa (*Thryssa baelama* Forsskål) di perairan Pantai Apui Kabupaten Maluku Tengah. *Perikanan*. 19(2). 61–66.
- [33] Jaganmohan, P., L. Kumari. 2018. Assessment of water quality in shrimp (*L. vannamei*) grow out ponds in selected villages of S.P.S.R Nellore district of Andhra Pradesh, India during winter crop season. *Int. J. Fish. Aquat. Stud*. 6(3). 260–266.
- [34] Tucker, C.S., L.R.D. Abramo. 2008. Managing High pH in Freshwater Ponds. *SRAC Publ*. 46(4604). 1–3.
- [35] Maicá, P.F., M.R. de Borba, T.G. Martins, W. Wasielesky. 2014. Effect of salinity on performance and body composition of Pacific white shrimp juveniles reared in a

- super-intensive system. *R. Bras. Zootec.* 43(7). 343–350.
- [36] Syukri, M., M. Ilham. 2016. Pengaruh salinitas terhadap sintasan dan pertumbuhan larva udang windu (*Penaeus monodon*). *Jurnal Galung Tropika.* 5(2). 86-96.
- [37] Furtado, P.S., B.R. Campos, F.P. Serra, M. Klosterhoff, L.A. Romano, W. Wasielesky. 2015. Effects of nitrate toxicity in the Pacific white shrimp, *Litopenaeus vannamei*, reared with biofloc technology (BFT). *Aquac. Int.* 23(1). 315–327.
- [38] Neto, I.A., H. Brandão, P.S. Furtado, W. Wasielesky. 2019. Acute toxicity of nitrate in *Litopenaeus vannamei* juveniles at low salinity levels. *Cienc. Rural.* 49(1). 1–9.
- [39] Saraswathy, R., M. Muralidhar, P. Ravichandran, A.G. Ponniah, A. Panigrahi, M. Kailasam, A. Nagavel. 2012. Effect of nutrient level on phytoplankton population in zero water exchange shrimp culture farms. *Indian J. Fish.* 59(2). 115–120.
- [40] Lin, Y.C., J.C. Chen. 2003. Acute toxicity of nitrite on *Litopenaeus vannamei* (Boone) juveniles at different salinity levels. *Aquac.* 224(4). 193–201.
- [41] Romano, N., C. Zeng. 2013. Toxic effects of ammonia, nitrite, and nitrate to decapod crustaceans: a review on factors influencing their toxicity, physiological consequences, and coping mechanisms. *Rev. Fish. Sci.* 21(1). 1–21.
- [42] Sukadi, M. F. 2016. Ketahanan dalam air dan pelepasan nitrogen & fosfor ke air media dari berbagai pakan ikan air tawar. *Jurnal Riset Akuakultur.* 5(1). 1.

## Preventive Effects of Yogurt Fortified With Purple Roselle Extract Against Cardiotoxicity in Rats Exposed With 2,3,7,8-tetrachlorodibenzo-p-dioxin

Ani Setianingrum<sup>1\*</sup>, Iffa Fanadila Febriani<sup>2</sup>, Herlina Pratiwi<sup>3</sup>, Ajeng Erika P. Haskito<sup>1</sup>

<sup>1</sup> Veterinary Public Health Laboratory, Faculty of Veterinary Medicine, University of Brawijaya, Malang, Indonesia

<sup>2</sup> Faculty of Veterinary Medicine, University of Brawijaya, Malang, Indonesia

<sup>3</sup> Veterinary Embryology Laboratory, Faculty of Veterinary Medicine, University of Brawijaya, Malang, Indonesia

### Abstract

Dioxin is one of the environment's persistent organic pollutants that harm animal and human health. Prolonged exposure to 2,3,7,8-tetrachlorodibenzo-p-dioxin (TCDD) can disrupt normal organ function including heart. Yogurt is known to have antioxidant properties, and fortification natural plant-based antioxidant purple roselle (*Hibiscus sabdariffa L*) extract into yogurt can improve the antioxidant potential. The purpose of this study was to determine the preventive effects of yogurt fortified with purple roselle on dioxin exposure rats (*Rattus norvegicus*) based on the levels of Malondialdehyde (MDA) and histopathological of the heart. This experimental study used a completely randomized design (CRD). A total of 30 male Wistar rats were divided into five groups (Negative Control, Positive Control, Treatment groups T1, T2, and T3), a dose of 200 ng.kg<sup>-1</sup> BW TCDD and 1 mL of roselle yogurt 0.5%, 1.0%, and 1.5% were given orally for 12 days. MDA levels were analyzed using the Thiobarbituric Acid (TBA) assay and histopathology of the heart using the Haematoxylin Eosin (HE) staining method. Statistical analysis used one-way Analysis of Variance (ANOVA). Histopathology changes were analyzed descriptively. The results showed that TCDD exposure induced oxidative stress in heart tissue, and yogurt roselle has the potential to prevent an increase of MDA levels significantly (p<0.05). Furthermore, TCDD can cause histopathological alterations, such as necrosis and hemorrhage, and yogurt roselle was proven to prevent cardiotoxicity due to TCDD exposure.

**Keywords:** heart, histopathology, MDA, purple roselle, TCDD, yogurt.

### INTRODUCTION

Development in Industrial activities is often followed by an increasing level of pollution to the environment. One of the pollutants that are considered toxic and produced by human activities is dioxins and their congeners. Due to the toxic, persistent, bioaccumulative nature of dioxins in the environment, the United Nations of Environmental Program (UNEP) is actively campaigning on the problem of dioxin pollution so that it has become a global concern [1]. Dioxins congener that have the highest toxicity is 2,3,7,8 -Tetrachlorodibenzo-p-dioxin (TCDD). In humans and laboratory animals, TCDD induced carcinogenesis, teratogenicity, reproductive toxicity, hepatotoxicity, endocrine disruption, wasting syndrome, and immunological dysfunction [2,3].

The aryl hydrocarbon receptor (AhR) pathway, which induces cytochrome P450 and other drug-metabolizing enzymes, can explain the toxicity of TCDD. Cardiotoxicity manifestations due to dioxins exposure include ischemic heart disease and an increase in blood pressure. In addition, cardiac tissue damage

caused by dioxin intoxication includes hemorrhage and necrosis [2,4]. Some in vivo investigations suggest that TCDD exposure has serious consequences for the cardiovascular system [5]. Chronic TCDD exposure caused degenerative cardiovascular diseases in rats, including cardiomyopathy and chronic active arteritis. Furthermore, TCDD accelerates the production of reactive oxygen species (ROS), which causes lipid peroxidation, cell membrane damage, DNA and protein damage at the cellular level. TCDD was found to cause oxidative stress in various organs [2]. Studies suggested that using antioxidant supplementation possible to counteract the adverse effect of TCDD toxicity.

Yogurt is a dairy product that has many health benefits due to its potent antioxidant activity. Milk proteins have shown antioxidant activity for the scavenging of reactive oxygen species [6]. Casein derived from yogurt can inhibit the lipoxygenase-catalyzed lipid autoxidation and increased superoxide dismutase (SOD) enzyme activity [7]. Furthermore, whey proteins can efficiently inhibit lipid oxidation [8]. Bioactive peptides are released from milk proteins by enzymatic breakdown during the fermentation of milk by lactic acid bacteria. These peptides have immunomodulatory activity, ACE inhibitory, antimicrobial, and antioxidative activity [9]. Fortification of yogurt with plant extracts that is rich in natural antioxidants is applied to improve

\* Correspondence address:

Ani Setianingrum

Email : ani.setia@ub.ac.id

Address: Faculty of Veterinary Medicine, Brawijaya  
University Malang, 65151, Indonesia

the nutritional and therapeutic quality of yogurt. One of the natural plant-based antioxidants is purple roselle flowers (*Hibiscus sabdariffa* L.). Roselle has been shown to have the capacity as an antioxidant due to the presence of components such as anthocyanins, vitamin C, flavonoids, and phenolic acids [10]. Natural plant-based antioxidants can be used to reduce the free radical formation and increase antioxidant capacity, as well as to substitute synthetic antioxidants that have adverse effects, such as liver damage and carcinogenesis [11].

This study aims to investigate the effect of yogurt fortified with purple roselle extract on the cardiotoxicity caused by 2,3,7,8-TCDD exposure. The protective effect of yogurt fortified with purple roselle extract was observed based on the level of malondialdehyde (MDA) and the histopathological changes of the cardiac tissue.

## MATERIAL AND METHOD

### Chemicals

Commercial cow's milk, purple roselle, Yóourmet® yogurt starter containing three strains lactic acid bacteria *L. bulgaricus*, *S. thermophilus* and *L. acidophilus*, corn oil, 2,3,7,8-TCDD (purity>99%) Supelco, Cat No: 48599, dried purple roselle (*Hibiscus sabdariffa* L) calyx from a local supplier, East Java, Indonesia. We also used distilled water, 10% formaldehyde, 70% ethanol, 80% ethanol, 90% ethanol, HE dyes, and paraffin.

### Making of Purple Roselle Extract

The dried roselle flowers were finely ground into flour, sieved using a 60-mesh sieve. The roselle flower flour was dissolved in water with a ratio of 20 g: 100 mL, pasteurized at 63-65°C for 30 minutes. The liquid was then carefully separated from the sediment [12].

### Making Yogurt Fortification With Purple Roselle Extract

Fresh cow's milk was pasteurized at 72°C for 15 seconds, then cooled down until the temperature reached 45°C. Yogurt starters were inoculated (3%), homogenized, then incubated at 45°C for 4 hours until the liquid starter reaches a pH of 4.5-5. The plain yogurt was then separated into different bottles and fortified with different concentrations of purple roselle extract, 0.5%, 1%, and 1.5%. The mixture was homogenized and stored at 4°C until used.

### Animals and Treatment

A total of 30 white male adult Wistar rats (*Rattus norvegicus*) were obtained from Experimental Animal Institute, LPPT UGM,

Indonesia. The animal was placed in group rat cages in 12-h light-dark cycle at room temperature of 25-26°C. Acclimatization to the laboratory environment was carried out for seven days. Standard commercial rat pellet and water were given ad libitum. The experiment was approved by the Institutional Ethics Committee of Brawijaya University number 1123-KEP-UB. Rats were randomly divided into five groups. Negative control (NC) group, given only distilled water by gavage. Group positive control (PC), TCDD in corn oil was administered orally with doses of 200 ng.kg<sup>-1</sup> BW daily. Treatment groups were given TCDD and yogurt fortified with purple roselle extract. Group T1 (TCDD + 0.5% roselle yogurt); group T2 (TCDD + 1% roselle yogurt); group T3 (TCDD + 1.5% roselle yogurt).

The experiment was conducted for 12 days. The animals were then euthanized to collect heart tissues. The heart organ was divided into two parts, one part was stored in 10% formaldehyde solution for histopathology analyses, and the other part was stored at -80°C for biochemical analysis.

### Tissue Malondialdehyde (MDA) Analysis

The examination of MDA levels was carried out by measuring Thiobarbituric acid reaction [13]. Heart tissue was cut into small pieces and weighed 0.1 gram, and then crushed. Furthermore, the homogenization process was carried out by centrifuge at a speed of 1000 rpm for 10 minutes. The resulting supernatant was then measured for absorption using a spectrophotometer at  $\lambda = 532$  nm.

### Histopathological analysis

For microscopic evaluation, heart samples were immersed in 10% formaldehyde solution as a fixation agent. The heart tissue samples were processed by routine tissue technique and were embedded in paraffin. Paraffin blocks are then collected, cut, and placed on a glass object, then dripped with Canadian balm and covered with a glass cover. After that, the glass object was put into the incubator at 37°C one night. Then, the preparations were ready for Hematoxylin-Eosin (HE) staining.

## RESULT AND DISCUSSION

### MDA Level From Heart Tissue

The malondialdehyde (MDA) assay of the heart shows in Table 1. MDA levels from groups with TCDD exposure showed an increase compared to the negative control (NC) group. A significant difference occurred between the negative control group compared to the positive



control group. Treatment groups given with yogurt fortified purple roselle extract (T2 and T3) show a significant decrease of MDA level compared to the positive control (PC) group.

**Table 1.** MDA level of rat's heart of all group in the study

Groups	MDA level (ng.mL <sup>-1</sup> ) ± SD
Negative Control (NC)	262.62±6.60 <sup>a</sup>
Positive Control (PC) TCDD	297.60±8.85 <sup>c</sup>
T1 (TCDD + 0.5% roselle yogurt)	276.89±1.20 <sup>ab</sup>
T2 (TCDD + 1.0% roselle yogurt)	289.11±1.57 <sup>bc</sup>
T3 (TCDD + 1.5% roselle yogurt)	274.71±6.77 <sup>ab</sup>

**Note:** The different superscript indicates a significant difference ( $p < 0.05$ ) between groups

MDA is formed from biochemical processes in the body as a consequence of lipid peroxidation. TCDD is known to induced toxic responses and increasing oxidative stress. Exposure to TCDD triggers the formation of Reactive Oxygen Species (ROS), lipid peroxidation, and oxidative stress has been indicated as factors leading to acute toxicity of TCDD [14]. In the current study, the MDA level increased in heart tissue which was induced by TCDD exposure, and yogurt fortified purple roselle extract at concentration 1.5% decreases the heart MDA level close to normal control levels.

TCDD exposure was found to cause considerable lipid peroxidation in cardiac tissue, as well as an increase in MDA levels. The peroxidation of fatty acids by reactive oxygen radicals produced MDA. Malondialdehyde is an indicator of lipid peroxidation and causes irreparable cell damage. Many disorders, including cardiovascular disease, are caused by TCDD-induced oxidative stress, which is defined as an imbalance between free radicals and the antioxidant state [5]. On the other hand, it was discovered that a therapy of yogurt fortified with purple roselle extract was able to protect against oxidative damage caused by TCDD by lowering MDA levels in cardiac tissue.

Yogurt and milk are the most consumed dairy products that have long been known to have health benefits, particularly in the case of yogurt, where the benefits are linked to gut health. The antioxidant capabilities of casein and whey proteins in yogurt are apparently due to their ability to bind transition metals and scavenge free radicals [15]. This study used three lactic acid bacteria *L. bulgaricus*, *S. thermophilus*, and *L. acidophilus*, as the yogurt starter. Some lactobacilli possess antioxidation activity and can

reduce the risk of ROS accumulation during the ingestion of food. Lactic acid bacteria are able to degrade the superoxide anion and hydrogen peroxide [8,16].

Purple roselle calyces are the source of natural bioactive molecules such as polyphenols and flavonoids, which have shown antioxidant potential. Fortification of yogurt with roselle extract has proven to improved antioxidant activity [17]. Fortification of purple roselle extract into yogurt with a concentration of 1.5% has the best activity in preventing oxidative stress induced by TCDD, hence preventing the lipid peroxidation to increase. Bioactive peptides in fermented milk can stabilize radicals by donating hydrogen atoms. Radicals are captured by bioactive peptides of the yogurt. Thus, it prevents the initiation of the formation of lipid radicals which are unstable because they lose one hydrogen atom from the lipid molecule. *Hibiscus sabdariffa L* contains anthocyanin with high antioxidant activity. Anthocyanins are believed to be the active components responsible for the antihypertensive and hypocholesterolemic effects [10].

#### Heart histopathology results

Figure 1 shows the heart histopathology of rats (*Rattus norvegicus*) from negative and positive control groups. Hematoxylin Eosin (H&E) stained sections of c left ventricle revealed a normal structural architecture of cardiomyocytes. Cardiac histopathology in the negative control group showed no significant tissue damage, there was a central cell nucleus, pink cytoplasm, and clear boundaries between cells. A normal picture of heart cells stained with H&E shows regular cardiac muscle fibers, clear boundaries between cells, and one or two nuclei in the center of the cell.

All treatment groups showed changes in heart muscle cells in the form of myocyte cells that experienced necrosis and hemorrhage in the myocardium. Histopathological damage was seen in the Positive Control (PC) group. The prominent changes consist of myocyte cell necrosis, hemorrhage, and extravasation of red blood cells between myocytes (Fig. 2B, 2B1). The PC group was exposed to TCDD as a toxic substance. Continuous administration of TCDD can induce damage to the heart tissue. The many foci of myocardial degeneration found in the rat heart were characteristic of the look of cardiomyopathy [2,5,18]. Apoptosis was indicated by the presence of pyknotic myonuclei

and dark eosinophilic cytoplasm in certain cardiomyocytes. Cardiomyopathy can occur as a result of anoxia caused by vascular alterations or as a result of direct damage to cardiac cells.

TCDD exposure to rats (*Rattus norvegicus*) will trigger an increase in Reactive Oxygen Species (ROS) in the heart. ROS bind to H atom molecules derived from lipids, proteins, and nucleotides contained in DNA and cell organelles, so that DNA and cardiac organs experience dysfunction and structural damage. Damage to cell protein structure and damage to cardiac cell organelles caused by ROS is the basic pattern of necrosis. High levels of ROS can cause damage and cell death [2,5].

TCDD toxin that enters the body will inhibit blood clotting so that it damages the endothelium of blood vessels. Damage to the walls of blood vessels causes blood to escape from the circulation, resulting in hemorrhage

[18]. The occurrence of hemorrhage can occur because high ROS are not inhibited effectively by endogenous antioxidants. Group T1 (TCDD and yogurt roselle 0.5%) showed myocyte cells with pyknotic necrosis accompanied by hemorrhage (Fig. 1C, C1).

Group T2 (TCDD and yogurt roselle 1.0%) shows necrosis of myocyte cells and irregular myofibril structures and is still accompanied by hemorrhage (Figure 1D, D1). Group T3 (TCDD and yogurt roselle 1.5%) showed that myocyte cells underwent necrosis, which was slightly accompanied by the presence of hemorrhage. However, the myofibril structure in the T3 group was seen to be organized and similar to the NC group (Fig. 1E, E1). The accumulation of free radicals in the heart will stimulate lipid peroxidation. Lipid peroxidation will cause damage to cell membranes and heart structures.

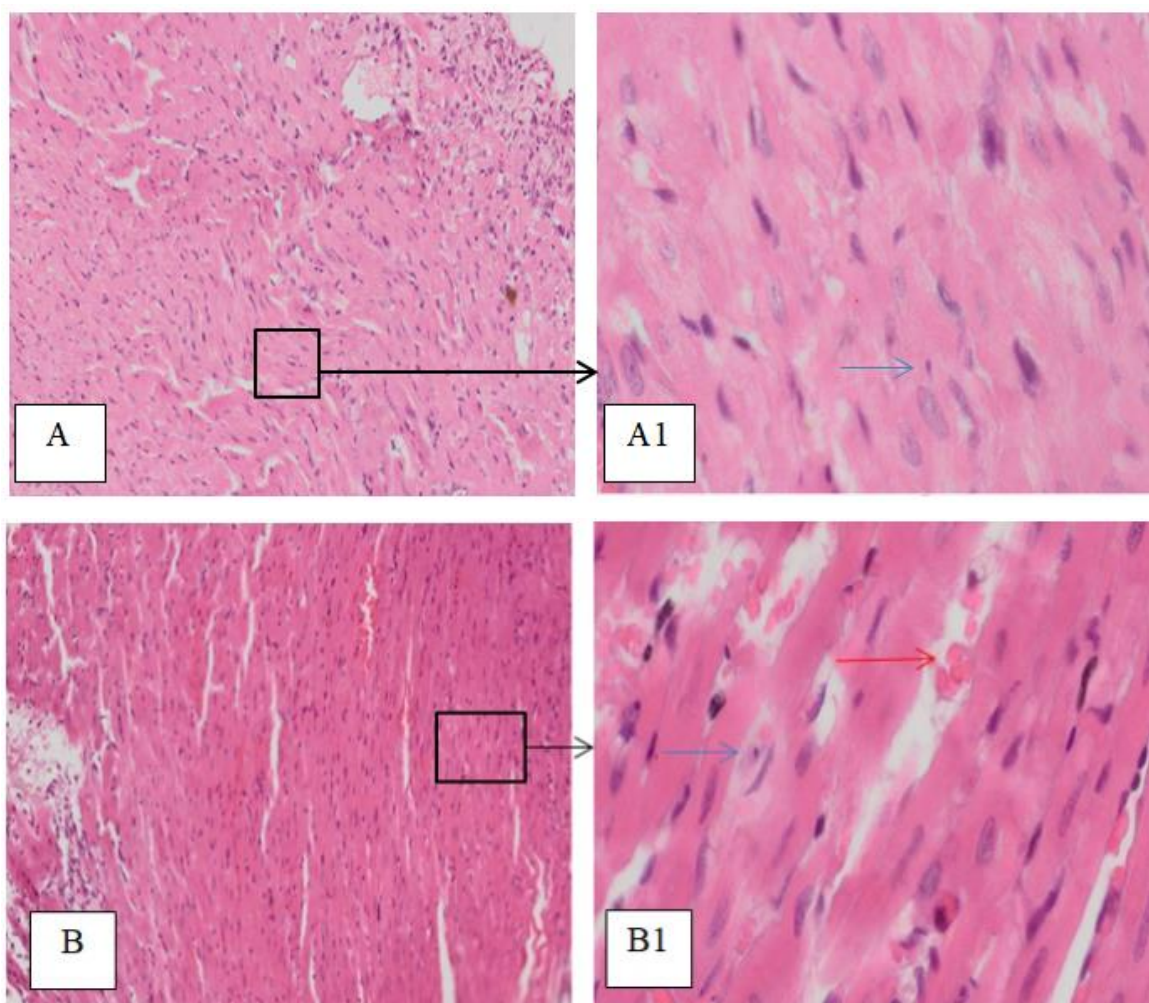


**Figure 1.** H&E stained sections of the left ventricular myocardium of control groups. A. Negative Control (NC) group (A: magnification 100x, A1: magnification 400x); B. Positive control (PC) group (B: blue arrow: necrosis; red arrow: hemorrhage)

Cardiac histopathology results in the T3 group were better and gave an optimal effect than the T2 and T1 groups. The mechanism in preventing the occurrence of histopathological damage to myocyte cells undergoing necrosis through the antioxidant activity of yogurt fortified with purple roselle extract is to donate H atoms to free

radicals so that free radicals will be stable. Bioactive peptides in fermented milk will stabilize radicals and prevent further damage to cardiac cells. Anthocyanin and other phenolic compounds present in purple roselle extract play a role in increasing antioxidant activity [10,11].

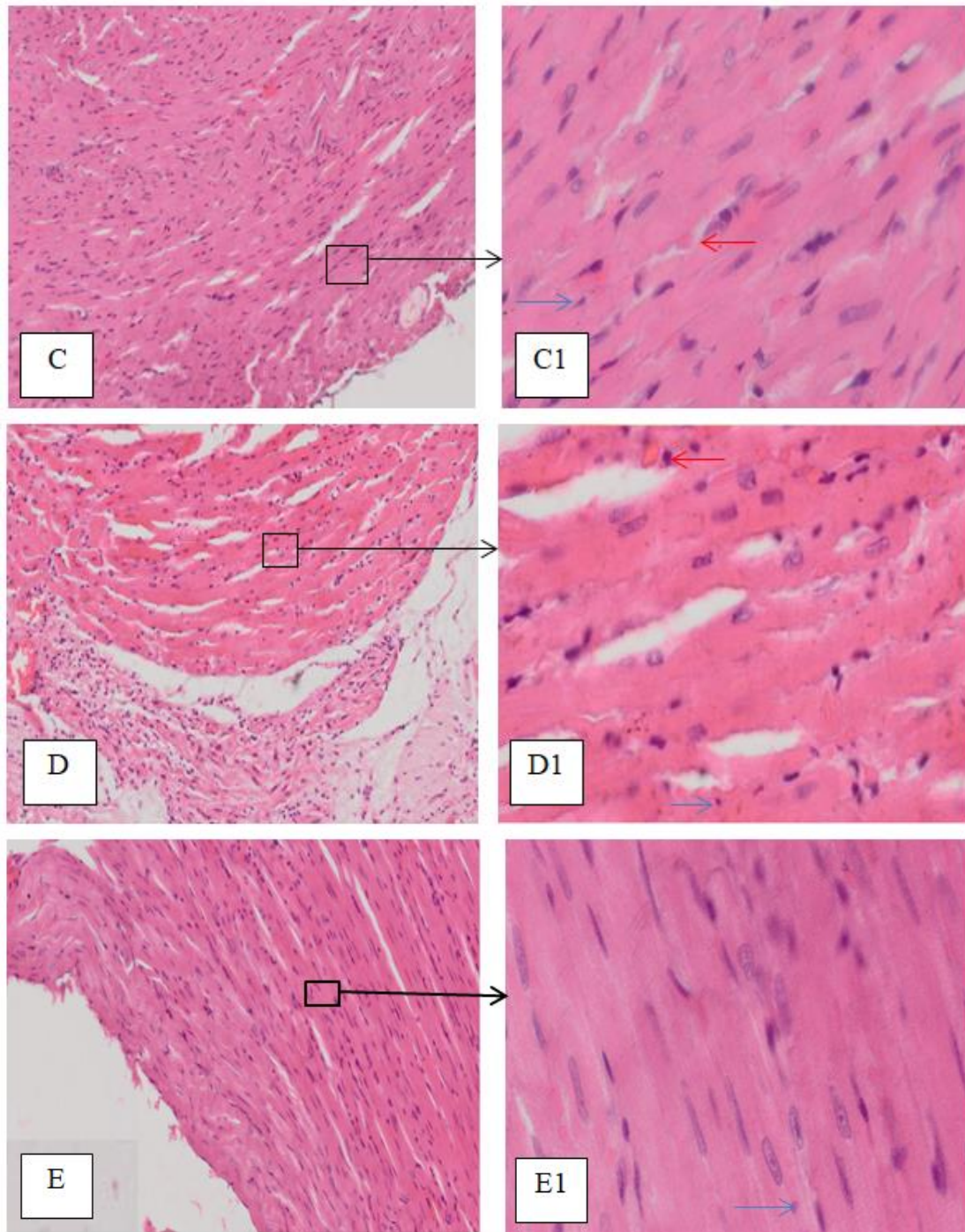


**Figure 2.** H&E stained sections of left ventricular myocardium of treatment groups. **C.** T1 group (TCDD + 0.5% roselle yogurt) C: magnification 100x, C1: magnification 400x; **D.** T2 group (TCDD + 1% roselle yogurt) D: magnification 100x, D1: magnification 400x; **E.** T3 group (TCDD + 1.5% rosele yogurt) E: magnification 100x, E1: magnification 400x; blue arrow: necrosis; red arrow: hemorrhage



According to the results, yogurt fortified with roselle extract enhanced antioxidant activities and cell viability. It proves that the antioxidants in yogurt fortified with purple roselle extract play a role in stabilizing reactive free radicals, so that tissue damage can be prevented.

#### CONCLUSION

Based on the present study results, it can be concluded that giving yogurt fortified with purple roselle extract with concentrations of 0.5 and 1.5% was potential in preventing increasing malondialdehyde (MDA) and preventing histopathological damage levels of rat heart (*Rattus norvegicus*) that have been exposed to TCDD. Thus, yogurt fortified with purple roselle extract, which decreases oxidative stress, could be a promising anti-TCDD toxicity option.

#### CONFLICT OF INTEREST

The authors have no conflicts of interest that are relevant to this article.

#### ACKNOWLEDGEMENT

This study was supported by research funding from the University of Brawijaya. The authors thank LPPM UB, Biosains Institute UB, and Faculty of Veterinary Medicine UB.

#### REFERENCES

- [1] United Nations of Environmental Programme. 2008. The 12 initial POPs under the Stockholm Convention. Available at: <http://chm.pops.int/TheConvention/ThePOPs/The12InitialPOPs/tabid/296/Default.aspx>
- [2] Ciftci, O., A.S. Duman, N.B. Turkmen, A. Taslidere. 2018. Beta-glucan prevents toxic effects of 2,3,7,8-TCDD in terms of oxidative and histopathological damage in heart tissue of rats. *Brazilian J. Pharm. Sci.* 54(3). 1–7.
- [3] Setianingrum, A., G.D. Satria, M.C. Padaga. 2019. Aktivitas antioksidan kasein yogurt susu kambing pada fungsi hati tikus model intoksikasi dioksin. *Vet. Biomed. Clin. J.* 1(1). 26–32.
- [4] Yoshioka, W., C. Tohyama. 2019. Mechanisms of developmental toxicity of dioxins and related compounds. *Int. J. Mol. Sci.* 20(3). 617. DOI: 10.3390/ijms20030617.
- [5] Ciftci, O., O.M. Disli, N. Timurkaan. 2012. Protective effects of protocatechuic acid on TCDD-induced oxidative and histopathological damage in the heart tissue of rats. *Toxicol. Ind. Health.* 29(9). 806–811.
- [6] Dziuba, B, M. Dziuba. 2014. Milk proteins-derived bioactive peptides in dairy products : molecular, biological and methodological aspects. *Acta Sci. Pol. Technol. Aliment.* 13. 5–25.
- [7] Setianingrum, A., A.E.P. Haskito. 2021. Antioxidant activity of casein yogurt against dioxin toxicity in rats liver. *IOP Conference Series: Earth and Environmental Science.* 762(012056).
- [8] Brandelli, A., D.J. Daroit, A.P.F. Correa. 2015. Whey as a source of peptides with remarkable biological activities. *Food Res. Int.* 73. 149–161.
- [9] Mohanty, D.P., S. Mohapatra, S. Misra, P. Sahu. 2016. Milk-derived bioactive peptides and their impact on human health – A review. *Saudi J. Biol. Sci.* 23(5). 577–83.
- [10] Izquierdo-Vega, J.A., D.A. Arteaga-Badillo, M. Sánchez-Gutiérrez, J.A. Morales-González, N. Vargas-Mendoza, C.A. Gómez-Aldapa, et al. 2020. Organic acids from Roselle (*Hibiscus sabdariffa L.*)- A brief review of its pharmacological effects. *Biomedicines.* 8(5). 1–16.
- [11] Alenisan, M.A., H.H. Alqattan, L.S. Tolbah, A.B. Shori. 2017. Antioxidant properties of dairy products fortified with natural additives : A review. *J. Assoc. Arab Univ. Basic Appl. Sci.* 1-7.
- [12] Noviatry, A, A. Setianingrum, A.E.P. Haskito. 2020. Organoleptic properties evaluation of purple *Hibiscus sabdariffa L* (Roselle) calyx extract-fortified yogurt. *J. Phys. Conf. Ser.* 1430(1). 8–13.
- [13] Ohkawa, H., N. Ohishi, K. Yagi. 1979. Assay for lipid peroxides in animal tissues by thiobarbituric acid reaction. *Anal. Biochem.* 95(2). 351–8.
- [14] Vijaya, V., P. Palaniswamy, K. Selvi. 2014. Protective effect of ellagic acid against TCDD-induced renal oxidative stress : Modulation of CYP1A1 activity and antioxidant defense mechanisms. *Mol Biol Rep.* 41. 4223–4232.
- [15] Farvin, K.H.S., C.P. Baron, N. Skall, J. Otte, C. Jacobsen. 2010. Antioxidant activity of yoghurt peptides : Part 2 – Characterisation of peptide fractions. *Food Chem.* 123(4). 1090–1097.
- [16] Fernandez, M.A., É. Picard-Deland, M. Le Barz, N. Daniel, A. Marette. 2017. Yogurt and health. In: Frias, J., C. Martinez-Villaluenga, E. Peñas (Eds). *Fermented foods*

- in health and disease prevention. Academic Press. Boston. 305–338.
- [17] Suharto, E.L.S., I.I. Arief, E. Taufik. 2016. Quality and antioxidant activity of yogurt supplemented with roselle during cold storage. *Media Peternak*. 39. 82–89.
- [18] Wahba, N.S., M.G. Amer, R.A. Karam, R.H. Mohamed. 2012. Pathology effect of persistent organic pollutants (dioxins) on rat myocardium and amelioration with antioxidant vitamins (role of aryl hydrocarbon receptors and cytochrome P450). *J. Clin. Exp. Pathol.* 2(7). 130. DOI: 10.4172/2161-0681.1000130.
- [19] Birnbaum, L.S. 2017. Dioxin and the AH receptor: Synergy of discovery. *Curr. Opin. Toxicol.* 2. 120–123.
- [20] Ambolet-camoit, A., C. Ottolenghi, A. Leblanc, M. Ji, N. Cagnard. 2015. Two persistent organic pollutants which act through different xenosensors (alpha-endosulfan and 2,3,7,8 tetrachlorodibenzo-p-dioxin) interact in a mixture and downregulate multiple genes involved in human hepatocyte lipid and glucose metabolism. *Biochimie*. 116. 79–91.

## Dynamical Analysis and Parameter Estimation of a Model of Hepatitis B Disease Spread in Malang

Fitroh Aulani<sup>1\*</sup>, Wuryansari Muharini Kusumawinahyu<sup>2</sup>, Isnani Darti<sup>2</sup>

<sup>1</sup>Master Program of Mathematics, Faculty of Mathematics and Natural Sciences, University of Brawijaya, Malang, Indonesia

<sup>2</sup>Department of Mathematics, Faculty of Mathematics and Natural Sciences, University of Brawijaya, Malang, Indonesia

### Abstract

In this article, a model representing the spread of Hepatitis B disease is constructed as a nonlinear autonomous system. The model divides the considered human population into three classes, namely susceptible, infected, and recovered class. The dynamical analysis shows that there are two equilibrium points in the model, namely a disease-free equilibrium point and an endemic equilibrium point. The existence and stability of the equilibrium points depend on the basic reproduction number ( $\mathcal{R}_0$ ). The disease-free equilibrium point is local asymptotically stable when  $\mathcal{R}_0 < 1$ , while the endemic equilibrium point exists and is local asymptotically stable if  $\mathcal{R}_0 > 1$ . The five parameters of the model are estimated by applying Downhill Simplex (Nelder-Mead) Algorithm and by using the infected data cases taken from such a hospital in Malang. The estimated parameters are the transmission of infection rate, the saturation rate, the vaccination rate, the recovery rate, and the immunity loss rate. The resulting parameter estimation supports the analytical result and is used to illustrate the analytical results numerically. Based on the considered model and the result of the parameters estimation, it can be concluded that the Hepatitis B spread in Malang is controllable.

**Keywords:** downhill simplex (Nelder-Mead) algorithm, dynamical analysis, hepatitis B model, parameter estimation.

### INTRODUCTION

Hepatitis B disease is a type of infectious disease caused by the Hepatitis B Virus (HBV). That virus is a type of the virus family Hepadnaviridae [1]. HBV is more easily spread than other viruses, like Hepatitis C Virus (HCV) or Human Immunodeficiency Virus (HIV). HBV can also be transmitted through sexual transmission [2]. According to a nationwide report in 2007 and 2013, Hepatitis B cases in Indonesia are indicated from high to moderate [3].

Many types of research have been conducted to describe the epidemic phenomenon by constructing mathematical models which divide the population into some classes. The classic epidemic model called the SIR model considers three classes, namely Susceptible, Infected, and Recovery class. The SIR model is introduced in 1927, and the model is governed by the bilinear incidence rate [4]. Many modifications are applied to the classic SIR model based on the disease character. Capasso and Serio [5] in 1978 modified the SIR model by applying a saturated incidence rate. In 2019, Khan *et al.* [6] constructed a SIR model Hepatitis B with a saturated transmission rate and added the vaccination factor to the model. Furthermore,

Khan *et al.* also assumed that recovered individuals have permanent immunity.

Generally, the mathematical models contain some parameters that can be used to predict the behavior of the disease spread as long as their values are known. To determine the parameter values, we can do the estimation process to approximate the actual data with the solution of the model. Golgeli [7] analyzed a SIR Hepatitis B model with a bilinear transmission rate and performed the parameter estimation using a data set taken in Turkey. This model consists of four parameters, and one of the parameters is estimated. Golgeli concluded that Hepatitis B in Turkey stabilizes into a disease-free state.

Based on the previous research, in this paper, a Hepatitis B disease model was constructed by modifying the model of Khan *et al.* [6] into the SIRS model. A dynamical analysis is conducted by determining the equilibrium point and the local stability of the equilibrium point. The parameter values of the SIRS model are obtained by employing the parameter estimation process. The infected cases data of Hepatitis B was retrieved from Dr. Saiful Anwar Hospital, a governmental hospital in Malang. Data from January 2015 to December 2019 were used in the estimation process. Furthermore, numerical simulation was performed to illustrate the analytical results related to the spread of Hepatitis B in Malang.

---

Correspondence address:

**Fitroh Aulani**

Email : fitrohaulani96@gmail.com

Address : Dept. Mathematics, University of Brawijaya,  
Veteran Malang, 65145

**MATERIAL AND METHOD**

**Model Formulation**

In this research, a Hepatitis B disease model was reconstructed and represented as a SIRS model by assuming that the recovered individuals can lose their immunity. Hence the recovered individual can be reinfected. The incidence rate is also modified into a saturated incidence rate. Based on those modifications, a nonlinear autonomous system consisting of three variables and eight parameters is proposed to describe the Hepatitis B spread.

**Equilibrium Point and Local Stability**

The equilibrium point of the model is obtained when the size of all class of population in the model are constant. The linearization process around the equilibrium point is carried out to analyze the local stability of the equilibrium point. The eigen values of the Jacobian matrix coming from the linearization process provides the information about the stability of the equilibrium point. If all of the eigen values of Jacobian matrix have negative real part, the equilibrium point is local asymptotically stable.

**Parameter Estimation**

The estimation process determines the value of the parameter in the model by minimizing the difference between the estimated solution of the model and the real data iteratively. Hence, the first step of the estimation process is considering the objective function which is used in [8]:

$$O_f = \sum_1^i R_i^2 = \sum_1^i (Y_i - f(x_i, \theta))^2 \quad (1)$$

where  $R_i$  is the  $i^{\text{th}}$  residual,  $Y_i$  is the  $i^{\text{th}}$  data, and  $f(x_i, \theta)$  is the numerical solution of the model with the vector of the parameters  $\theta$ . The objective function is minimized by using the Nelder-Mead Algorithm [9,10], as follows.

1. Choose the initial value of the parameter  $\theta$  and the initial value of population as the variable in the model.
2. Generate the population of the model  $f(x_i, \theta)$  using the Runge-Kutta 4<sup>th</sup> order method.
3. Determine the objective function (1) and sorted the values of objective function from smallest to largest values

$$O_f(\vec{\theta}_1) \leq O_f(\vec{\theta}_2) \leq O_f(\vec{\theta}_3) \leq \dots \leq O_f(\vec{\theta}_{i+1}).$$

4. Calculate the reflection point

$$\vec{\theta}_r = \vec{\theta} + \rho (\vec{\theta} - \vec{\theta}_{i+1})$$

where  $\vec{\theta} = \sum_1^i \frac{\vec{\theta}_i}{i}$ . The standard value for the coefficient of reflection is  $\rho = 1$ .

5. If  $O_{f_1} \leq O_{f_r} < O_{f_i}$ , the reflection point is accepted. Terminate the iteration.

6. If  $O_{f_r} < O_{f_1}$ , calculate the expansion point

$$\vec{\theta}_e = \vec{\theta} + \chi (\vec{\theta}_r - \vec{\theta}).$$

The standard value for the coefficient of expansion is  $\chi = 2$ . If  $O_{f_e} < O_{f_r}$ , accepted the expansion point  $\vec{\theta}_e$  and terminated the iteration. If  $O_{f_e} \geq O_{f_r}$ , accepted the reflection point  $\vec{\theta}_r$  and terminated the iteration.

7. Determination of the contraction point.

- a. Outside. If  $O_{f_i} \leq O_{f_r} < O_{f_{i+1}}$  calculate the outside contraction point

$$\vec{\theta}_c = \vec{\theta} + \hat{\gamma} (\vec{\theta}_r - \vec{\theta}).$$

The standard value for the coefficient of contraction is  $\hat{\gamma} = \frac{1}{2}$ . If  $O_{f_c} \leq O_{f_r}$ ,  $\vec{\theta}_c$  is accepted and terminated the iteration otherwise go to the next step.

- b. Inside. If  $O_{f_r} \geq O_{f_{i+1}}$  calculate the inside contraction point

$$\vec{\theta}_{cc} = \vec{\theta} - \hat{\gamma} (\vec{\theta} - \vec{\theta}_{i+1}).$$

If  $O_{f_{cc}} \leq O_{f_{i+1}}$ ,  $\vec{\theta}_{cc}$  is accepted and terminated the iteration otherwise go to the next step.

8. Shrink (reduction). Evaluate the objective function  $O_f$  at each point  $\vec{v}_k$ , which the point is obtained based on

$$\vec{v}_k = \vec{\theta}_1 + \sigma (\vec{\theta}_k - \vec{\theta}_1)$$

where  $k = 2, \dots, i + 1$ . Replace the  $\vec{\theta}_k$  point with  $\vec{v}_k$ . The next iteration consist of  $\vec{\theta}_1, \vec{v}_2, \dots, \vec{v}_{i+1}$ . The standard value for the coefficients of shrink (reduction) is  $\sigma = \frac{1}{2}$ .

9. The iteration ends if the tolerance criteria have been reached as [11].

$$\|\vec{\theta}_{i+1} - \vec{\theta}_i\| \leq \epsilon_\theta \text{ and } O_f(\vec{\theta}_i) - O_f(\vec{\theta}_{i+1}) \leq \epsilon_f.$$

**Numerical Simulation**

The parameter values obtained from the parameter estimation process are used in this part. The model is simulated numerically by using Runge-Kutta 4<sup>th</sup> order method to confirm the analytical results and to show the dynamic of the model.



**Data Collection**

This research uses secondary data of the number of infected Hepatitis B from January 2015 to December 2019. The data was taken from RSUD Dr. Saiful Anwar Malang. The data of the infected individuals are presented at Table 1.

**Table 1.** The number of HBV infected individuals

Times	Number of infected				
	2015	2016	2017	2018	2019
January	27	6	12	14	7
February	13	5	6	14	7
March	14	2	10	6	7
April	8	5	8	11	11
May	4	4	9	12	16
June	5	8	5	2	7
July	2	8	10	12	14
August	13	7	15	7	9
September	3	3	18	7	12
October	4	12	16	13	15
November	6	10	18	13	11
December	6	11	10	11	10

**RESULT AND DISCUSSION**

**Model Formulation**

Based on the assumption and the modification on the model of Khan *et al.* in 2019 [6] that have been described before, we propose a model of Hepatitis B transmission as follows.

$$\frac{dS(t)}{dt} = \Lambda - \frac{\alpha S(t)I(t)}{1 + \gamma I(t)} - (\mu_0 + v)S + \delta R(t),$$

$$\frac{dI(t)}{dt} = \frac{\alpha S(t)I(t)}{1 + \gamma I(t)} - (\mu_0 + \mu_1 + \beta)I(t), \quad (2)$$

$$\frac{dR(t)}{dt} = \beta I(t) + vS(t) - (\mu_0 + \delta)R(t),$$

where  $S(t)$ ,  $I(t)$ , and  $R(t)$  represent the susceptible individual, the infected individual, and the recovered individual at time  $t$ , respectively. The parameters  $\Lambda, \alpha, \mu_0, \mu_1, \gamma, v, \beta$ , and  $\delta$  represent the birth rate, the transmission of infection rate, the natural mortality rate, the death rate because of Hepatitis B infection, the saturation rate, the vaccination rate, the recovery rate, and the immunity loss rate respectively. The density of the total population considered in the model is the sum of the density of susceptible, infected, and recovered classes, namely  $N(t) = S(t) + I(t) + R(t)$ .

**Equilibrium Point of Model**

Since the equilibrium point of the model (2) is obtained when the size of all class of population in the model are constant, then it is reached when

$\frac{dS}{dt} = \frac{dI}{dt} = \frac{dR}{dt} = 0$ . It can be proved easily, that there are two equilibrium points, namely the disease-free equilibrium point

$$E_0 = (S_0, I_0, R_0) = \left( \frac{\Lambda(\mu_0 + \delta)}{\phi}, 0, \frac{v\Lambda}{\phi} \right)$$

and the endemic equilibrium point  $E^* = (S^*, I^*, R^*)$

$$S^* = \frac{\eta(1 + \gamma I^*)}{\alpha},$$

$$I^* = \frac{\Lambda \alpha(\mu_0 + \delta) - \eta\phi}{\eta(\alpha \mu_0 + \gamma \phi) + \alpha\delta(\mu_0 + \mu_1)},$$

$$R^* = \frac{\beta I^* + v S^*}{\mu_0 + \delta}.$$

Here  $\eta = \mu_0 + \mu_1 + \beta$  and  $\phi = \mu_0(\mu_0 + \delta + v)$ . Furthermore, by applying the Next Generation Matrix method [12], the basic reproduction number ( $\mathcal{R}_0$ ) is easily formulated, namely

$$\mathcal{R}_0 = \frac{\alpha\Lambda(\mu_0 + \delta)}{\eta\phi}.$$

It is clear that the disease-free equilibrium always exists, while the endemic equilibrium exists when  $\mathcal{R}_0 > 1$ .

**Stability of the Equilibrium Point**

The local stability of the equilibrium point can be determined through the linearization process, which provide the Jacobian matrix

$$J = \begin{pmatrix} -\frac{\alpha I}{1 + \gamma I} - \mu_0 - v & -\frac{\alpha S}{(1 + \gamma I)^2} & \delta \\ \frac{\alpha I}{1 + \gamma I} & \frac{\alpha S}{(1 + \gamma I)^2} - \eta & 0 \\ v & \beta & -\mu_0 - \delta \end{pmatrix}.$$

The result of the stability analysis is presented in the following theorems.

**Theorem 1.** if the basic reproduction number is less than one ( $\mathcal{R}_0 < 1$ ), the disease-free equilibrium point ( $E_0$ ) of system (2) is local asymptotically stable.

**Proof.** The Jacobian matrix at  $E_0$  is

$$J(E_0) = \begin{pmatrix} -\mu_0 - v & -\frac{\alpha\Lambda(\mu_0 + \delta)}{\phi} & \delta \\ 0 & \frac{\alpha\Lambda(\mu_0 + \delta)}{\phi} - \eta & 0 \\ v & \beta & -\mu_0 - \delta \end{pmatrix}.$$

$J(E_0)$  has three eigenvalues, namely  $\lambda_1 = -(\mu_0 + \delta + v)$ ,  $\lambda_2 = -\mu_0$  and  $\lambda_3 = \eta(\mathcal{R}_0 - 1)$ . All eigenvalues are negative if  $\mathcal{R}_0 < 1$ . Hence, the disease-free equilibrium  $E_0$  is local asymptotically stable when  $\mathcal{R}_0 < 1$ .

**Theorem 2.** If  $\mathcal{R}_0 > 1$ , the endemic equilibrium point ( $E^*$ ) of system (2) exist and is local asymptotically stable.

**Proof.** The Jacobian matrix at  $E^*$  is

$$J(E^*) = \begin{pmatrix} -\frac{\alpha I^*}{\omega_1} - \omega_2 & -\frac{\alpha S^*}{\omega_1^2} & \delta \\ \frac{\alpha I^*}{\omega_1} & \frac{\alpha S^*}{\omega_1^2} - \eta & 0 \\ v & \beta & -\omega_3 \end{pmatrix}$$

where

$$\omega_1 = 1 + \gamma I^*, \omega_2 = \mu_0 + v, \omega_3 = \mu_0 + \delta$$

Based on calculated  $|J(E^*) - \lambda I|$ , we get a polynomial equation of third degree.

$$\lambda^3 + a_1 \lambda^2 + a_2 \lambda + a_3 = 0, \quad (3)$$

where

$$a_1 = \omega_2 + \omega_3 + \frac{I^*}{\omega_1} (\alpha + \eta \gamma),$$

$$a_2 = \frac{I^*}{\omega_1} (\alpha \omega_3 + \alpha \eta + \eta \gamma \omega_3 + \eta \gamma \omega_2) + \phi,$$

$$a_3 = \frac{I^*}{\omega_1} (\alpha \mu_0 \eta + \alpha \delta \mu_0 + \alpha \delta \mu_1 + \phi \eta \gamma).$$

Routh-Hurwitz criterion stated that all of the root of the equation (3) have negative real part if  $a_1 > 0$ ,  $a_3 > 0$ , and  $a_1 a_2 - a_3 > 0$  [13]. It is clear that  $a_1 > 0$  and  $a_3 > 0$ . By applying such a simple algebraic manipulation, it can be proved that  $a_1 a_2 - a_3 > 0$ . Hence, the endemic equilibrium point is local asymptotically stable.

**Parameter Estimation**

There are eight parameters in the SIRS model (2). In this paper, the three parameters are fixed, and the other five parameters are estimated. The idea of the estimation parameter is to minimize the objective function (1) so that the parameter values correspond to the real data. The first step to estimate the parameter is to define the initial values  $\vec{\theta}_0 = (\alpha, \gamma, v, \delta, \beta) = (0.000010260, 1.4, 0.3816, 0.982, 0.1667)$ . In the first period January 2015, the total population in Malang is 866801, so we choose the initial values of the population as  $(S_0, I_0, R_0) = (866774, 27, 0)$ . By following step 1 until step 9 in the Nelder Mead algorithm, which was described in the previous section, the iteration ends after the error tolerance is met. The parameter that makes the minimum objective function is the best one. The

minimum values of the objective function was reached in the 1412<sup>th</sup> iteration. The best parameter values were presented at Table 2, and they can be used to determine the value of the basic reproduction number, namely  $\mathcal{R}_0 = 0.00000167$ .

**Table 2.** Estimated parameter value

Parameter	Value	Source
$\Lambda$	0.0025128	Dispendukcapil Malang
$\alpha$	0.0000311	Estimated
$\gamma$	0.022	Estimated
$\mu_0$	0.0024205	Dispendukcapil Malang
$v$	0.965	Estimated
$\delta$	1.788	Estimated
$\mu_1$	0.0000018	RSUD Dr. Saiful Anwar
$\beta$	1.248	Estimated

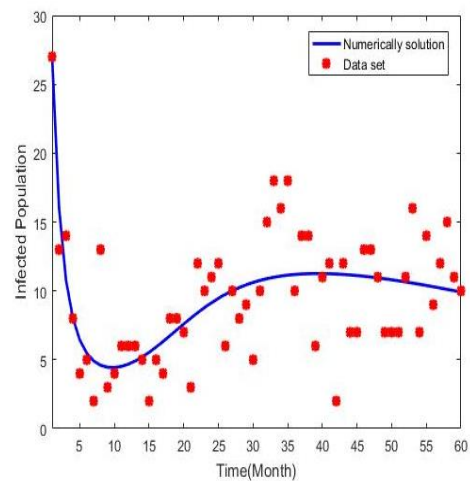


**Figure 1.** Comparison of SIRS model of Hepatitis B and the infected data

**Numerical Simulation**

The SIRS model (2) is simulated by using the best parameter presented at Table 2. Figure 1 shows that the numerical solution of the model approach the trend of the infected data of Hepatitis B.

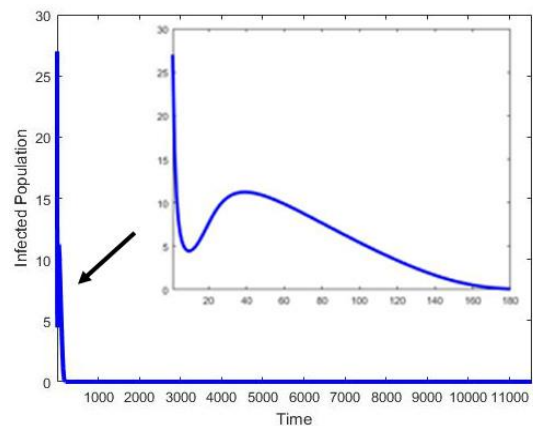


**Figure 2.** Simulation SIRS model of Hepatitis B

Figure 2 shows the profile of the density of the infected population when the length of the interval time is enlarged becomes  $t = 11544$ . In accordance with the analytical result, eventually, the size of the infected population decreases and converges to 0 because the basic reproduction number  $\mathcal{R}_0 < 1$ .

### CONCLUSION

A SIRS model representing the spread of the Hepatitis B disease model has been reconstructed in the form of a three-dimensional nonlinear autonomous differential equation system with eight parameters. The performed dynamical analysis shows that the model has a disease-free equilibrium point and an endemic equilibrium point. By applying the Next Generation Matrix method, the basic reproduction number  $\mathcal{R}_0$  has been formulated. The existence and the stability of the equilibrium points depend on the basic reproduction number  $\mathcal{R}_0$ . The disease-free point always exists, while the endemic point only exists when  $\mathcal{R}_0 > 1$ . By applying linearization around each equilibrium point, the local stability of the equilibrium points is investigated. The disease-free point is local asymptotically stable when  $\mathcal{R}_0 < 1$ . Referring to the Routh-Hurwitz criteria, it can be shown that the endemic point is local asymptotically stable when this point exists.

Based on the data of infected cases taken from a hospital in Malang, Indonesia, the five parameters of the model have been estimated. The numerical simulation of the SIRS model by using the estimated parameters reach the minimum error if compared to the infected data. The result of the simulation of the proposed model predicts that eventually, Malang can be a Hepatitis B-disease-free state. This result agrees with the analytical result since the estimated parameters give  $\mathcal{R}_0 < 1$ .

### REFERENCES

- [1] Wong, D.J., S.A. Locarnini. 2018. Molecular virology and life cycle. In: Kao, J.H., D.S. Chen (Eds). Hepatitis B Virus and Liver Disease. Springer. Singapore. 1-23.
- [2] Konerman, M.A., A.S. Lok. 2018. Epidemiology, diagnosis, and natural history of Hepatitis B. In: Sanyal, A.J., T.D. Boyer, K.D. Lindor, N. A. Terrault. Zakim and Boyer's Hepatology: A Textbook of Liver Disease, 7<sup>th</sup> Ed. Elsevier. 474-484.
- [3] Muljono, D.H. 2017. Epidemiology of Hepatitis B and C in Republic of Indonesia. *Euroasian. J. Hepatogastroenterol.* 7(1). 55–59.
- [4] Kermack, W.O., McKendrick A.G. 1927. A Contribution to the mathematical theory of epidemics. *Proceedings of the Royal Society of London. Series A.* 115(772). 700-721.
- [5] Capasso, V., G. Serio. 1978. A generalization of the Kermack-McKendrick deterministic epidemic model. *Math.I Biosci.* 42(1-2). 43-61.
- [6] Khan, T., Z. Ullah, N. Ali, G. Zaman. 2019. Modeling and control of the Hepatitis B virus spreading using an epidemic model. *Chaos Solitons Fractals.* 124. 1-9.
- [7] Golgeli, M. 2019. A mathematical model of Hepatitis B transmission in Turkey. *Communication Faculty of Sciences, University of Ankara Series A1 Mathematics and Statistics.* 68. 1586-1595.
- [8] Wolberg, J. 2006. Data Analysis using the Method of Least Squares: extracting the most information from experiments. Springer-Verlag. Berlin Heidelberg. Germany.
- [9] Lagarias, J.C., J.A. Reeds, M.H. Wright, P.E. Wright. 1998. Convergence properties of the Nelder-Mead Simplex Method in low dimensions. *Soc. Ind. Appl. Math.* 9. 112-147.
- [10] Gao, F., L. Han. 2010. Implementing the Nelder-Mead Simplex algorithm with adaptive parameters. *Comput. Optim. Appl.* 51. 259-277.
- [11] Isermann, R., M. Munchhof. 2011. Identification of dynamic systems: an introduction with applications. Springer-Verlag. London, New York.
- [12] Brauer, F., C.C. Chavez. 2012. Mathematical models in population biology and epidemiology, 2<sup>nd</sup> Ed. Springer-Verlag. New York.
- [13] Murray, J.D. 2002. Mathematical biology I. An introduction, 3<sup>rd</sup> Ed. Springer-Verlag. Berlin Heidelberg.

## **In Silico Study to Predict the Potential of Beta Asarone, Methyl Piperonylketone, Coumaric Acid in *Piper Crocatum* as Anticancer Agents**

Ahmed Hasan Abkar\*, Moch. Sasmito Djati<sup>2</sup>, Widodo<sup>2</sup>

Department of Biology, Faculty of Mathematics and Natural Sciences, University of Brawijaya, Malang, Indonesia

### **Abstract**

*Piper Crocatum* Ruiz & Pav leaves often be used to treat various diseases, including cancer, empirically. This study aimed to analyze the anticancer activities of *Piper Crocatum* bioactive compounds via *In Silico* analysis. The methods were biological activity analysis, cell line cytotoxicity activity, SwissADME, STITCH, molecular docking, and molecular dynamics simulation. The investigated bioactive compounds were  $\beta$ -asarone, methyl piperonylketone, and coumaric acid. The results showed the biological activities of the compounds related to anticancer were anti-mutagenic, TNF expression inhibitive, and MMP9 expression inhibitive. The prediction of cytotoxicity analysis results showed that investigated bioactive compounds were toxic on various tumor cell lines. Based on swissADME results, almost all compounds have good pharmacological properties, except coumaric acid. Docking analysis demonstrated the presence of bioactive compounds inhibited TNF $\alpha$ , HER2, and MMP9 as the target protein. The molecular dynamic result was confirmed using molecular dynamic and it shows that  $\beta$ -asarone interaction was stable against MMP9 and TNF protein showed by the low RMSD value. The study found the investigated bioactive compounds of *Piper crocatum* have the activity of anti-cancer via the inhibition of TNF $\alpha$  and MMP9 protein. However, further research still needs to be done to confirm the prediction results of this *In Silico* study.

**Keywords:** anticancer, *In Silico*, molecular docking, *Piper crocatum*.

### **INTRODUCTION**

Cancer is one of the leading causes of death and a significant barrier to increasing life expectancy all over the world. Cancer is a disease that arises from the abnormal growth of body cells which turn into cancer cells. The urgency of finding effective cancer treatment has become one of the oncology researchers' primary focuses. Commonly, the development of an anticancer drug is conducted through in vitro and in vivo studies, which is time and cost-consuming. *In Silico* study is reported to be the alternative to screening herbal-based anticancer agents and cancer drug discovery [1]. The screening of anticancer from several herbal plants through the *In Silico* method is effective due to advancements, such as web servers that provide prediction tools and databases. The web servers that often to be used in anticancer in silico study are STITCH (<http://stitch.embl.de/>), Prediction of Activity Spectra for Substances (PASS) online (<http://way2drug.com/PassOnline/>), and SwissADME (<http://www.swissadme.ch/>) [2]. In addition, in silico software-based analyses such as molecular docking and molecular dynamics can

be used to determine the interaction of bioactive compounds against the cancer-related protein.

Red Betel Leaf (*Piper crocatum* Ruiz & Pav) is a medicinal plant that is often used to treat various diseases such as cancer, cough, asthma, nasal inflammation, and sore throat [3]. Empirically, the formulation of *Piper crocatum* leaf extract with other medicinal plants demonstrates the eradication of various diseases, such as inflammation, bleeding, breast cancer, uterine cancer, leukemia, and liver swelling [4].

The chemical content of *Piper Crocatum* leaf plants based on chromatography analysis are flavonoids, polyphenols, alkaloids, tannins, and essential oils [5]. The flavonoid content is included in the class of polyphenols that are distributed in parts of the plant body and have the activities to inhibit tumor cell growth, migration, metastasis, and endothelial activation [6]. *Piper Crocatum* also has cytotoxic activity against 4T1 metastasis of breast cancer cells at IC<sub>50</sub> 120  $\mu$ g/mL and inhibits migration activity at a concentration of 30  $\mu$ g/mL ( $\frac{1}{4}$  of IC<sub>50</sub>) [6]. *Piper crocatum* also inhibited the proliferation of T47D and HeLa, and cytotoxic against colon cancer cells [6].

Several proteins play a significant role in the progression and development of cancer, such as HER2 (human epidermal growth receptor 2), MMP9 (matrix metalloproteinase-9), and TNF $\alpha$  (tumor necrosis factor  $\alpha$ ). The activity of HER2 leads to the

\* Correspondence address:

Ahmed Hasan Abkar

E-mail : hamadah118850@gmail.com

Address : Dept. Biology, University of Brawijaya, Veteran  
Malang, 65145.

initiation of signaling pathways and possession of cell proliferation and tumorigenesis [7]. The MMP9 protein is a well-known protein found to be associated with the pathogenesis of tumors, such as metastasis and angiogenesis [8]. Besides, TNF $\alpha$  is a pro-inflammatory cytokine that is associated with carcinogenesis inflammation [9]. Based on the role of some proteins mentioned above, the inhibition of those proteins is the potential to be the target in cancer therapy.

Previous studies on  $\beta$ -asarone, methyl piperonylketone, and coumaric acid interaction against HER2, MMP9, and TNF $\alpha$  proteins in cancer remain unclear. To address this unclarity, the study aims to determine the potential of  $\beta$ -asarone, methyl piperonylketone, and coumaric acid from *Piper crocatum* as an anticancer agent via the blockade of HER2, MMP9, and TNF $\alpha$  proteins through in silico study.

## METHODS

The study was a qualitative study that used an observational descriptive research design using exploratory research as secondary data since in vitro and in vivo studies cost and time constraints. Thus, this study was a preliminary study and screening method for the prediction of anticancer agents from bioactive compounds of herbal plants.

The anticancer effects of *Piper crocatum* bioactive compounds such as  $\beta$ -asarone, methyl piperonylketone, and coumaric acid were conducted through *In Silico* study. The analysis of this study included biological activity, cell line cytotoxicity activity, SwissADME, STITCH, molecular docking, and molecular dynamics simulation.

## Data Collection

The canonical smile of the compounds used in the analysis of biological activity, cell line cytotoxicity activity, and SwissADME, and the 3D structure of investigated compounds were retrieved from PubChem (<https://pubchem.ncbi.nlm.nih.gov/>). The the canonical smile and compound ID of PubChem retrieval were  $\beta$ -asarone CC=CC1=CC(=C(C=C1)OC)OC (CID\_5281758), p-coumaric acid C1=CC(=CC=C1C=CC(=O)O)O (CID\_637542), and methyl piperonylketone CC(=O)CC1=CC2=C(C=C1)OCO2 (CID\_78407). The

protein 3D structure of TNF $\alpha$  and TNF $\alpha$  receptors (TNFR2), HER2, and MMP9 were obtained from protein data bank PDB (<https://www.rcsb.org/>) with protein ID of PDB retrieval were MMP9 (PDB ID 1gkc), HER2 (PDB ID 1n8z), and TNF $\alpha$  and TNFR2 (PDB ID 3alq).

## Data Analysis

The analysis of the biological activity of investigated bioactive compounds was performed by the PASS web server (<http://way2drug.com/PassOnline/index.php>), and the canonical smile of each bioactive compound was inserted. The parameters Pa as "being active" and Pi as "being inactive" were obtained in this study. The higher the Pa value, the bigger potential of the biological activity of the compound [1]. The study used the cut-off value of Pa value in 0.7. Additionally, the cytotoxic activity was also done in PASS through different weblinks (<http://www.way2drug.com/cell-line/>). It was used to predict the cytotoxic activity of compounds in cancer and normal cell lines. The highest potential of anticancer activity against a specific protein (represented by the highest Pa value) based on PASS analysis was then used for further analysis.

The pharmacological properties of investigated bioactive compounds were analyzed using the SwissADME web server (<http://www.swissadme.ch>) by inserting the canonical smile of each compound. The STITCH analysis was done through a web server (<http://stitch.embl.de/>) by inserting the name of investigated bioactive compounds.

The molecular docking analysis was done to determine the interaction of investigated bioactive compounds against the TNF $\alpha$ , TNFR2, HER2, and MMP9 proteins. Molecular docking was performed by HEX software and visualized using Discovery Studio ver 19.0. The lowest binding affinity of protein-ligand interaction based on molecular docking analysis results was then analyzed further for a molecular dynamics simulation using YASARA software [10].

## RESULT AND DISCUSSION

### Biological Activity Analysis using PASS Online

Based on PASS analysis, coumaric acid showed higher probabilities for the antimutagenic (0.886/0.002), TNF expression inhibitor (0.737/0.005), and MMP9 expression inhibitor (0.818/0.003). Congruently, methyl piperonylketone

also showed biological activity as an MMP9 expression inhibitor (0.745/0.004). Additionally, the  $\beta$ -asarone showed higher probabilities for the TNF expression inhibitor (0.739/0.005) and MMP9 expression inhibitor (0.809/0.003). The prediction of the bioactive compound's biological activity through PASS analysis was shown in Table 1. In line with these results, the flavonoid activity contained in *Piper crocatum* was reported to have the activity of inhibiting cancer cell migration via suppressing MMP-9 expression and FAK phosphorylation [8].

Table 1. Biological activity of coumaric acid, beta asaron, and Methyl piperonyl ketone.

Bioactive compounds	Anticancer Activity	Pa	Pi
4-coumaric acid	Anti-mutagenic	0.886	0.002
	TNF expression inhibitor	0.737	0.005
	MMP9 expression inhibitor	0.818	0.003
Methyl Piperonylketone	MMP9 expression inhibitor	0.745	0.004
	TNF expression inhibitor	0.739	0.005
$\beta$ - Asarone	MMP9 expression inhibitor	0.809	0.003

### Cell Line Cytotoxicity Prediction through CLC-Pred Analysis

A CLC-Pred is a well-known tool in cheminformatics and medicinal chemistry, was used to predict the toxicity of compounds against the cell line type and tissue to the respective tumor type. The maximum number of different cell line predictions were collected and tabulated with the respective cell line and type of cell.

Table 2. CLC-Pred analysis of cell line cytotoxicity prediction

Bioactive compound	Cell line	Tumor type	Pa	Pi
4-Coumaric acid	IGROV-1	Adenocarcinoma	0.628	0.009
Methyl Piperonyl Ketone	Hs 683	Glioma	0.659	0.015
$\beta$ -Asarone	K562	Leukemia	0.484	0.029

The compound of coumaric acid and methyl piperonylketone showed significant cytotoxicity against adenocarcinoma (Pa value = 0.628) and Glioma (Pa value = 0.659). Likewise,  $\beta$ -asarone

cytotoxic against leukemia cells showed a Pa value of 0.484 (Table 2).

### Investigated Bioactive Compound-Protein Interaction Analysis Using STITCH

The STITCH analysis results showed only p-coumaric acid having compound-protein interaction. However, methyl piperonylketone and  $\beta$ -asarone showed no interaction with any protein. Based on the data, there were several proteins involved in the interaction against the p-coumaric acid (Figure 1). The network showed several biological processes in the body that can be summarized and confirmed using the KEGG pathway (Table 3).

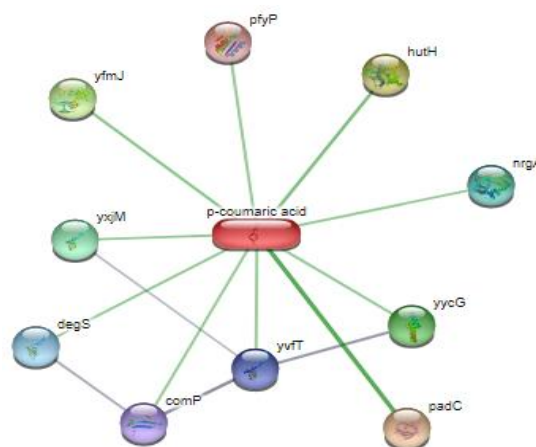


Figure 1. STITCH analysis results of p-coumaric acid-protein interaction

The gene set was involved in several pathways such as peptidyl-histidine phosphorylation, signal transduction by protein phosphorylation, the phosphorelay signal transduction system, single organism signaling, response to stimulus, cell communication, cellular response to stimulus, aromatic compound catabolic process, and two-component systems. One of the pathways associated with cancer was histidine phosphorylation which was reported to be involved in the development of hepatocellular carcinoma [11].

Histidine phosphorylation was also linked to the migration and differentiation of neuroblastoma cells and tumors through the expression of NME1 and NME2 [12]. In addition, protein phosphorylation induced signal transduction that affected several cancer-related processes, including cell apoptosis, proliferation, angiogenesis, metastasis, and several cancer therapies through the phosphorylation of key proteins (p38, MAPK, ERK, PI3K, STAT3, and p53)[13].

Table 3. Protein involvement based on the KEGG pathway

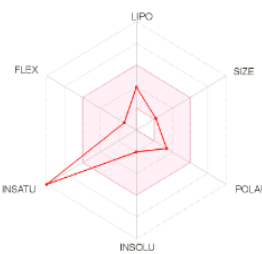
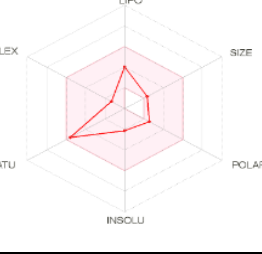
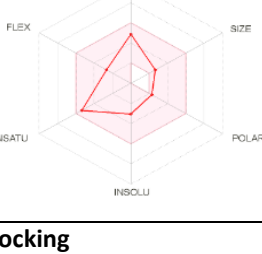
Pathway ID	Pathway Description	Gene set	False discovery rate
0018106	peptidyl-histidine phosphorylation	DEGS, COMP, YVFT, YYCG, YXJM, PFYP	1.18e-07
0023014	signal transduction by protein phosphorylation	DEGS, COMP, YVFT, YYCG, YXJM, PFYP	1.18e-07
0000160	phosphorelay signal transduction system	DEGS, COMP, YVFT, YYCG, YXJM, PFYP	4.1e-06
0044700	single organism signaling	DEGS, COMP, YVFT, YYCG, YXJM, PFYP	7.63e-06
0050896	response to stimulus	DEGS, COMP, YVFT, YYCG, YXJM, PFYP, PADC, YFMJ	2.09e-05
0007154	cell communication	DEGS, COMP, YVFT, YYCG, YXJM, PFYP	0.000103
0051716	cellular response to stimulus	DEGS, COMP, YVFT, YYCG, YXJM, PFYP	0.000519
0019439	the aromatic compound catabolic process	PADC, YFMJ, HUTH	0.022
02020	two-component system	DEGS, COMP, YVFT, YYCG	0.0141

### Pharmacological Property Analysis

The pharmacological property analysis was done using the SwissADME server to determine the ability of adsorbs, distribution, metabolism, and excretion of compounds. In Table 4, the radar image showed by the pink zone was the optimum zone. The optimum characteristics of the compound for oral consumption were as follows:

having a molecular weight of 150-500 g.mol<sup>-1</sup>, a polarity with the TPSA being between 20-130Å<sup>2</sup>, a solubility with a log S not more than 6, flexibility with no more than nine rotatable bonds, and lipophilicity XLOGP3 between -0.7 and +5.0 [14]. Based on the data in Table 4, almost all compounds have good pharmacological properties, except the fairly low saturation of coumaric acid.

**Table 4.** Pharmacological property of SwissADME Analysis

Bioactive compound	Character	Value
<b>4-coumaric acid</b> 	Formula	C9H8O3
	Molecular weight	164.16 g.mol <sup>-1</sup>
	Lipophilicity (XLOGP3)	1.46
	Water solubility (Log S)	-2.27
	Polarity	57.53 Å <sup>2</sup>
	Fraction Csp3	0.00
	GI absorption	High
	Lipinski	Yes; 0 violation
	Synthetic accessibility	1.61
	<b>Methyl piperonylketone</b> 	Formula
Molecular weight		178.18 g.mol <sup>-1</sup>
Lipophilicity (XLOGP3)		1.56
Water solubility (Log S)		-2.14
Polarity		35.53 Å <sup>2</sup>
Fraction Csp3		0.30
GI absorption		High
Lipinski		Yes; 0 violation
Synthetic accessibility		2.02
<b>β-asaron</b> 		Formula
	Molecular weight	208.25 g.mol <sup>-1</sup>
	Lipophilicity (XLOGP3)	3.00
	Water solubility (Log S)	-3.25
	Polarity	27.69 Å <sup>2</sup>
	Fraction Csp3	0.33
	GI absorption	High
	Lipinski	Yes; 0 violation
	Synthetic accessibility	2.39

### Molecular Docking



Based on the molecular docking results, the interaction of investigated bioactive compounds against HER2 protein is shown in Table 5 and Figure 2. The interaction of complex  $\beta$ -asarone and HER2 protein was the strongest compared to other complexes shown by the lowest binding energy (-196.7 cal.mol<sup>-1</sup>) followed by coumaric acid (-180.9 cal.mol<sup>-1</sup>) and methyl piperonylketone (-172.2 cal.mol<sup>-1</sup>). The interaction of  $\beta$ -asarone and HER2 protein demonstrated the higher number of hydrogen bonds via GLU873, GLN902, and GLU964.

$\beta$ -asarone also has the lowest binding energy in the interaction against the MMP9 protein. The binding energy of  $\beta$ -asarone against the MMP9 protein was -216.09 cal.mol<sup>-1</sup> in the form of 3 hydrogen bonds. Additionally, the binding energy of methylpiperonyl ketone and coumaric acid against MMP9 protein interaction was -203.41 and -220.9 cal.mol<sup>-1</sup>, respectively (Table 6, Fig. 3). The complex of  $\beta$ -asarone and MMP9 protein also showed higher hydrogen bonds compared to the other ligand-protein complexes.

**Table 5.** The interaction of complex ligand-HER2 proteins

Complex Ligand-Protein	Interaction	Category	Binding energy (cal.mol <sup>-1</sup> )
$\beta$ -Asarone-HER2	:LIG1:H - B:GLU837:OE1	Hydrogen Bond	-196.7
	:LIG1:H - B:GLN902:OE1	Hydrogen Bond	
	:LIG1:H - B:GLU964:OE2	Hydrogen Bond	
	:LIG1:H - B:GLU964:OE2	Hydrogen Bond	
Methylpiperonyl ketone-HER2	:LIG1:H - A:VAL754:O	Hydrogen Bond	-172.2
	A:THR793:CG2 - :LIG1	Hydrophobic	
	:LIG1 - A:VAL754	Hydrophobic	
p-Coumaric acid-HER2	:UNK1:H19 - A:SER728:O	Hydrogen Bond	-180.9
	A:SER728:CB - :UNK1:O11	Hydrogen Bond	
	A:ARG849:CD - :UNK1:O10	Hydrogen Bond	
	:UNK1 - A:ALA730	Hydrophobic	

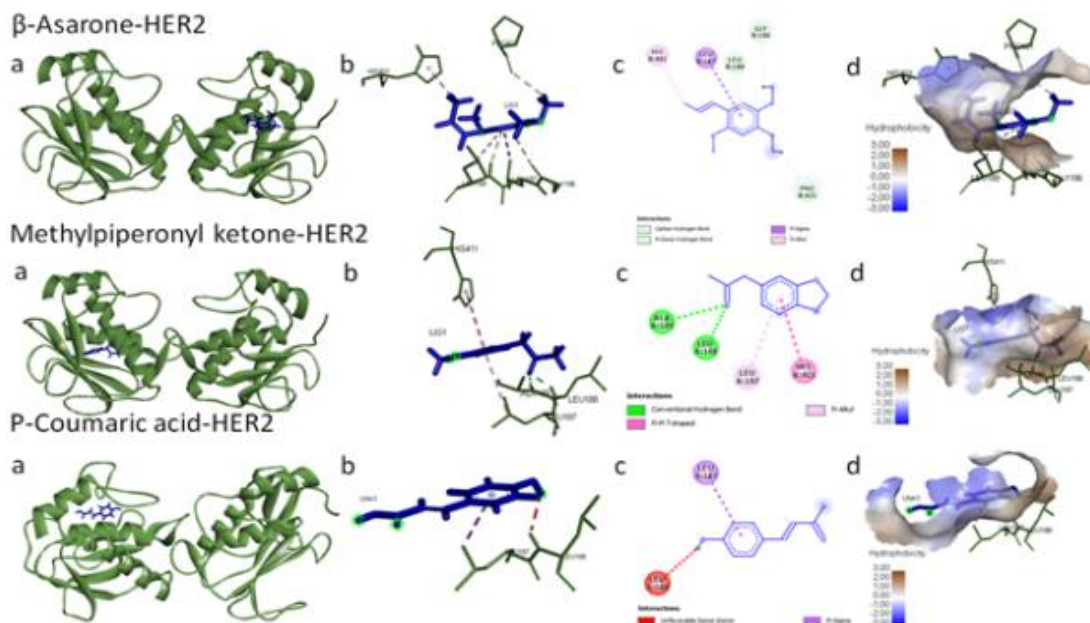


**Figure 2.** Interaction between  $\beta$ -Asarone, Methyl piperonylketone, and P-Coumaric acid on HER2 protein, **a.** overview of the ligand-protein complex, **b.** the active site of ligand-protein complex interactions, **c.** the 2D structure of the ligand-protein complex, **d.** hydrophobicity of the ligand-protein bond complex. The green color is the HER2 protein, the blue color is a compound.

**Table 6.** The interaction of complex ligand-MMP9 proteins

Complex Ligand-Protein	Interaction	Category	Binding energy (cal.mol <sup>-1</sup> )
β-Asarone-MMP9	:LIG1:H - B:GLY186:O	Hydrogen Bond	-216.09
	:LIG1:H - B:PRO421:O	Hydrogen Bond	
	B:LEU188:HN -:LIG1	Hydrogen Bond	
	B:LEU187:CD1 - :LIG1	Hydrophobic	
	B:HIS401 - :LIG1:C	Hydrophobic	
Methylpiperonyl ketone-MMP9	:LIG1 - B:LEU188	Hydrophobic	-203.41
	A:LEU188:HN -:LIG1:O	Hydrogen Bond	
	A:ALA189:HN - :LIG1:O	Hydrogen Bond	
	A:HIS411 - :LIG1	Hydrophobic	
p-Coumaric acid-MMP9	:LIG1 - A:LEU187	Hydrophobic	-220.9
	A:LEU187:CD1 - :UNK1	Hydrophobic	
	A:LEU188:HN - :UNK1:H2O	Unfavorable	

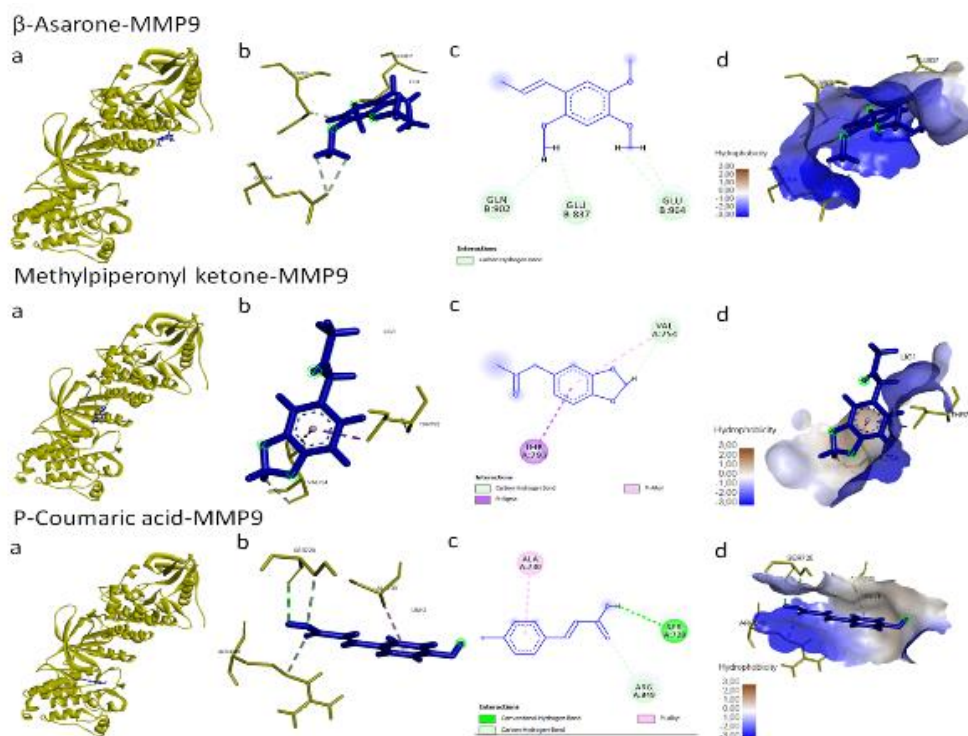


**Figure 3.** Interaction between B-Asarone, Methylpiperonyl ketone, and P-Coumaric acid on the matrix metalloproteinase-9 protein, **a.** overview of the ligand-protein complex, **b.** the active site of ligand-protein complex interactions, **c.** the 2D structure of the ligand-protein complex, **d.** hydrophobicity of the ligand-protein bond complex. The yellow color is the MMP9 protein, the blue color is a compound.

**Table 7.** The interaction of complex ligand-TNFα

Complex Ligand-Protein	Interaction	Category	Binding energy (cal.mol <sup>-1</sup> )
β-Asarone-MMP9	B:GLN102:HN - :LIG1:O	Hydrogen Bond	-192
	:LIG1:H - A:GLU116:OE2	Hydrogen Bond	
	B:PRO100:C,O;CYS101:N - :LIG1	Hydrophobic	
Methylpiperonyl ketone-MMP9	:LIG1:H - A:PRO100:O	Hydrogen Bond	-178.2
	:LIG1:H - B:GLN102:OE1	Hydrogen Bond	
	B:ARG98:NH2 - :LIG1	Hydrogen Bond	
p-Coumaric acid-MMP9	:UNK1:H2O - F:PRO100:O	Hydrogen Bond	-175.7
	F:ARG98:NH2 - :UNK1	Electrostatic	

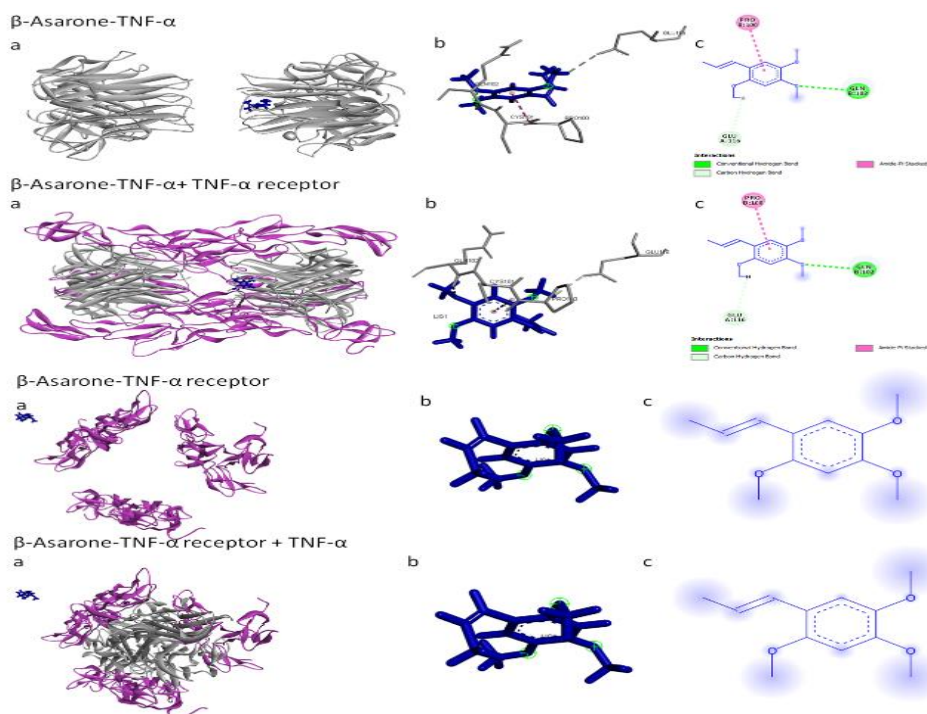


**Figure 4.** Interaction between B-Asarone against TNF- $\alpha$  inhibition and TNF- $\alpha$  receptors, **a.** overview of the ligand-protein complex, **b.** the active site of ligand-protein complex interactions, **c.** the 2D structure of the ligand-protein complex.

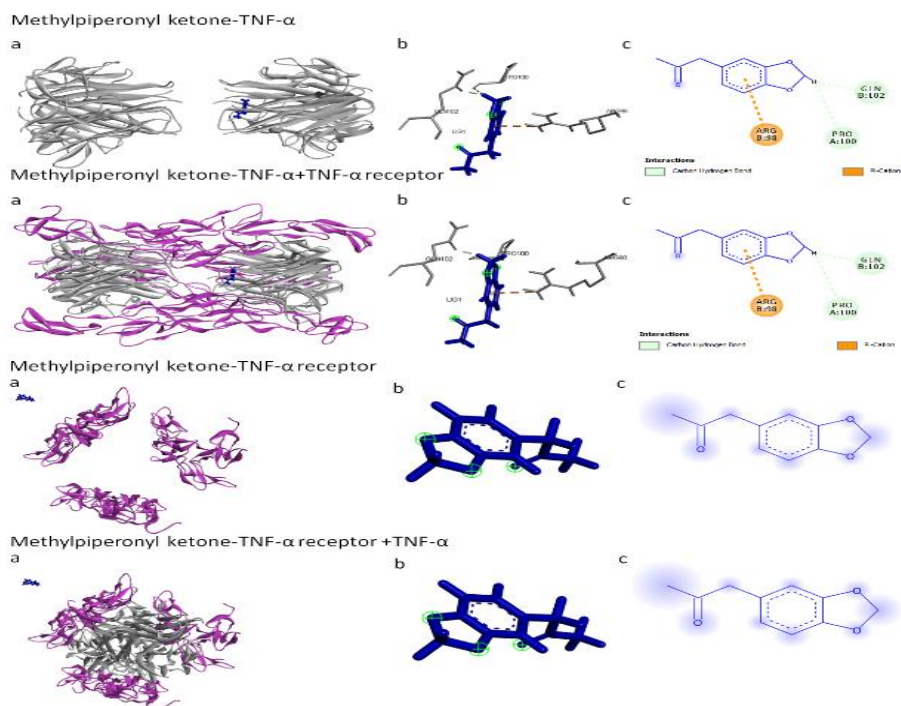


**Figure 5.** Interaction between Methyl piperonylketone against TNF- $\alpha$  inhibition and TNF- $\alpha$  receptors, **a.** overview of the ligand-protein complex, **b.** the active site of ligand-protein complex interactions, **c.** the 2D structure of the ligand-protein complex.

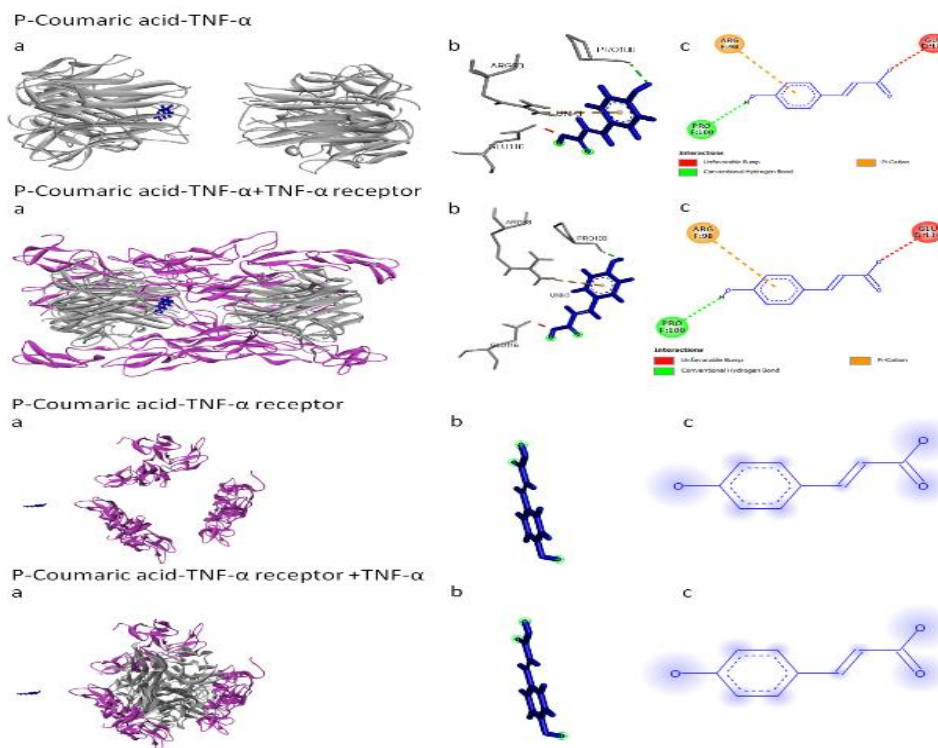


**Figure 6.** Interaction between P-Coumaric acid against TNF- $\alpha$  inhibition and TNF- $\alpha$  receptors, a. overview of the ligand-protein complex, b. the active site of ligand-protein complex interactions, c. the 2D structure of the ligand-protein complex.

Molecular docking analysis showed that  $\beta$ -Asarone can bind to TNF- $\alpha$  at the same residue as TNF- $\alpha$  binds to the TNF- $\alpha$  receptor (Fig. 4). Key residues involved in the interaction of TNF- $\alpha$  and TNF- $\alpha$  receptors include GLN100, GLU116, and PRO100. This study found  $\beta$ -asarone were also able to bind GLN100, GLU116, and PRO100 from TNF- $\alpha$  stabilized by hydrogen bonds and hydrophobic bonds with a binding energy of  $-192 \text{ kcal.mol}^{-1}$  (Table 7) and assumed to have the ability to interfere with the interaction of TNF- $\alpha$  and the receptor. Besides, methyl piperonylketone compound was also predicted to inhibit TNF- $\alpha$  binding to the TNF- $\alpha$  receptor via the involvement of key residues PRO100, GLN102, ARG98 residues of TNF- $\alpha$  (Fig. 5, Table 7).

The interaction of TNF- $\alpha$  and methyl piperonylketone was formed by hydrogen and electrostatic forces with a binding energy of  $-178.2 \text{ cal.mol}^{-1}$ . The results of the molecular docking showed that this compound was unable to interact with the TNF- $\alpha$  receptor. The compound of p-coumaric acid can inhibit TNF- $\alpha$  binding to the TNF- $\alpha$  receptor shown by the binding of coumaric acid to the PRO100 and ARG98 key residues of TNF- $\alpha$

(Fig. 6, Table 7). The interaction of TNF- $\alpha$  and coumaric acid was formed by hydrogen bonds and electrostatic forces with a binding energy of  $-175.7 \text{ cal.mol}^{-1}$ .

The hydrogen bonds formed between ligands and proteins are crucial for the interactions because hydrogen bonds hugely contribute to the structure of the bonds, which can increase the stability of the interaction [8]. The molecular docking analysis showed the strongest and most stable interaction among the three bioactive compounds was  $\beta$ -asarone against each protein. This interaction was also predicted to potentially inhibit the protein target, including HER2, MMP9, and TNFa, via the involvement of key amino acid residues. Furthermore, the interaction of  $\beta$ -asarone against each protein was confirmed and further analyzed using a molecular dynamics simulation.

Based on the molecular docking analysis and supporting data from the previous studies, the possible mechanisms of the action from the bioactive compound that may occur were presented in Figure 7. Under normal conditions, cells can grow, move and invade cells through two pathways, namely the TNFa/TNFR2 and HER2



pathways. In the TNF $\alpha$ /TNFR2 pathway, proinflammatory cytokines such as TNF $\alpha$  bind to TNFR2 and indirectly activate NF $\kappa$ B. Likewise, the active HER2 will induce AKT phosphorylation and NF $\kappa$ B activation. The active NF $\kappa$ B will stimulate the expression of the NTN1 gene that encodes the NETRIN1 protein. The NETRIN1 protein causes invasive cells. On the other hand, the HER2 protein also activates FAK and Src, both of which activate the JNK protein for phosphorylation and induce MMP9 activity for cell motility and development. The presence of *Piper Crocatum* bioactive compounds inhibits TNF $\alpha$ , HER2, and MMP9, causing motility and invasiveness, preventing cell development from occurring.

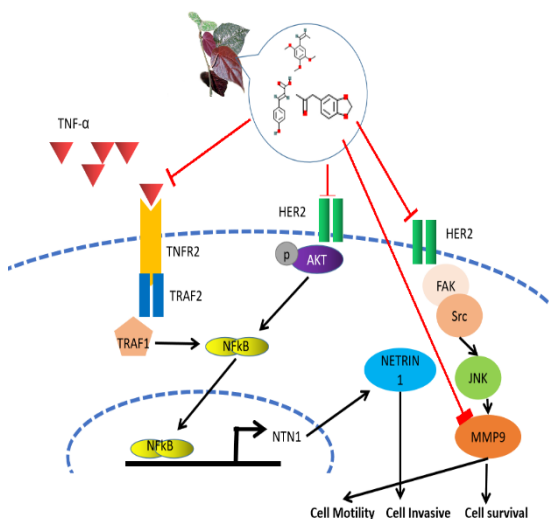


**Figure 7.** Mechanism of *Piper crocatum* Ruiz & Pav bioactive compounds as anticancer through inhibition of the TNF $\alpha$ /TNFR2, HER2, and MMP9 pathways. The mechanism pathway is based on Wang *et al* [15] and Rossi *et al* [16].

### Molecular Dynamics

The molecular dynamic study was done to analyze the complex of  $\beta$ -asarone, as the most potential of bioactive compounds in inhibiting each target protein that showed by the lowest binding affinity in molecular docking results. The Root Mean Square Deviation (RMSD) value of complex protein-ligand is shown in Figure 8.

RMSD was the average displacement of atoms during a simulation towards their corresponding structure. The RMSD value was used to determine whether the structure was stable over a certain period from the simulation of changes [17]. RMSD

was a calculation of the average distance between the backbone atoms of a protein superimpose [18]. A good RMSD value was 3 Å range or below. However, when the RMSD value reaches 3 Å or exceeds 3 Å, it indicates that the protein structure has changed [17].

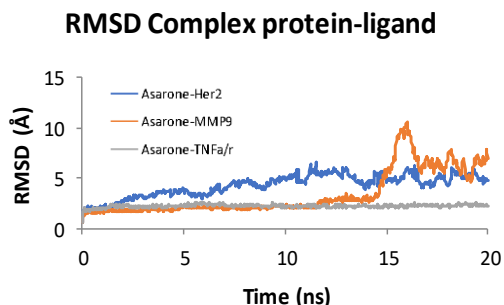


**Figure 8.** The simulation results of molecular dynamics of RMSD Complex protein-ligand

Based on the molecular dynamics data results, there were three charts on the graph, such as green ( $\beta$ -asarone and TNF), orange ( $\beta$ -asarone and MMP9), and blue ( $\beta$ -asarone and HER2) (Fig. 8). The study found that the most stable interaction of complex protein-ligand was  $\beta$ -asarone and TNF, which was shown by a flat graph with an RMSD value of under 4Å [19] compared to a higher RMSD value and fluctuating chart of  $\beta$ -asarone against MMP9 and HER2.  $\beta$ -asarone and MMP9 were initially formed stable molecules until the 15ns. It was assumed there was a change in the position of the ligand-protein complex. A change in position can be caused by the release of the ligand from the protein or by its movement.

To support the result of complex protein-ligand RMSD, the molecular dynamics analysis also showed the RMSD ligand movement, as shown in Figure 9. RMSD ligand movement was used to see how the ligand moves when it interacted with proteins. The study found that the ligand movement in the complex of  $\beta$ -asarone with TNF and MMP9 protein were stable compared to the HER2 protein. The instability of  $\beta$ -asarone against HER2 protein showed by a high RMSD ligand value that indicates instability of the ligand in the structure so that the ligand will continue to move [17]. RMSD ligands demonstrate the translational and rotational movement of ligands and characterize the binding or dissociation process [18]. Based on this information, it was concluded

that  $\beta$ -asarone has an unstable interaction (or even can be detached from its interaction) with the HER2 protein. However, the ligand conformation of  $\beta$ -asarone appeared stable when interacting with MMP9, HER2, and TNFa/r showed by all the RMSD ligand conformation value were 1-2 Å.

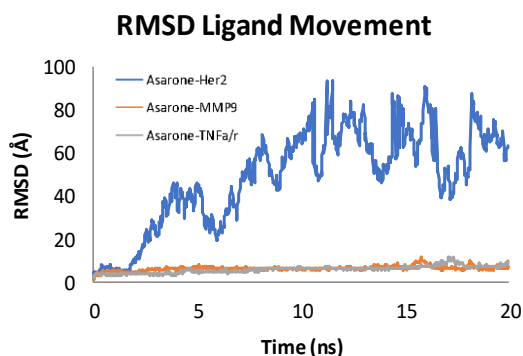


Figure 9. Results of molecular dynamics simulation results of RMSD Ligand movement

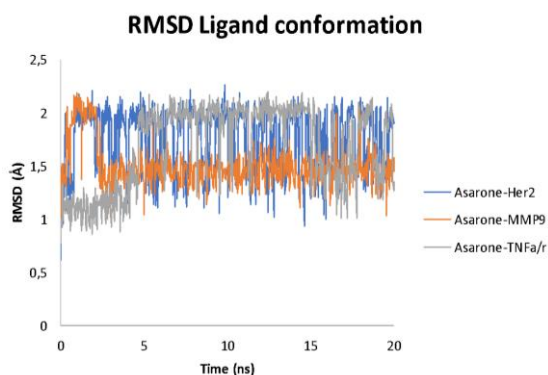


Figure 10. Results of molecular dynamics simulation results of RMSD Ligand

The stability of ligand-protein is demonstrated by the distance between the ligand-protein. This study found that  $\beta$ -asarone interaction against MMP9 and TNF protein was stable, at least until 14ns for MMP9 (Fig. 8). These results were confirmed by the RMSD value of ligand movement that showed the stable movement of  $\beta$ -asarone against MMP9 and TNF interaction (Fig. 9). In addition, the ligand conformation against all target proteins were demonstrating a 1-2 Å RMSD value showing a stable conformation of the ligand.

We demonstrate that the best interaction of  $\beta$ -asarone based on molecular dynamic analysis against target protein were the complex of  $\beta$ -asarone with MMP9 and TNFa, showed by the stable ligand-protein complex, ligand movement,

and ligand conformation. The interaction of  $\beta$ -asarone and HER2 may also potential but these complex remain unstable in the condition of living systems as a study of molecular dynamic.

## CONCLUSION

The results showed the biological activities of coumaric acid, methyl piperonylketone, and  $\beta$ -asarone were anti-mutagenic, TNF expression inhibitor, and MMP 9 expression inhibitor. The study also found the investigated bioactive compounds were cytotoxic on various tumor cells, including glioma, adenocarcinoma, and leukemia. Based on swissADME results, almost all compounds have optimum pharmacological properties, such as molecular weight, polarity, solubility, flexibility, and lipophilicity, except for coumaric acid, which has a fairly low saturation. Based on the docking analysis result, the investigated bioactive compounds inhibit TNFa, HER2, and MMP9 causing motility, invasiveness, and tumor cell development to not occur.

Based on these findings, it can be concluded that the methyl piperonylketone,  $\beta$ -asarone, and coumaric acid in *Piper crocatum* have the potential to be anticancer. The molecular dynamics of  $\beta$ -asarone and the protein target interaction showed that the TNF a/r protein was stable when interacting with the  $\beta$ -asarone ligand. The RMSD ligand movement showed that  $\beta$ -asarone ligand conformation appeared stable when interacting with MMP9, HER-2, and TNFa/r because the RMSD value was seen from the minimum fluctuation of the RMSD ligand conformation value and did not exceed 3 Å. In addition, this in silico study still needs further research to confirm this finding using in vitro or in vivo study to the respective cancer type.

## REFERENCES

- [1] Lagunin, A.A., V.I. Dubovskaja, A.V. Rudik, P.V. Pogodin, D.S. Druzhilovskiy, T.A. Glorizova, D.A. Filimonov, N.G. Sastry, V.V. Poroikov. 2018. CLC-Pred: a freely available web service for in silico prediction of human cell line cytotoxicity for drug-like compounds. *PLoS one*. 13(1). p.e0191838.
- [2] Nafisah, W., H.N. Pinanti, Y.I. Christina, M. Rifa'i, M.S. Djati. 2021. Computational biological activity and pharmacological properties analysis for anticancer Cyperus

- rotundus bioactive compounds. AIP Conference Proceedings 2353(1). 030118. AIP Publishing LLC.
- [3] Haryadi, R.B. 2010. Daya antibakteri ekstrak daun sirih (*Piper betle*) dan daun sirih merah (*Piper crocatum*) terhadap pertumbuhan bakteri *Staphylococcus aureus* secara *In Vitro* sebagai materi praktikum mikrobiologi. Master Thesis. Postgraduate Program, State University of Malang.
- [4] Mangesa, R., I. Irsan. 2020. Efektifitas fraksi aktif methanol daun sirih merah (*Piper crocatum*) yang berpotensi sebagai antibakteri *Salmonellas typhi*: (the effectiveness of methanol active fraction of red better leaves [*Piper crocatum*] that potential as an antibacterial *Salmonellas typhi*). *Uniqbu Journal of Exact Sciences*. 1(2). 40-45.
- [5] Juliantina, R.F., M.D.A., Citra, B. Nirwani, T. Nurmasitoh, E.T. Bowo, 2009. Manfaat sirih merah sebagai agen antibakterial terhadap bakteri gram positif dan gram negatif. *Jurnal Kedokteran dan Kesehatan Indonesia*. 1(1). 12-20.
- [6] Zulharini, M., Sutejo, I.R., Fadliyah, H. and Jenie, R.I., 2018. Methanolic extract of red betel leaves (*Piper crocatum* Ruiz & Pav) performs the cytotoxic effect and antimigration activity toward metastatic breast cancer. *Indones. J. Cancer Chemoprevention*. 8(3). 94-100.
- [7] Iqbal, N., N. Iqbal. 2014. Human epidermal growth factor receptor 2 (HER2) in cancers: overexpression and therapeutic implications. *Mol. Biol. Int*. 852748.
- [8] Huang, H. 2018. Matrix metalloproteinase-9 (MMP-9) as a cancer biomarker and MMP-9 biosensors: recent advances. *Sensors*. 18(10). p.3249.
- [9] Wang, X., Y. Lin, 2008. Tumor necrosis factor and cancer, buddies or foes? *Acta Pharmacol. Sin*. 29(11). 1275-1288.
- [10] Krieger, E., G. Vriend. 2015. New ways to boost molecular dynamics simulations. *J. Comput. Chem*. 36(13). 996-1007.
- [11] Masuda, M. 2019. Hunting hidden pieces of signaling pathways in hepatocellular carcinoma. *Hepatobiliary Surg. Nutr*. 8(1). 74.
- [12] Adam, K., J. Lesperance, T. Hunter, P.E. Zage. 2020. The potential functional roles of NME1 histidine kinase activity in neuroblastoma pathogenesis. *Int. J. Mol. Sci*. 21(9). 3319.
- [13] Liu, X., Y. Zhang, Y. Wang, M. Yang, F. Hong, S. Yang. 2021. Protein phosphorylation in cancer: role of nitric oxide signaling pathway. *Biomolecules*. 11(7). 1009.
- [14] Daina, A., O. Michielin, V. Zoete. 2017. SwissADME: a free web tool to evaluate pharmacokinetics, drug-likeness, and medicinal chemistry friendliness of small molecules. *Sci. Rep*. 7(1). 1-13.
- [15] Bare, Y., D.R.T. Sari, Y.T. Rachmad, G.C. Krisnamurti, A. Elizabeth, A. Maulidi. 2019. In silico insight the prediction of chlorogenic acid in coffee through Cyclooxygenase-2 (COX2) Interaction. *Biogenesis: Jurnal Ilmiah Biologi*. 7(2). 100-105.
- [16] Wang, L., X. Zhi, Y. Zhu, Q. Zhang, W. Wang, Z. Li, J. Tang, J. Wang, S. Wei, B. Li, J. Zhou. 2015. MUC4-promoted neural invasion is mediated by the axon guidance factor Netrin-1 in PDAC. *Oncotarget*. 6(32). 33805.
- [17] Rossi, A.F.T., J.C. Contiero, F. da Silva Manoel-Caetano, F.E. Severino, A.E. Silva. 2019. Up-regulation of tumor necrosis factor- $\alpha$  pathway survival genes and the receptor TNFR2 in gastric cancer. *World J. Gastrointest. Oncol*. 11(4). 281.
- [18] Fusani, L., D.S. Palmer, D.O. Somers, I.D. Wall, 2020. Exploring ligand stability in protein crystal structures using binding pose metadynamics. *J. Chem. Inf. Model*. 60(3), 1528-1539.
- [19] Wibowo, S., S. Widyarti, A. Sabarudin, D.W. Soeatmadji, S.B. Sumitro, 2019. The role of astaxanthin compared with metformin in preventing glycosylated human serum albumin from possible unfolding: a molecular dynamic study. *Asian J. Pharmaceut. Clin. Res*. 12(9). 276-282.



## Screening of Potential Biosurfactant Producing Bacteria from Tanjung Perak Port, Surabaya

Marlinda Elvina Susanti<sup>1\*</sup>, Maftuch<sup>2</sup>, Asep Awaludin Prihanto<sup>2</sup>

<sup>1</sup>Master Program of Aquaculture, Faculty of Fisheries and Marine Sciences, University of Brawijaya, Malang, Indonesia

<sup>2</sup>Faculty of Fisheries and Marine Sciences, University of Brawijaya, Malang, Indonesia

### Abstract

Bacteria are bioremediation agents that are advised to overcome water pollution. This study aims to isolate biosurfactant-producing bacteria for bioremediation from Tanjung Perak Port, Surabaya. The isolates grown in specific media were tested for drop collapse, oil spreading test, and emulsification index. A total of 12 bacterial isolates were isolated from Tanjung Perak seawater contaminated with diesel oil. In the drop collapse test, four isolates had the highest positive score from this test, isolate LU-5, LU-7, LU-9, and LU-11. While in the second test, the oil spreading test, the highest positive score results were obtained in three isolates, isolates LU-2, LU-7, and LU-11. The emulsification index (E24) value showed that isolates LU-7, LU-9, and LU-11 were significantly higher than the others, which was above 10%. This study concludes that in Tanjung Perak, seawater-contaminated oil isolated several bacteria that produce biosurfactants, which have the potential to be developed as bioremediation agents.

**Keywords:** bacteria, bioremediation, biosurfactant, diesel oil

### INTRODUCTION

Water pollution is a crucial environmental issue that continues to occur, especially in marine waters. The primary source of marine contamination is derived from oil spills both from offshore drilling processes and from activities by ships that cross the ocean [1]. A site that gets an opportunity of an oil spill is the port. Tanjung Perak is the second most significant and active port in Indonesia after Tanjung Priok. To this day, Tanjung Perak is a port used as a trading center in eastern Indonesia. Bunkering activities in the port area or refueling diesel oil when ships are more frequently contributing waste oil spills. This activity can harm life resources, disrupt marine activities, including fishing, marine culture, and decrease seawater quality, up to human health problems [2].

There are different approaches to reduce the impact of oil contamination physically, chemically, and biologically. Biological treatment of oil spills in bioremediation techniques is the most effective and economical way. As well as having a small environmental effect, this method can significantly reduce the oil spills impacts [3]. Bioremediation works by decomposing or reducing toxic organic and inorganic waste in the environment into other harmless compounds. A SWOT analysis for bioremediation technologies

showed that the bioremediation agents are predominantly bacteria (57%), enzymes (19%), fungi (13%), algae (6%), plants (4%), and protozoa [4]. Indigenous bacteria as a bioremediation agent are advised. Bacteria are one type of microorganism with a very high abundance in nature, both in terms of number and type. Bacteria that can degrade compounds contained in petroleum hydrocarbons are called hydrocarbonoclastic bacteria.

Biosurfactants are surfactants produced by microorganisms, especially bacteria. Currently, this active compound has gained significant attention as an emulsifier and oil recovery agent. It is because biosurfactants have high efficiency and selectivity. Biosurfactants can work in extreme conditions (salinity, pH, and temperature) with high biodegradability and low toxicity [5]. Several types of bacteria can produce surfactants that allow them to degrade or alter insoluble organic compounds, one of which is diesel oil. In addition, biosurfactants can increase surface area and oil solubility. Therefore, this study will discuss the potential of bacteria indigenous from the Tanjung Perak Port in producing biosurfactants by several screening methods.

### MATERIAL AND METHOD

#### Samples Collection

Water samples were collected from the port of Tanjung Perak Surabaya, 7°19'97,60' south latitude and 112°73'18,42' east longitude (Fig. 1). The sampling method in this study used the purposive sampling method. A sample of 1000 mL of seawater was taken from the port of

\*Correspondence address:

Marlinda Elvina Susanti

Email : marlindaelvina@gmail.com

Address : Faculty of Fisheries and Marine Sciences,  
University of Brawijaya, Veteran Malang, 65145.

Tanjung Perak, Surabaya. The sampling site was in an area that had experienced an oil spill. In-site water quality measurements are carried out directly at the location. Water temperature and pH were measured by a pH meter (Lutron PH-220). Other water quality parameters measured in the laboratory include salinity with a salinometer and oil content (APHA.5220 B-2017). The water sample was then placed in sterilized bottles and stored in an icebox at 4°C. It was stored for around 2 hours until arriving at the laboratory for further analysis.

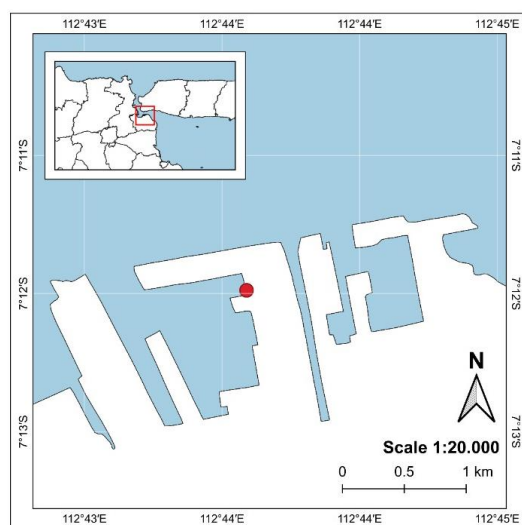


Figure 1. Sampling Location at Tanjung Perak Port

### Isolation of Bacteria

The pure water samples were homogenized using a water bath incubator shaker (Memmert wnb 22, Germany) at 30°C for 1 hour, 170 rpm speed shaker. Then, one ml of the sample was transferred to a tube containing 9 ml of 0.85% NaCl, followed by serial dilutions up to 10<sup>-5</sup>. Next, the isolation was carried out using the spread plate method, and 0.1 mL of water sample from 10<sup>-5</sup> dilutions were cultured in Nutrient Agar (NA) medium + 1% diesel oil (as an additional carbon source) and incubated for 24-48 hours at 30°C [6].

### Morphological Characterization of Bacteria Colony

After incubation, different bacterial colonies that appeared on the agar surface were taken and transferred for characterization. The morphological characterization of bacterial colonies was carried out macroscopically and microscopically. Macroscopic observations mark the shape, color (pigmentation), elevation, and margins in this study. While the microscopic

characterization was carried out by Gram staining using a microscope with a magnification of 400x. This physical characterization was determined based on Harley-Prescott [7]. The selected colonies were purified into NA medium using the streak plate method. The pure isolates were stored in slanted agar and Nutrient Broth (NB) medium with glycerol, then stored in a refrigerator at 4°C for further analysis.

### Screening of Biosurfactant-Producing Isolates

#### Drop collapse test

All of the screening tests in this study used Nutrient Broth as a medium. The drop collapse test was performed by dripping two microliters of diesel oil onto a parafilm surface followed by five microliters drops of 24 h culture supernatants of each isolate. After 1 minute of observation, the supernatant made the oil drop collapse and will be flat if it contains biosurfactants [8]. It scored as positive results. On the other hand, if the droplets remain spherical, the isolate was scored as negative results. These results can be compared with distilled water as a control.

#### Oil spreading assay

The oil spreading test was performed by pouring 50 ml of distilled water into a petri dish (9 cm diameter). Later, 50 µL of diesel oil was dropped onto the surface of the water. The 24 h culture supernatant (10 µL) of each isolate was then added to the diesel oil surface. The clear zone was observed if the biosurfactant was present, and, subsequently, the diameter of the clear area was measured after 30 s [8].

#### Emulsification index (E<sub>24</sub>)

The emulsification test is used to determine the ability of biosurfactants to emulsify liquids of different polarities. The 24 h culture supernatant incubated at 30°C of each isolate was mixed with diesel oil. The test was used a test tube (16 mm diameter, 100 mm high) in a 1:1 ratio (1.5 mL supernatant mixed with 1.5 mL diesel oil). The mixture was vortexed at high speed for 2 minutes and then left for 24 hours to form a stable emulsion. Emulsification test results are expressed as the emulsification index [9]. The percentage of emulsification index was calculated following the formula.

$$E_{24}(\%) = \frac{HE}{HT} \times 100$$

#### Description:

HE : the height of emulsion layer (cm)

HT : total height of liquid column (cm)

### Statistical Analysis

All emulsification indexes were performed in duplicate. Ms. Excel version 2008 was used for statistical analysis. Data presented are mean value  $\pm$  standard deviation.

## RESULT AND DISCUSSION

### Physicochemical Properties of Water Sample

Water samples were collected from the Tanjung Perak port area that contaminated diesel oil. In addition to seawater sampling, physical and chemical parameters were measured. The physicochemical properties of the water analyzed from the sample will affect the results of the isolated microorganisms. The results of the analysis are shown in Table 1.

Table 1. Water Quality Analysis

No.	Parameter	Result	Unit
1	Temperature	31.4	°C
2	pH	6.58	-
3	Salinity	26.2	ppt
4	Oil Content	2.0	mg.L <sup>-1</sup>

Temperature can affect the rate of biochemical reactions. The reaction rate will double for every 10°C increase in temperature. At a temperature of 31.4°C, the bacteria that grow well are mesophilic. The results of the salinity measurement of 26.2 ppt indicate that the location is brackish waters. With this salinity, bacteria that can live are a group of halophilic bacteria [10].

According to the Government Regulation (PP) Number 22, in the year 2021, the detected oil concentration still fulfills the standard of port water quality. However, these are not suitable for marine biota that lives in this area [11]. The concentration of oil that pollutes the waters will also affect the number of isolates found. Hydrocarbonoclastic bacteria in their life activities require carbon molecules as a source of

nutrition and energy to metabolize and reproduce [12]. These bacteria can degrade oil waste by using existing carbon as a source of energy and nutrients for growth.

### Isolation and Morphology Characterization of Bacteria

Twelve pure isolates were obtained from the isolation process. The results of the morphological characterization are visualized in Table 2. Based on the morphological characteristics process, from the 12 isolates, the average colony was irregular. Several isolates were circular in shape, and one isolate was punctiform. Most of the colors of the colonies were cream, while only three colonies were white. The elevation of the 12 isolates was dominated by prominent convex colonies. Only some colonies had raised elevations. Characteristics based on margin indicate entire and undulate. Meanwhile, the Gram staining results showed that 66.7% of the isolates were gram-negative bacteria, and 83.3% were rods. Similar to another study reported that gram-negative bacteria isolated from water contaminated with diesel oil is more than the gram-positive bacteria [6].

Several studies report the results of bacteria that have been isolated from waters affected by oil spills, and there are *Vibrio alginolyticus* [13], *Bacillus cereus* [14], *Alcanivorax nanhaiticus* and *Halomonas meridiana* [15], *Aeromonas hydrophila*, *Enterobacter agglomerans*, *Shewanella putrefaciens*, and *Acinetobacter haemolyticus* [3]. In addition, biosurfactants are secondary metabolite products from bacteria that can increase hydrocarbons emulsification and help facilitate the degradation process. In this study, all identified isolates were evaluated for their ability to produce biosurfactants.

Table 2 . Morphology of Colony Characterization

Isolates Code	Macroscopic				Microscopic	
	Form	Colour	Elevation	Margin	Gram	Shape
LU-1	Punctiform	Cream	Raised	Undulate	Positive	Cocci
LU-2	Irregular	Cream	Convex	Undulate	Positive	Rods
LU-3	Circular	Cream	Convex	Entire	Positive	Rods
LU-4	Circular	Cream	Raised	Entire	Negative	Rods
LU-5	Circular	White	Convex	Entire	Negative	Rods
LU-6	Irregular	Cream	Convex	Entire	Negative	Rods
LU-7	Irregular	Cream	Convex	Undulate	Negative	Rods
LU-8	Irregular	White	Raised	Undulate	Negative	Rods
LU-9	Circular	Cream	Convex	Entire	Negative	Rods
LU-10	Irregular	White	Raised	Undulate	Negative	Cocci
LU-11	Irregular	White	Convex	Undulate	Negative	Rods
LU-12	Irregular	White	Convex	Undulate	Positive	Rods

### Biosurfactant-Producing Bacteria Screening

The results of this study confirm that the oil-contaminated area is a potential place to obtain biosurfactant-producing microorganisms. Twelve isolates with different morphologies are able to produce biosurfactants with varying ability levels (Table 3).

**Table 3.** Screening of Biosurfactant Producing Bacteria

Isolate Code	Screening Biosurfactant	
	Drop Collapse Test	Oil Spreading Test (mm)
Control	-	-
LU-1	+	++
LU-2	+	++++
LU-3	+	+++
LU-4	+	+++
LU-5	++	+++
LU-6	+	+++
LU-7	++	++++
LU-8	+	++
LU-9	++	+++
LU-10	+	+++
LU-11	++	++++
LU-12	+	+

\*Drop collapse test (DCT) [24] :

(-) completely spherical, (+) slightly flat, and (++) flat.

\*\*Oil spreading test (OST) based on the diameter of the clear zone : (-) no diameter, (+) diameter ≤ 10 mm, (++) diameter 10-30 mm, (+++) diameter 30-50 mm and (++++) diameter ≥ 50 mm.

#### Drop collapse test

The biosurfactant test using the drop collapse method is based on the destabilization of the bacterial supernatant droplets containing the biosurfactant [16]. If the droplets are round and stable, the polar water molecules will attract the water surface of the hydrophobic surface of the oil [17]. The results of the drop collapse test in this study showed that none of the isolates produced round and stable droplets as in the control. So, it was revealed that the 12 isolates were able to produce biosurfactants. Of all isolates producing biosurfactants, LU-5, LU-7, LU-9, and LU-11 showed the highest positive score with flat drops. The droplet is flat because the interfacial tension between the sample and the oil decreases.

#### Oil spreading test

The oil spreading test is a fast, easy and sensitive method used to detect biosurfactant activity. The results of oil spreading showed that the 12 bacterial isolates dripped onto a layer of oil and water could form a clear zone. The

diameter of the clear zone indicates the activity of surfactants, which is also known as oil displacement [18]. In contrast to the control, which did not form a clear area. It was due to the absence of the addition of bacterial isolates to the test medium so that there was no bacterial activity to utilize carbon sources in producing biosurfactants [19].

The diameter of the clear zone diameter formed in isolates LU-2, LU-7, and LU-11 was greater than 50 mm. The diameter of the clear zone of the three isolates was more significant than that of the other isolates. Thus, this indicates the presence of a higher concentration of biosurfactant. Oil spreading test results were in corroboration with drop collapse test results. Strains found with positive drop collapse results were positive for the oil spreading test also. These two methods are recommended for testing biosurfactant production [20].

#### Emulsification index (E<sub>24</sub>)

The emulsification assay technique as the quantitative method can be used for screening of the biosurfactant producers. This method is the most promising one because they are more reliable and accurate to confirm the presence of biosurfactant [21]. The emulsification ability of the biosurfactants produced by the 12 bacterial isolates was determined based on the measurement of the emulsification index (E<sub>24</sub>). The results showed that all isolates had different emulsification index values (Fig 2).

The highest E<sub>24</sub> value was produced by isolating LU-7 and LU-11 with the same percentage of 14.81%. The LU-9 isolate also had a relatively high E<sub>24</sub> value of 12.96%. Based on the characteristic isolates LU-7, LU-9, and LU-11 were gram-negative bacteria. Similar to another study, the gram-negative bacteria have a high emulsification capacity. Gram-negative bacterium O15 isolated from seawater produced 65% of the highest emulsification and demonstrated biosurfactant production in the other biosurfactant screening method [22].

Thus, from this test, three isolates were obtained, which could be considered potential biosurfactant producers. Isolates with better emulsification value show the ability to utilize oil more effectively. It is related to the mechanism of biosurfactants in increasing oil degradation. It increases the bioavailability of the substrate through emulsification [23].

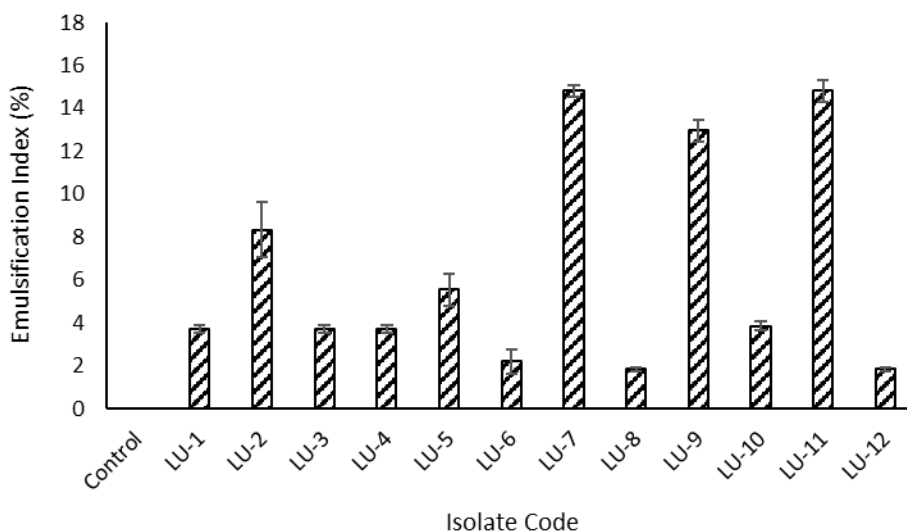


Fig 2. Emulsification Index ( $E_{24}$ ). Error bars indicate standard deviation

## CONCLUSION

Indigenous bacteria that produce biosurfactants are found quite a lot in the waters of the Tanjung Perak Port. A total of 12 isolates were found, and all of them can produce biosurfactants with different abilities. The screening results found that the three best isolates were LU-7, LU-9, and LU-11 isolates. The discovery of biosurfactant-producing bacteria indicates that in this area can be found biosurfactant-producing bacteria that have the potential as bioremediator. However, further research is needed to identify these potential bacteria and determine their ability to degrade the oil.

## REFERENCES

- [1] Sulistyono. 2013. Dampak tumpahan minyak (oil spill) di perairan laut pada kegiatan industri migas dan metode penanggulangannya. *Forum Teknologi*. 3(1). 49–57.
- [2] Beiras, R. 2018. Basic concepts : Sources, fate and effects of pollutants in coastal ecosystems. *Mar. Pollut*. 147. 1–11.
- [3] Yeti, D., N.F. Afianti. 2017. Penerapan dan tingkat efektivitas teknik bioremediasi untuk perairan pantai tercemar minyak. *OSEANA*. XLII. 55–69.
- [4] Quintella, C. M., A.M.T. Mata, L.C.P. Lima. 2019. Overview of bioremediation with technology assessment and emphasis on fungal bioremediation of oil contaminated soils. *J. Environ. Manage*. 241. 156–166.
- [5] Ismail, A. S., H.S. El-Sheshtawy, N.M. Khalil, 2019. Bioremediation process of oil spill using fatty-lignocellulose sawdust and its enhancement effect. *Egypt. J. Pet*. 28(2). 205–211.
- [6] Pranowo, P.P., H.S. Titah. 2016. Isolation and screening of diesel-degrading bacteria from the diesel contaminated seawater at Kenjeran Beach, Surabaya. *EnvironmentAsia*. 9(2). 165–169.
- [7] Harley, J.P., L.M. Prescott. 2002. Laboratory Exercise in Microbiology 5th edition. McGraw-Hill. New York.
- [8] Almansoor, A. F., M. Idris, S. Abdullah, N. Anuar. 2014. Screening for potential biosurfactant producing bacteria from hydrocarbon-degrading isolates. *Adv. Environ. Biol*. 8(3). 639-647.
- [9] Mouafo, T.H., A. Mbawala, R. Ndjouenkeu. 2018. Effect of different carbon sources on biosurfactants' production by three strains of *Lactobacillus* spp. *BioMed Research International*. 2018(1). 1-15.
- [10] Lubis, S.S. 2015. Penapisan bakteri laut penghasil antimikroba dari Pesisir Serdang Bedagai Sumatera Utara. *J. Islam. Sci. Technol*. 1(1). 87–96.
- [11] Republic of Indonesia. 2021. Government Regulation No. 22 about Implementation of Environmental Protection and Management: Seawater Quality Standards. Republic of Indonesia. Jakarta.
- [12] Rahayu, Y.S., Yuliani, G. Trimulyono. 2019. Isolation and identification of hydrocarbon degradation bacteria and phosphate solubilizing bacteria in oil contaminated soil

- in Bojonegoro, East Java, Indonesia. *Indonesian J. Sci. Technol.* 4(1). 134–147.
- [13] Imron, M.F., S.B. Kurniawan, H.S. Titah. 2019. Environmental technology and innovation potential of bacteria isolated from diesel-contaminated seawater in diesel biodegradation. *Environ. Technol. Innov.* 14. 2–10.
- [14] Ramadhani, A., T. Wahyuni, E.Y. Herawati, A. Kurniawan, A.A. Amin. 2019. Isolation, and identification of diesel oil degrading bacteria in water contamination site and preliminary analysis with potential bacterial *Gordonia terrae*. *Res. J. Life Sci.* 6(2). 141–149.
- [15] Puspitasari, I., A. Trianto, J. Suprijanto. 2020. Eksplorasi bakteri pendegradasi minyak dari perairan Pelabuhan Tanjung Mas, Semarang. *J. Mar. Res.* 9(3). 281–288.
- [16] Ewida, A.Y.I., W.S. El-din Mohamed. 2019. Isolation and characterization of biosurfactant producing bacteria from oil-contaminated water. *Biosci. Biotechnol. Res. Asia.* 16(4). 833–841.
- [17] Wibisana, A. 2018. Isolasi dan skrining mikroba penghasil biosurfaktan dari air laut yang tercemar minyak. *Jurnal Ilmiah Teknik Kimia.* 2(2). 55.
- [18] Syakti, A.D., P. Lestari, S. Simanora, L.K. Sari, F. Lestari, F. Idris, T. Agustiadi, S. Akhlus, N.V. Hidayati, Riyanti. 2019. Culturable hydrocarbonoclastic marine bacterial isolates from Indonesian seawater in the Lombok Strait and Indian Ocean. *Heliyon.* 5(5). e01594.
- [19] Najiyah, D., N. Vita, C. Nanda. 2013. Manfaat surfaktan dari bakteri laut hidrokarbonoklastik untuk akselerator proses hidrokarbon minyak bumi. *Lembaran Publikasi Minyak dan Gas Bumi.* 47(2). 97–104.
- [20] Thavasi, R., S. Sharma, S. Jayalakshmi. 2013. Evaluation of screening methods for the isolation of biosurfactant producing marine bacteria. *J. Pet. Environ. Biotechnol.* 4(2). DOI: 10.4172/2157-7463.S1-001.
- [21] Sidkey, N., H. Mohamed, H. Elkhoully. 2016. Evaluation of different screening methods for biosurfactant producers isolated from contaminated Egyptian samples grown on industrial olive oil processing waste. *Br. Microbiol. Res. J.* 17(4). 1–19.
- [22] Hassanshahian, M. 2014. Isolation and characterization of biosurfactant producing bacteria from Persian Gulf (Bushehr provenance). *Mar. Pollut. Bul.* 86(1–2). 361–366.
- [23] Patowary, K., R. Patowary, M.C. Kalita, S. Deka. 2017. Characterization of biosurfactant produced during degradation of hydrocarbons using crude oil as sole source of carbon. *Front. Microbiol.* 8(2). 1–14.
- [24] Wu, Y., M. Xu, J. Xue, K. Shi, M. Gu. 2019. Characterization and enhanced degradation potentials of biosurfactant-producing bacteria isolated from a marine environment. *ACS Omega.* 4(1). 1645–1651.

## Expression Virus-Like Particles (VLPs) at Geomembrane and Concrete in Asian Pacific Shrimp Culture (*Litopenaeus vannamei*)

Venny Nur Hidayah<sup>1</sup>, Muhammad Musa<sup>2</sup>, Yuni Kilawati<sup>2</sup>

<sup>1</sup>Master Program of Aquaculture, Faculty of Fisheries and Marine Science, University of Brawijaya, Malang, Indonesia

<sup>2</sup>Departement of Aquatic Resources Management, Faculty of Fisheries and Marine Science, University of Brawijaya, Malang, Indonesia

### Abstract

Asian Pacific Shrimp is an invertebrate that the most culture in aquaculture. But the high demand for shrimp makes farmers cultivate a high density. There are several ways to increase the density of shrimp culture, usually called *geomembrane* plastic and concrete ponds. The ponds are located in the Laboratory of Brackishwater and Seawater Fisheries, Probolinggo and Lucky Windu, Situbondo. Day of Culture (DOC) on Laboratory of Brackishwater and Seawater Fisheries in Probolinggo pond is 85 days both, while in Lucky Windu Situbondo is 81 days on pond 2, and pond 3B 133 days. The study aimed to evaluate correlations of VLPs towards geomembrane and concrete ponds. The research method has two observations: 1. Periodic observations; nitrite, ammonium, and shrimp were observed; 2. Last observation; sampling water for analysis VLPs was observed. Data of sampling water in the different ponds were then analyzed using Pearson correlation analysis to look for the level of tightness and direction of the relationship. The results have obtained that *geomembrane* VLPs and concrete VLPs has a very strong relationship, while the type of *geomembrane* and concrete was close to  $1 > 0.5$  and the result is 0.90, 0.96, 0.69, and 0.82. Water quality showed pH 8.1 at *geomembrane*, nitrite  $0.2 \text{ mg.L}^{-1}$  at *geomembrane*, and ammonium of  $0.44 \text{ mg.L}^{-1}$  at concrete. The pond area in *geomembrane* pond 1 and 2 was  $1600 \text{ m}^2$ , meanwhile in concrete both is  $4300 \text{ m}^2$ , which mean in concrete ponds more the existence of VLPs is because due to the different pond area factors and indicates from detections of WSSV that the result was positive that makes environment factor in abundances VLPs. But VLPs have no effect on the growth of shrimp vaname during the cultivated process.

**Keywords:** Asian Shrimp Pasific (*L. vannamei*), Virus-Like Particles (VLPs), Water Quality, and WSSV.

### INTRODUCTION

Asian shrimp pacific (*Litopenaeus vannamei*) is widely cultivated in Indonesia as an alternative to the cultivation of shrimp tiger (*P. monodon*) [1]. The high demand for vannamei shrimp increased annually in 2015 by 615,871 tons, in 2016 amounted to 698,138 tons, in 2017 amounted to 920,051 tons, in 2018 amounted to 931,338 tons and in 2019 amounted to 1,053,205 tons [2].

With the high demand for shrimp among the community, farmer's cultivation increases density, one of which is the use of geomembrane ponds and concrete. Geomembrane plastic has the function to coat or cover the entire pool to the bottom (ground level). Concrete ponds themselves can prevent water leakage as well as improve uneven or stable soil texture [3]. In addition to density, monitoring water quality is also important to maintain the stability of aqua culture ecosystems. When the lack of water quality control and weather changes are significant, it can cause shrimp to experience

stress. Stress factors affect the immune response in shrimps that are then susceptible [4]. Because water is an important requirement because it can affect the survival of fish, the development, growth, and level of shrimp production [5].

If the water quality decreases, it will be easier for harmful pathogenic organisms to multiply rapidly. The spread of pathogenic organisms can be vertically and horizontally. Vertically, from the base of the pond sediment to the surface of the pond [6] and horizontally from a particle can transfer the intergenic genes that enter into other particles. The particles can be called VLPs (Virus-Like Particles).

Virus-like particles (VLPs) are particles derived from protein capsids that belong to viruses but do not contain biological DNA structures [7]. VLPs contain bacterial and viral genes, where VLPs exist, the host must have the potential infecting bacteria and viruses [8]. The content of VLPs in the aquatic environment of shrimp farms will directly affect the accumulation of VLPS in the shrimp body through the respiratory.

The presence of VLPS can cause primary and secondary infections by bacteria, which commonly occur on a large scale due to virus-infected organisms, resulting in decreased production in aquaculture and leading to large

\*Correspondence Address:

Venny Nur Hidayah

Email : vennyhidayah@gmail.com

Address : Faculty of Fisheries and Marine Science,

University of Brawijaya, Veteran Malang, 65145

economic losses. Precise observation of the abundance of VLPS particles is very important as ecological monitoring in a business of shrimp farming [9]. Based on previous research, the VLPS expression of the sample can be observed using a Confocal Laser Scanning Microscope (CLSM).

The relationship of VLPs with sample water depends on temperature, pH, complexions, encapsulated molecules. VLPs are formed through the nucleation process, aided by electro static interactions between dimer capsid proteins and the genome of viruses. Further interaction is carried out by capsid proteins. Capsid proteins then form a wall of capsid protein structure. In dimers, capsid proteins stick together to form complex proteins and show the condition of intact protein capsids [10]. From the description above, it is necessary to conduct research related to the correlation of VLPs geomembrane and concrete.

## **MATERIAL AND METHOD**

### **Water Sampling**

The research was in February-May 2021. Water collected in two locations: Laboratory of Brackishwater and Seawater Probolinggo, East Java and Lucky Windu Situbondo, East Java. Water samples took to Laboratory in Probolinggo, using two ponds of geomembrane, and the spot taking the sample in the inlet and outlet. The detail spot for taking water sampling at the surface with depths of 40 cm and above sediment (pool bottom) is 4 cm [11]. It is also applied at Lucky Windu concrete ponds. The reason why used two types of ponds (geomembrane and concrete) is geomembrane plastic has the function to coat or cover the entire pool to the bottom (ground level). Concrete ponds themselves can prevent water leakage as well as improve uneven or stable soil texture [3]. The water sample was given PFA (paraformaldehyde) 4% tightly closed and coated with aluminum foil and stored in a coolbox with a temperature of 7°C and in closed conditions.

### **VLPs water sample Analysis Procedure**

The water sample obtained was then taken 5 mL (3.5 mL of water sample and 1.5 PFA 4%). Samples were processed between 24 hours and 96 hours [12]. Water samples taken 1 mL were dripped over a simple vacuum (membrane 0.025 µL and filter 0.2 µm in syringe) little by little. Then it is pumped slowly until the water is filtered and enters the syringe. The membrane (Anodisc or Whatman) with pore 0.025 µL wait

until wind-cooled. Bacteria and viruses were stained by slightly modifying the protocol [13] after collecting viruses and bacteria on an Anodisc or Whatman filter with a pore size of 0.025 µL. Create a staining solution by adding (97.6 µL deionized Water Sterile + 2.5 µL SYBR DNA Gel Stair) to Eppendorf Tubes 2 mL in dark conditions. Using SYBR Gold dissolved 10,000 times in dimethyl sulfoxide, at a final concentration of 3.3 times this stain, higher fluorescence yield compared to SYBR Green I or II. The staining solution is homogenized. Given a staining solution of 100 µL, then drip on a petridish. The 0.025 µL membrane is placed on top of the staining solution and incubated for 18 minutes. The membrane of 0.025 µL is wind-cooled. Given one drop of fluorescent mounting on the glass cover. The membrane is placed on the glass cover and closed [12]. Observations were made using CLSM (Confocal Laser Scanning Microscope). For further calculations, digital images were created using a DMIRE 2 confocal scanning laser microscope with a TCS SP2 confocal system (Leica Microsystems, Germany).

### **Sampling Shrimp Organ and DNA Isolations**

The DNA isolation from shrimp is 6 cm and took gills by opening the carapace of the head, swimming legs (pleopods), or tail. After that, pooling or merging and then put in microtube 1.5 mL and labeled each microtube. Furthermore, shrimp samples were counted and weighed as much as 0.05 g for DNA extraction. The next stage is DNA quantifiable testing, amplification, and electrophoresis [14]. Pleopods and tails are one of the target organs that are easily infected with WSSV. In addition, WSSV (which is still infectious in soil sediments) allows transmission of WSSV through mobile devices (including pleopods). Meanwhile, gill was in direct contact with the environment [14,15].

### **Detection WSSV Virus with RT-PCR**

PCR test conducted using primary ICP11 (Wsv230\_19F22:5'GACGCCGATTCTTGCTGGTGG 3'danWsv230\_202R24:5'GGGTTGAATCTCCAGCG TTGAATC3') with PCR program: Hotstart: 95°C for 3 minutes, Denaturation: 94°C for 1 minute, Annealing: 59°C for 1 minute, extension: 72°C for 1 minute (35 cycles), Postextension: 72°C for 7 minutes. Then visualized using geldoc [15].

### **VLPs at Convocal Laser Scanning Microscopy (CLSM)**

The membrane pore 0.025 µL is placed on the microscope preparation table and then



observed with a magnification of 400x. The acquired image is then marked, then the image that has been calculated the number of VLPs is stored in a folder that has been named. The images to be analyze dare adapted to the data in Microsoft Excel to make it easier to group the data [12].

#### pH

pH measurements are carried out periodically for three weeks and obtained the average pH per week. The procedure for using a pH meter based on SNI (2004) is as follows: The pH meter is calibrated with a buffer solution according to the tool's working instructions each time. It will take measurements. Rinse the electrodes with mineral-free water, then dry them with soft tissue. Dipping electrodes into test samples up to pH meters shows a steady reading. Record the scale or number readings on the display from the pH meter. Record the temperature at the time of pH measurement and report the result. Rinse the electrodes again with mineral-free water after measurement [16].

#### Nitrite

Nitrite measurements are carried out periodically for three weeks and obtained the average Nitrite per week. Nitrite measurement procedure was using Nitrite Testkit Hanna Instrument HI: 3873. The following nitrite measurement fills the cuvet glass with 10 mL of the sample until the mark is stated. We added one package of hi 3873-0 Nitrite Reagent. The lid was reattached, and the sample was shaken for 1 minute, and we wait for 1 minute to allow the color to develop. The lid was removed, and the color comparison cube was filled with 5 mL of a treated water sample. We determined which color matches the solution in the cube and record the result in  $\text{mg.L}^{-1}$  (or ppm) nitrite. It is better to match the color 20 with a white cloth to make it visible about 10 cm behind the comparison. The reading to  $\text{mg.L}^{-1}$  nitrite was converted, then multiply the reading by a factor of 4.43 [17,18].

#### Ammonium

Ammonium measurements are carried out periodically for three weeks and obtained the average ammonium per week. The measurement of ammonium content can be done using the Nessler method in spectrophotometry with a wave length of 425 nm. How to measure ammonium content in the sample is: water samples are filtered using Whatman No. 42 filter

paper, filtered sample water is then picked up as much as 10 mL and inserted into the reactor tube. Nessler reagents of four drops were added and homogenized using a vortex mixer for 30 seconds, and waited for 10 minutes. Measured using a spectrophotometer at a wavelength of 425 nm. Ammonium levels in the sample are calculated by the formula = Sample Absorbance/ Slope [17].

#### Growth Asian Pacific Shrimp Analyze

Shrimp sampling was needed to calculate the initial weight at stocking and final weight at the beginning of stocking until harvest time. The initial weight and final weight are measured [19].

#### Data Analysis

Pearson correlation analysis is used to look for the level of tightness and direction of the relationship of VLPs in geomembrane and concrete pond. The higher correlation value, the higher the tightness of the relationship between the two variables. Minus (-) and plus (+) signs on correlation values represent the nature of the relationship. Correlation values are 0.00 to 0.5 medium correlations and if > 0.5 correlations are very strong [20]. If the corrective value is minus, the relationship between the two tables is unidirectional. If the correlation value is marked plus, the relationship between the two tables is in the opposite direction [21]. The formula for Pearson correlation analysis is as follows [22]:

$$r_{pm} = \frac{n(\sum xy) - (\sum x)(\sum y)}{\sqrt{\{n(\sum x^2) - (\sum x)^2\}\{n(\sum y^2) - (\sum y)^2\}}}$$

## RESULTS AND DISCUSSION

### Detection of Vaname Shrimp infected with WSSV in RT-PCR

Shrimp samples obtained after the PCR test were positive. In this case, the virus replicates repeatedly in other target organs.

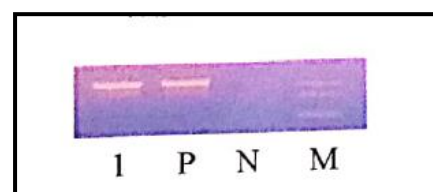


Figure 1. WSSV PCR results are positive; numbers 1= sample wells; M=DNA marker indicator (100-1000 bp); N= negative control and P = positive control.

The transmission of WSSV consists vertically or horizontally [23]. Vertically, it is transmitted generatively through the infected broodstock to

heredity, while horizontally can go through the food chain, so that virion in the environment enters the body of the shrimp. In addition, it can also occur due to transmission factors and reservoir infections [24].

The result from PCR was positive (Fig. 1) because virus infection is a vector in the spread of shrimp disease presence of VLPs [25] and the abundance of bacteria with correlation with viruses [26]. Pathogens or foreign bodies that enter the body can VLPs, viruses, or bacteria that are harmful if the VLPs are high, then the virus bacteria ratio (VBR) can easily infect the host. Although largely unproven, viral infections remain the main possible vector for the spread of shrimp disease [27].

**Analysis of Water Quality**

**pH**

pH is the degree of acidity used to express the level of acidity or wetness possessed by water [28]. pH in the range of 7.5–8.5 [29].

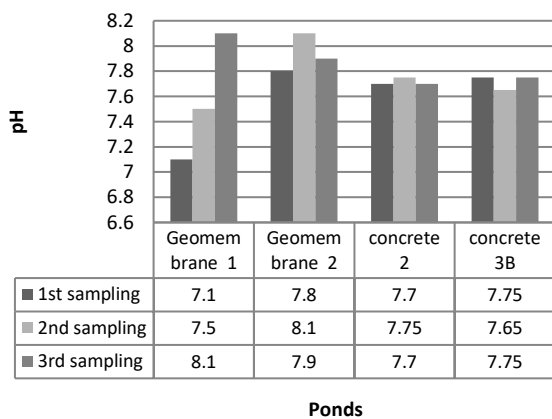


**Figure2.** pH measurements performed on sampling in Geomembrane and Concrete.

The highest pH in the 1<sup>st</sup> sampling was geomembrane 2 for 7.8, while for the 2<sup>nd</sup> sampling was found in geomembrane 2 by 8.1. In the 3<sup>rd</sup> sampling, the highest pH was measured in geomembrane 1 for 8.1. Meanwhile, the lowest pH in 1<sup>st</sup> sampling was geomembrane 1 for 7.1, 2<sup>nd</sup> sampling was concrete 3B for 7.65, and 3<sup>rd</sup> sampling was concrete 2 for 7.7 (Fig. 2).

The average pH in a shrimp pond is 6.2-10.2 [30]. Reducing carbon dioxide during the day is helped by the process of photosynthesis, and at night, carbon dioxide increases because it is produced from shrimp. If there is heavy rain and acidic soil, then the pH can reach 4.1 [31]. The stability of structure VLPs under different pH and

ions does not play a major role in the abundance of VLPs [32].

Factors that caused an abundance of VLPs are nutrient availability and the primary productivity of coral ecosystems concerning other microorganisms (prokaryotes) that was determined [33]. According to the new experiment about VLPs, the relationship between the abundance of VLPs and hydrographic factors, nutrient availability, as well as primary productivity in the coral ecosystem was clarified [9]. Parameters that significantly had negative relations are dissolved oxygen, temperature, pH, salinity, and total phytoplankton [9]. The stability of the structure of VLPs under different pH and ions does not play a major role in the abundance of VLPs [32].

**Nitrite**

Nitrite is an unstable gas affected by dissolved oxygen and is a transition from ammonium and nitrates to the nitrification process [34]. The highest nitrite in 1<sup>st</sup> sampling was measured in geomembrane 1 for 0.2 ppm, while in the 2<sup>nd</sup> sampling was measured in geomembrane 2 for 0.2 ppm, and in 3<sup>rd</sup> sampling was measured in geomembrane 1 for 0.1 ppm. The lowest nitrite in the 1<sup>st</sup> sampling was found in concrete 3B for 0.02 ppm, in the 2<sup>nd</sup> sampling was found in concrete 2 for 0.03 ppm, and for the 3<sup>rd</sup> sampling was in concrete 3B for 0.03 ppm (Fig. 3).

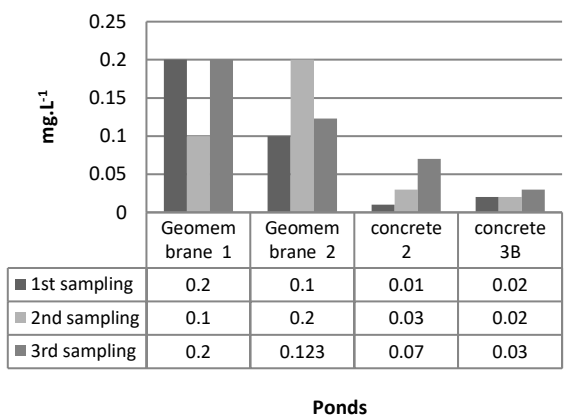


**Figure3.** Nitrite measurements performed on sampling in Geomembrane and Concrete.

In the previous study, nitrite and nitrate concentrations in the treatment ponds were lower during most of the experimental period [35]. During the nitrification process, hydrogen ions are produced and released in to the water column [36], which is likely to cause the

reduction of pH in there environment. In this study also, a similar trend was observed. The pH in the treatment ponds decreased with an increase in rearing time. The increase in turbidity of the water column could be the result of the increase in levels of suspended particles [37] and the addition of large amounts of artificial feed in the rearing environment [38]. Nitrite levels based on SNI01-7246 200 are < 0.01 mg.L<sup>-1</sup> [39]. Factors that cause the abundance of VLPs are because the organic matter in the water enters the host, including algae, and in the water wastewater [40].

During the process of ammonia oxidation to nitrite, alkalinity in form of carbonated or bicarbonates is consumed, which causes the system pH to go down and the ammonia oxidation to slow down. Evidence that low pH induces prophage in ammonia oxidizers is novel [41]. A positive significant correlation was found between VLPs, bacteria, and VBR and nutrients (nitrate, ammonium, DIN) [9].

**Ammonium**

Ammonium and nitrate compounds are an important part of the watered nitrogen cycle. Denitrification is a reaction of reducing nitrates to nitrites, nitrite oxides, and nitrogen gases. Meanwhile, nitrogen fixation is the binding of nitrogen gas to ammonia and organic nitrogen. This process occurs in a trial involving symbiosis between algae and bacteria [42].

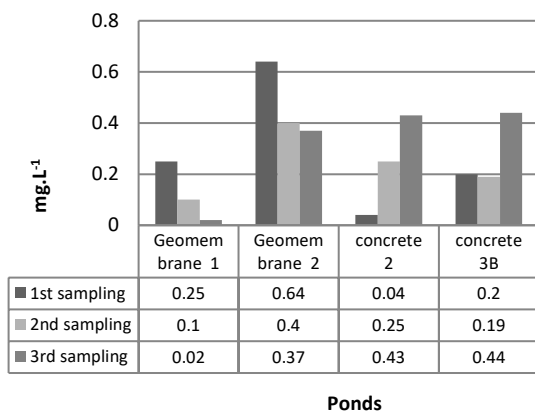


**Figure4.** Ammonium measurements were performed on sampling in Geomembrane and Concrete.

The highest ammonium in the 1<sup>st</sup> sampling was found in geomembrane 2 for 0.64 ppm, in the 2<sup>nd</sup> sampling was found in geomembrane 2 for 0.4 ppm, and in the 3<sup>rd</sup> sampling, was found in concrete 3B for 0.44 ppm. Conversely, the lowest ammonium in the 1<sup>st</sup> sampling was measured in concrete 2 for 0.04 ppm, 2<sup>nd</sup> sampling in concrete

3B for 0.19 ppm, and 3<sup>rd</sup> sampling in geomembrane 1 for 0.02 ppm.

Ammonium levels can also increase due to the influence of the pH of the waters. If the pH value of an expansion is lower, then the level of ammonium in the water becomes higher [43]. Ammonium concentration in ponds exceeding 0.45 ppm can inhibit shrimp growth by up to 50%. For shrimp to grow well enough, ammonium contained in pond water should not be more than 0.01 ppm [39]. The presence of high amounts of ammonium in the waters affects stress in biota [44].

These viral-mediated lysates will enhance the transfer of nutrients from particulate to dissolved and will be then utilized by uninfected bacteria. As a result, viruses play an important role in the recycling of nutrients and carbon. These viral lysates are rich in free and combined amino acids and therefore, are a potentially important source of labile organic N, which is taken by bacteria and produced ammonium as a by-product.

Furthermore, the bacterial counts indicate that uninfected bacteria might convert the dissolved organic nitrogen into inorganic resulting in a higher concentration of nitrite and ammonium. Then, the latter will be consumed by phytoplankton, thus increasing its biomass, which explains the high abundance and biomass of plankton in located B, particularly the diatoms. Hence, the viral lysates at located Bare triggered mostly by infection of bacterial cells, owing to the high VBR and its low biomass. This state explained the positive significant correlation between VLPs, bacteria, and VBR, and nutrients (nitrate and ammonium). As a result, the viral lysis will stimulate bacterial metabolism characterized as a major N source that drives primary production in the ocean. In other words, viral activity will indirectly fuel plankton productivity that requires enough amounts of nutrients for its growth [9].

**Growth of Asian Pacific Shrimp**

The daily average growth (ADG) of vaname shrimp after the age of over 60 days generally ranges from 0.2 g -0.3 g. The growth of Asian Pacific Shrimp was showed in following Table 1. Daily growth obtained in this study after the age of 80 days is 0.10 g -1.14 g. The rate of growth of individuals shows a decrease with the increase in average weight as the maintenance period increases [19].

Shrimp growth is influenced by many factors, namely internal and external factors. Internal

factors include sex, age, size, and maturity level of the gonads, while external factors are divided into two groups, namely biotic and abiotic factors. Biotic factors are feed and stocking density, while the dominant abiotic factors are temperature, oxygen, salinity, light, and toxic materials [45]. That besides being supported by good feed and environment. Shrimp growth is also determined by stocking density. High stocking density of shrimp will result in slow growth due to competition for space and feed. Such condition will affect the growth of the reared shrimp [46]. The growth of white shrimp is influenced by a combination of several factors, namely water quality (including water temperature), seed quality, feed quality, amount of feed, and stocking density [47].

Environment can affect replication virus and the production of VLPs at the rate of cell growth under metabolism, DNA transcription and replication, mRNA translation and protein PTM. The environment in question includes the concentration of dissolved oxygen (DO), pH, temperature, agitation rate, cell and substrate concentration, inlet gas composition flow, volume, pressure, dynamics and fluids [48]. abundance of VLP in each plot significantly correlated with turbidity. there is a correlation between the abundance of VLP and particles suspended in eutrophic water columns and oligotrophic estuaries. Particles suspended in Water is mainly composed of organic matter [49].

**Table 1.** The growth of Asian Pacific Shrimp

Sampling	Ponds	Weight (g)	Size (Σ.g <sup>-1</sup> )
1 <sup>st</sup>	Geomembrane 1		
	DOC 42	3.36	297
	Geomembrane 2		
	DOC 42	2.18	100
	Concrete 2		
	DOC 42	4.7	212
2 <sup>nd</sup>	Concrete 3B		
	DOC 42	4.5	222
	Geomembrane 1		
	DOC 54	7.9	126
	Geomembrane 2		
	DOC 52	2.8	35
3 <sup>rd</sup>	Concrete 2		
	DOC 49	6.8	147
	Concrete 3B		
	DOC 49	6.8	147
	Geomembrane 1		
	DOC -	-	-
3 <sup>rd</sup>	Geomembrane 2		
	DOC -	-	-
	Concrete 2		
	DOC 56	8.8	133
	Concrete 3B		
	DOC 56	8.7	114

**Analysis Correlation of VLPs in Geomembrane and Concrete**

The data provide that geomembrane and concrete pondshave strong correlations. VLPs in geomembrane 1 has abundance VLPs in CLSM of 22 particles.m<sup>-3</sup>, and geomembrane 2 has 250 particles.m<sup>-3</sup>. Meanwhile, concrete 2 has an abundance VLPs in CLSM, which is 314 particles.m<sup>-3</sup>, and concrete 3B has 139 particles.m<sup>-3</sup>. The pond area in geomembrane pond 1 and 2 was 1600 m<sup>2</sup>. Meanwhile in concrete, both are 4300 m<sup>2</sup>, which means concrete ponds have more VLPs due to the different pond area factors [33]. Besides pond, other factors that caused the abundance VLPs were bacterial cycles and nutrients [6,9].

Compared to the abundance of VLPs in aquaculture waters, VLPs are often found in the sea [50]. Usually, VLPs are found in coral reef areas or the depths of the sea [27]. The concentration of VLPs in the ocean ranges from 1.7 x10<sup>6</sup>particles.m<sup>-3</sup> to 4.0 x 10<sup>7</sup>particles.m<sup>-3</sup> [8]. The environment can affect viral replication and production of VLPs at the rate of cell growth in a state of metabolism, DNA transcription, and replication, translation of mRNA, and PTM proteins. The environment in question includes dissolved oxygen concentration (DO), pH, temperature, agitation rate, cell and substrate concentration, incoming gas composition flow, volume, pressure, dynamics, and fluids [48].

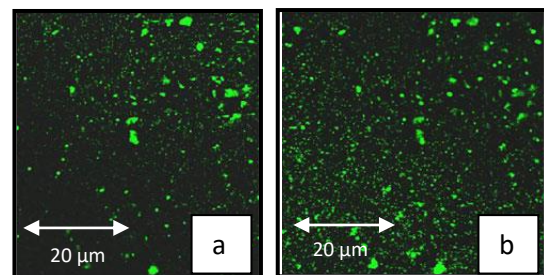


**Figure 5.** Visualisation VLPs in Confocal Laser Scanning Microscopy (CLSM), abundance VLPs in geomembrane (a) and VLPs in concrete (b)

**Table 2.** Correlations VLPs in Geomembrane and Concrete

No	Pond	Correlation of VLPs
1	Geomembrane 1 – Concrete 2	0.90
2	Geomembrane 2 – Concrete 3B	0.96
3	Geomembrane 1 – Concrete 2	0.69
4	Geomembrane 2 – Concrete 3B	0.82

There is a correlation between the abundance of VLPs and suspended particles in eutrophic water columns and oligotrophic estuaries.

Suspended particles in the waters are mainly composed of organic matter [49]. Depth can affect the distribution of virus-like particles (VLP). The range of VLPs abundance in the sample of pelagic organisms attached to the sediment is smaller than the VLPs abundance range in benthic samples [6].

#### CONCLUSION

Pearson correlation value showed that VLPs in geomembrane and concrete have a strong relationship, close to 1. Concrete ponds have more VLPs due to the different pond area factors. Detections of WSSV result was positive that indicates environment factor in abundances VLPs. However, VLPs have no effect on the growth of shrimp vaname during the cultivated process.

#### ACKNOWLEDGEMENT

We would like to thank University Leading Applied Research (PTUPT), Institute of Research and Community Service through Non-Tax State Revenue Funds (PNBP) University of Brawijaya, in accordance with the Budget Implementation List (DIPA) for funding this research.

#### REFERENCES

- [1] Srinivas, D., Ch. Venkatrayulu, B. Swapna. 2016. Sustainability of exotic shrimp *Litopenaeus vannamei* (Boone, 1931) farming in coastal Andhra Pradesh, India: Problems and Issues. *Eur. J. Exp. Biol.* 6(3). 80–85.
- [2] Ministry of Marine and Fisheries. 2019. Performance Report of Direktorat General of Fisheries Aquaculture, Ministry of Marine and Fisheries. Republic of Indonesia. Jakarta.
- [3] Novitasari, D., S.M. Prayitno, Sarjito. 2016. Analisa faktor risiko yang mempengaruhi serangan *Infectious Myonecrosis Virus* (IMNV) pada budidaya udang vanamei (*Litopenaeus vannamei*) secara intensif di Kabupaten Kendal. Prosiding Seminar Nasional Hasil-Hasil Penelitian Perikanan dan Kelautan ke-VI. Faculty of Fisheries and Marine Science - Research Center for Disaster Mitigation and Coastal Rehabilitation. Diponegoro University. 640-649.
- [4] Liu, G., S. Zhu, D. Liu, X. Guo, Z. Ye. 2017. Effects of stocking density of the white shrimp *Litopenaeus vannamei* (Boone) on immunities, antioxidant status, and resistance against *Vibrio harveyi* in a biofloc system. *Fish Shellfish Immunol.* 67. 19–26.
- [5] Fauzia, S.R., S.H. Suseno. 2020. Resirkulasi air untuk optimalisasi kualitas air budidaya ikan nila nirwana (*Oreochromis niloticus*). *Jurnal Pusat Inovasi Masyarakat.* 2(5). 887-892.
- [6] Filippini, M., M. Middleboe. 2007. Viral abundance and genome size distribution in the sediment and water column of marine and freshwater ecosystems. *FEMS microbiol Ecol.* 60. 397-410.
- [7] Jariyapong, P., C. Chotwiwatthanakun, S. Direkbusarakom, I. Hirono, S. Wuthisuthimethavee, W. Weerachatanukul. 2015. Delivery of double stranded RNA by *Macrobrachium rosenbergii* nodavirus-like particles to protect shrimp from white spot syndrome virus. *Aquaculture.* 435. 86–91.
- [8] Prussin, A.J., E.B. Garcia, L.C. Marr. 2015. Total concentrations of virus and bacteria in indoor and outdoor air. *Environ. Sci. Technol. Lett.* 2(4). 84–88.
- [9] Ramphul, C., E.C. Beatriz, S.Y. Toshiyuki, Koichi, Y. Thamasak, S. Yoshimi. 2015. Abundance of Virus-like Particles and its links to phytoplankton, bacteria and nutrients cycling in coastal coral ecosystem. *Eco-Engineering.* 27(3). 81-90.
- [10] Strugala, A., J. Jagielski, K. Kamel, G. Nowaczyk, M. Radom, M. Figlerowicz, A. Urbanowicz. 2021. *Virus-like particles* produces using the brome mosaic virus recombinant capsid protein expressed in bacterial system. *Int. J. Mol. Sci.* 22(3098): 1-15.
- [11] Maia, E.P., G.A. Modesto, L.O. Brito, A.O. Galvez and T.C.V. Gesteira. 2016. Intensive culture system of *Litopenaeus vannamei* in commercial ponds with zero water exchange and addition of molasses and probiotics. *Revista de biología marina y oceanografía.* 51(1). 61–67.
- [12] Peduzzi, P., M. Agis, B. Luef. 2013. Evaluation of confocal laser scanning microscopy for enumeration of virus-like particles in aquatic systems. *Environ. Monit. Assess.* 185(7). 5411–5418.
- [13] Noble, R.T., J.A. Fuhrman. 1998. Use of SYBR Green I for rapid epifluorescence counts of marine viruses and bacteria. *Aquat. Microb. Ecol.* 14. 113–118.
- [14] Arafani, L., M. Ghazali, M. Ali. 2016. Pelacakan virus bercak putih pada udang vaname (*Litopenaeus vannamei*) di Lombok

- dengan Real-Time Polymerase Chain Reaction. *Jurnal Veteriner*. 17(1). 88–95.
- [15] Amrillah, A.M., S. Widyarti, Y. Kilawati. 2015. Dampak stres salinitas terhadap prevalensi white spot syndrome virus (wssv) dan survival rate udang vannamei (*Litopenaeus vannamei*) pada kondisi terkontrol. *Res. J. Life Sci*. 2(2). 110–123.
- [16] SNI. 2004. SNI 06-6989.11-2004. Water and Waste – part 11<sup>th</sup>, pH measurement.
- [17] Supriatna., M. Mahmudi, M. Musa, Kusriani. 2020. Hubungan pH dengan parameter kualitas air pada tambak intensif udang vannamei (*Litopenaeus vannamei*). *J. Fish. Mar. Res*. 4(3). 368-374.
- [18] Hasuti, Y.P. 2011. Nitrifikasi dan denitrifikasi di tambak. *Jurnal Akuakultur Indonesia*. 10(1). 89-98.
- [19] Tahe, Suwardi, H.S. Suwoyo. 2011. Pertumbuhan dan sintasan udang vaname (*Litopenaeus vannamei*) dengan kombinasi pakan berbeda dalam wadah terkontrol. *Jurnal Riset Akuakultur*. 6(1). 31.
- [20] Pratomo, D.S., E.Z. Astuti. 2015. Analisis regresi dan korelasi antara pengunjung dan pembeli terhadap nominal pembelian di Indomaret Kedungmundu Semarang dengan metode kuadrat terkecil. *Jurnal Statistika*. 1-12.
- [21] Sihombing, Yennita, L. Hutahaean. 2019. Uji komparasi model korelasi dalam menganalisis efektivitas pendampingan petani. *Informatika Pertanian*. 28(1).1–10. doi: 10.21082/ip.v28n1.2019.p1-10.
- [22] Ariani, S., A. Al-Idrus, L. Japa, D. Santoso. 2020. Struktur komunitas makroalga sebagai indikator ekologi ekosistem perairan pada kawasan konservasi laut daerah di Gili Sulat Lombok Timur. *Jurnal Biologi Tropis*. 20(1). 132-138.
- [23] Rahma, H.N., S.B. Prayitnon, A.H.C. Haditomo. 2014. Infeksi white spot syndrom virus (WSSV) pada udang windu (*Penaeus monodon* Fabr.) yang dipelihara pada salinitas media yang berbeda. *J. Aquac. Manage. Technol*. 3(3). 25-33.
- [24] Rukish, R., G.I. Satriani, R. Rasyid. 2019. Monitoring penyakit WSSV pada budidaya udang windu (*Penaeus monodon*) di Tambak Tradisional Kota Tarakan. *Jurnal Harpodon Borneo*. 12(2). 89-95.
- [25] Ferreira, N.C., C. Bonetti, W.Q. Seiffert. 2011. Hydrological and Water Quality Indices as management tools in marine shrimp culture. *Aquaculture*. 318(4). 425–433.
- [26] Davy, J.E., N.L. Patten. 2007. Morphological diversity of virus-like particles within the surface microlayer of scleractinian corals. *Aquat. Microb. Ecol*. 47(1). 37–44.
- [27] Seymour, J.R., N. Patten, D.G. Bourne, J.G. Mitchell. 2005. Spatial dynamics of virus-like particles and heterotrophic bacteria within a shallow coral reef system. *Mar. Ecol. Prog. Ser*. 288. 1–8.
- [28] Zulus, A. 2017. Rancang BANGUN MONITORING pH air menggunakan *soil moisture sensor* di SMK N 1 Tebing Tinggi Kabupaten Empat Lawang. *JUSIKOM*. 2(1). 37-43.
- [29] Arsad, S., A. Afandy, A.P. Purwadhi, B. Maya, D.K. Saputra, N.R. Buwono. 2017. Studi kegiatan budidaya pembesaran udang vaname (*Litopenaeus vannamei*) dengan penerapan sistem pemeliharaan berbeda. *Jurnal Ilmiah Perikanan dan Kelautan*. 9(1). 1-14.
- [30] George, A., G. A. And N. James. 2018. Effect of pond type on physicochemical parameters, phytoplankton diversity and primary production in, Kisii, Kenya. *Int. J. Fish. Aqua. Stud*. 6(6). 125-130.
- [31] Kathyayani, S. A., M. Poornima, S. Sukumaran, A. Nagavel and M. Muralidhar. 2019. Effect of ammonia stress on immune variables of Pacific white shrimp *Penaeus vannamei* under varying levels of pH and susceptibility to white spot syndrome virus. *Ecol. Environ. Saf*. 184. 1-13.
- [32] Samandougou, I., R. Hammami, R. M. Rayas, I. Fliss and J. Jean. 2015. Stability of Secondary and Tertiary Structures of Virus-Like Particles Representing Noroviruses: Effects of pH, Ionic Strength, and Temperature and Implications for Adhesion to Surfaces. *Journal ASM.org*. 81. 7680-7686
- [33] Roundnew, B., J.R. Seymour, T.C. Jeffries, T.J. Lavery, R.J. Smith, J.G. Mitchell. 2012. Bacterial and Virus-Like Particle abundances in purged and unpurged groundwater depth profiles. *Groundwater Monit. Remediat*. 32(4). 72-77.
- [34] Makmur, M., H. Kusnopranto, S. S. Moersidik, D. S. Wisnubroto. 2012. Pengaruh Limbah Organik Dan Rasio N/P Terhadap Kelimpahan Fitoplankton Di Kawasan Budidaya Kerang Hijau Cilincing.

- Jurnal Teknologi Pengelolaan Limbah (J. Waste Manage. Technol)*. 15(2). 51-64.
- [35] Raja, A.R., N. Kalaimani, A. Panigrahi, A.G. Ponniah. 2014. Effect of season and treatment of seed with antibiotics on growout culture of *Penaeus monodon* (Fabricius, 1798) at Sunderban. *India. Turk. J. Fish. Aquat. Sci.* 14. 879-885.
- [36] Henriksen, K. and W. M. Kemp. 1988. Nitrification in estuarine and coastal marine sediments. In: Blackburn, T.H., J. Sorensen. (Eds). Nitrogen cycling in coastal marine environments. Wiley, New York, USA. 207-249.
- [37] Wasielesky, W., H. Atwood, A. Stokes, C.L. Browdy. 2006. Effect of natural production in a zero exchange suspended microbial floc based super intensive culture system for white shrimp *Litopenaeus vannamei*. *Aquaculture*. 258. 396-403.
- [38] Chithambaran, S., M. Harbi, M. Broom, K. Khobrani, O. Ahmad, H. Fattani, A. Sofyani And N. Ayaril. 2017. Green water technology for the production of Pacific white shrimp *Penaeus vannamei* (Boone, 1931). *Indian J. Fish.* 64(3). 43-49.
- [39] Kilawati, Y. dan Y. Maimunah. 2015. Kualitas Lingkungan Tambak Insentif *Litopenaeus vannamei* Dalam Kaitannya Dengan Prevalensi Penyakit White Spot Syndrome Virus. *Res. J. Life Sci.* 2(1). 50-59.
- [40] Hisee, A.R., M. Hisee, J. C. McKerral, S. R. Rosenbauer, J. S. Paterson, J. G. Mitchell and H. J. Fallowfield. 2020. Changes of viral and prokaryote abundances in a high rate algal pond using flow cytometry detection. *Water Sci. Technol.* 82(6). 1-8.
- [41] Choi, J., S. M. Kotay and R. Goel. 2010. Various physico-chemical stress factors cause prophage induction in *Nitrosospira multiformis* 25196- an ammonia oxidizing bacteria. *Water Res.* 44. 4450-4558.
- [42] Carneiro, M.A. Amaral, J.F.J. Resende, S.R. Oliveira, F.O. Fernandes, H.D.S. Borburema, M.S. Barbosa-Silva, A.B.G. Ferreira, E. Marinho-Soriano. 2020. Performance of the agarophyte *Gracilariopsis tenuifrons* in a multi-trophic aquaculture system with *Litopenaeus vannamei* using water recirculation. *J. Appl. Phycol.* 1-10.
- [43] Irawan, D. Dan L. Handayani. 2021. tуди kesesuaian kualitas perairan tambak ikan bandeng (*Chanos chanos*) di Kawasan Ekowisata Mangrove Sungai Tatah. *Budidaya Perairan.* 9(1). 10-18
- [44] Xue, S., J. Wei, J. Li, X. Geng and J. Sun. 2015. Effects of total ammonia, temperature and salinity on the mortality and viral replication of WSSV-infected Chinese shrimp (*Fenneropenaeus chinensis*). *Aquac. Res.* 48(1). 236-245.
- [45] Effendie, M.I. 1979. Fishery biological methods. Yayasan Dewi Sri. Bogor.
- [46] Mujiman, A., S.R. Suyanto. 1993. Tiger shrimp cultivation. Penebar Swadaya. Jakarta.
- [47] Wijayanto, D., D.B. Nursanto, F. Kurohman, R.A. Nugroho. 2017. Profit maximization of whiteleg shrimp (*Litopenaeus vannamei*) intensive culture in Situbondo Regency, Indonesia. *AAFL Bioflux.* 10. 1436-1444.
- [48] Roldao, A., A.C., Sliva, M.C.M. Mellado. 2017. Viruses and Virus-Like Particles in biotechnology: fundamentals and applications. Modul of New University of Lisbon, Institute of Experimental Biology and Technology, Oeiras, Portugal. doi: 10.1016/B978-0-12-809633-8.09046-4.
- [49] Nakayama, N., Mami. O. Katsuhiko. I. Susumu. A and Makoto. K. 2007. Seasonal variations in the abundance of viruslike particles and bacteria in the floodwater of a Japanese paddy field. *Soil Sci. Plant Nutr.* 53(4). 420-429.
- [50] Wu, S., L. Zou, H. Wang, J. Xiao, S. Yan, Y. Wang. 2020. Diverse and unique viruses discovered in the surface water of the East China Sea. *BMC Genomic.* 21(441). 1-15.

## MANUSCRIPT SUBMISSION

### FOCUS AND SCOPE

Journal of Experimental Life Science (JELS) is scientific journal published by Graduate Program of Brawijaya University as distribution media of Indonesian researcher's results in life science to wider community. JELS is published in every four months. JELS published scientific papers in review, short report, and life sciences especially nanobiology, molecular biology and cellular biology. JELS is scientific journal that published compatible qualified articles to academic standard, scientific and all articles reviewed by expert in their field.

Journal of Experimental Life Science (JELS) have vision to become qualified reference media to publish the best and original research results, and become the foundation of science development through invention and innovation on cellular, molecular, and nanobiology rapidly to community.

Journal of Experimental Life Science (JELS) have objectives to published qualified articles on research's results of Indonesian researchers in life science scope. JELS encompasses articles which discuss basic principles on nature phenomenon with cellular, molecular, and nanobiology approach.

### PEER REVIEW PROCESS

Publication of articles by JITODE is dependent primarily on their validity and coherence, as judged by peer reviewers, who are also asked whether the writing is comprehensible and how interesting they consider the article to be. All submitted manuscripts are read by the editorial staff and only those articles that seem most likely to meet our editorial criteria are sent for formal review. All forms of published correction may also be peer-reviewed at the discretion of the editors. Reviewer selection is critical to the publication process, and we base our choice on many factors, including expertise, reputation, and specific recommendations. The editors then make a decision based on the reviewers' advice, from among several possibilities:

*Accepted*, with or without editorial revisions  
Invite the authors to revise their manuscript to address specific concerns before a final decision

*Rejected*, but indicate to the authors that further work might justify a resubmission

*Rejected outright*, typically on grounds of specialist interest, lack of novelty, insufficient conceptual advance or major technical and/or interpretational problems

### PUBLICATION FREQUENCY

JELS publish 2 Issues per year until 2017. JELS started to publish 3 Issues per year since 2018.

### OPEN ACCESS POLICY

This journal provides immediate open access to its content on the principle that making research freely available to the public supports a greater global exchange of knowledge.

### COPYRIGHT NOTICE

Authors who publish with this journal agree to the following terms:

Authors retain copyright and grant the journal right of first publication with the work simultaneously licensed under a Creative Commons Attribution License that allows others to share the work with an acknowledgement of the work's authorship and initial publication in this journal.

Authors are able to enter into separate, additional contractual arrangements for the non-exclusive distribution of the journal's published version of the work (e.g., post it to an institutional repository or publish it in a book), with an acknowledgement of its initial publication in this journal.

Authors are permitted and encouraged to post their work online (e.g., in institutional repositories or on their website) prior to and during the submission process, as it can lead to productive exchanges, as well as earlier and greater citation of published work (The Effect of Open Access).

### PRIVACY STATEMENT

The names and email addresses entered in this journal site will be used exclusively for the stated purposes of this journal and will not be made available for any other purpose or to any other party.

### ETHICS PUBLICATION

Research that using animal, human, and clinical testing is should already have ethical clearance certificate from authorized institution.





**Title Typed in Bold, Capitalize each First Letter of Each Word, Except  
Conjunctive, *Scientific name* should not be Abbreviated  
(Calibri 14 Bold Center, should not exceed 12 words, except conjunctive)**

First Author<sup>1\*</sup>, Second Author<sup>2</sup>, Third Author<sup>3</sup> (Calibri 12 Center, without title)

<sup>1</sup>First Author Affiliation, Correspondence author should be indicated by \* symbol (Calibri 9 Center)

<sup>2</sup>Department of Biology, Faculty of Mathematics and Natural Sciences, University of Brawijaya, Malang, Indonesia

<sup>3</sup>Laboratorium of Physiology, Faculty of Medicine, University of Brawijaya, Malang, Indonesia

**Abstract (Calibri 9 Bold Center)**

This article illustrates preparation of your paper using MS-WORD (.doc or .rtf). Manuscript was numbered consecutively. Main text typed in two columns (67 characters), except title and abstract in one column. The manuscript should be written in English. The length of manuscript should not exceed 10 pages including table and figure in this format using A4 paper single space. The text should be in the margin of 3 cm up, down and left side, 2.5 cm on right side. Abstract includes the research purposes, research method and research results in one paragraph of *essay*, not *enumerative*. No citation in abstract. Abstract should not exceed 200 words. Keywords typed after abstract. (Calibri 9 Justify).

**Keywords:** manuscript, English, format, 5 words maximum (Calibri 9 Left)

---

**INTRODUCTION**\*(Calibri 10 Bold, Left, Capslock)

All submitted manuscripts should contain original research which not previously published and not under consideration for publication elsewhere. Articles must be written in ENGLISH and manuscripts may be submitted for consideration as research report articles, short reports or reviews.

The introduction explains the background of the problem, the study of literature and research purposes. Some initial introduction paragraphs explain the problem and background to these problems [1]. The next few paragraphs explain the study of literature that contains recent knowledge development which is directly related to the issues. The last paragraph of the introductory section contains a description of the purposes of the study. (Calibri 10 Justify)

**MATERIAL AND METHOD**(Calibri 10 Bold, Left, Capslock)

This section describes the types of methods (qualitative, quantitative or mixed-method) with details of methods of data collection and data analysis [2]. This section also describes the perspective that underlying the selection of a particular method. (Calibri 10 Justify)

**Data Collection** (Calibri 10 Bold, Left)

Explain the data collection methods, i.e. surveys, observations or archive, accompanied by details of the use of such methods. This section also describes the population, sampling and sample selection methods. (Calibri 10 Justify)

The use of English language should followed proper grammar and terms. Name of organism should be followed by its full scientific name in the first mention, in *italic* [3]. Author of the scientific name and the word of “var.” typed regular. Example: *Stellaria saxatillis* Buch. Ham. First abbreviation typed in colon after the abbreviated phrase.

Author must use International Standard Unit (SI). Negative exponent used to show the denominator unit. Example: g l<sup>-1</sup>, instead of g/l. The unit spaced after the numbers, except percentage [4]. Example: 25 g l<sup>-1</sup>, instead of 25gl<sup>-1</sup>; 35% instead of 35 %. Decimal typed in dot (not coma). All tables and figures should be mentioned in the text.

**RESULT AND DISCUSSION** (Calibri 10 Bold, Left, Capslock)

This section contains the results of the analysis and interpretation or discussion of the results of the analysis. Describe a structured, detailed, complete and concise explanation, so that the reader can follow the flow of analysis and thinking of researchers [5]. Part of the results study should be integrated with the results of the

---

Correspondence address: (Calibri 8 Bold, Left)

**Full name of correspondence author**

Email : sapto@jurnal.ub.ac.id

Address : affiliation address include post code

analysis and the results and discussion are not separated.

**Table**

Table should be submitted within the manuscript and in separated file of *Microsoft Excel* (xls.). Table should not exceed 8 cm (one column) and 17 cm (two columns). Table should be embedded in different page after references.

Table should be numbered in sequence. Table title should be brief and clear above the table, with uppercase in initial sentence. Vertical line should not be used. Footnote use number with colon and superscripted. Symbol of (\*) or (\*\*) was used to show difference in confidence interval of 95 and 99%.

**Table 1.** Example of the Table (Calibri 8.5 Left)

No	Point (Calibri 8.5 Justify)	Description
1		
2		
3		
4		
5		

Sources: Journal of PPSUB (Calibri 8.5 Left)

**Figures**

Figures should be in high resolution and well contrast in JPEG or PDF with the following conditions:

- Monochrome image (line art), figures of black and white diagram (solid/no shades of gray), resolution 1000-1200 dpi (dot per inch).
- Combination Halftone, combine figure and text (image containing text) and coloured graphic or in grayscale format. Resolution 600-900 dpi.
- Halftone, coloured figure or grayscale format without text. Resolution 300 dpi.

- Black and white figure should be in the grayscale mode, while coloured figures should be in RGB mode.
- Figure should not exceed the width of 8 cm (one column), 12.5 cm (1.5 columns) or 17 cm (two columns).
- Figures title typed clearly below the figure.
- Figure with pointing arrow should be grouped (grouping).
- Figures were recommended in black and white.
- Legend or figure description should be clear and complete. If compressed, the figure should be readable.
- Statistic graphic should be supplemented with data sources.
- If the figures come from the third party, it should have the copyright transfer from the sources.

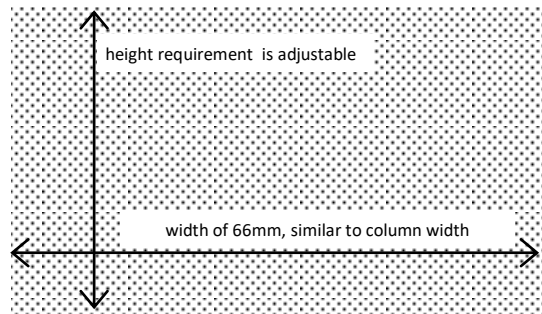


**Figure 1.** Illustration of Dimensional Figure of one column width. Figure dimension adjusted to the width of one column. Name the figure (diagram) written below the image. (Calibri 8.5 Justify)

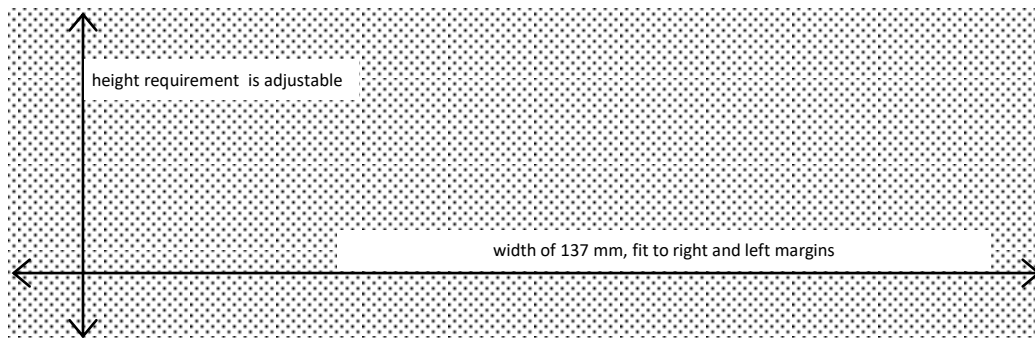


**Figure 2.** Illustration of Dimensional Figure of two column width. Figure dimension adjusted to the width of two columns (137 mm). Figure were align top or bottom of the page. (Calibri 8.5 Justify)

## References

1. Primary references include journal, patent, dissertation, thesis, paper in proceeding and text book.
  2. Avoid self citation.
  3. Author should avoid reference in reference, popular book, and internet reference except journal and private ana state institution.
  4. Author was not allowed to use abstract as references.
  5. References should been published (book, research journal or proceeding). Unpublished references or not displayed data can not be used as references.
  6. References typed in numbering list (format number 1,2,3,...), ordered sequentially as they appear in the text (system of Vancouver or author-number style).
  7. Citation in the manuscript typed only the references number (not the author and year), example: Obesity is an accumulation of fat in large quantities which would cause excessive body weight (overweight) [1]. Obesity is a risk factor of diabetic, hypertension dan atherosclerosis [2].
- [4].Syafi'i, M., Hakim, L., dan Yanuwiyadi, B. 2010. Potential Analysis of Indigenous Knowledge (IK) in Ngadas Village as Tourism Attraction. pp. 217-234. In: Widodo, Y. Noviantari (eds.) Proceed-ing *Basic Science National Seminar 7* Vol.4. Universitas Brawijaya, Malang. (Article within conference proceeding)
- [5].Dean, R.G. 1990. Freak waves: A possible explanation. p. 1-65. In Torum, A., O.T. Gudmestad (eds). Water wave kinetics. CRC Press. New York. (Chapter in a Book)
- [6].Astuti, A.M. 2008. The Effect of Water Fraction of *Stellaria* sp. on the Content of TNF- $\alpha$  in Mice (*Mus musculus* BALB-C). Thesis. Department of Biology. University of Brawijaya. Malang. (Thesis)

## CONCLUSION (Calibri 10 Bold, Left, Capslock)

Conclusion of the study's findings are written in brief, concise and solid, without more additional new interpretation. This section can also be written on research novelty, advantages and disadvantages of the research, as well as recommendations for future research.(Calibri 10 Justify)

## ACKNOWLEDGEMENT (Calibri 10 Bold, Left, Capslock)

This section describes gratitude to those who have helped in substance as well as financially.(Calibri 10 Justify)

## REFERENCES (Calibri 10 Bold, Left, Capslock)

- [1].(Calibri 10 Justify, citation labelling by references numbering)
- [2].Vander, A., J. Sherman., D. Luciano. 2001. Human Physiology: The Mecanisms of Body Function. McGraw-Hill Higher Education. New York. (Book)
- [3].Shi, Z., M. Rifa'i, Y. Lee, K. Isobe, H. Suzuki. 2007. Importance of CD80/CD86-CD28 interaction in the recognition of target cells by CD8<sup>+</sup>CD122<sup>+</sup> regulatory T cells. *Journal Immunology*. 124. 1:121-128. (Article in Journal)

**Cover Image**  
3D Structure of EGCG (Epigallocatechin-3-Gallate)  
Green Tea Component  
**Created by ::**  
Prof. Widodo, S.Si.,M.Si.,Ph.D MED Sc.

**Address :**

Building B, 1st Floor, Graduate Program Universitas Brawijaya  
Jl. Mayor Jenderal Haryono 169, Malang, 65145,  
East Java, Indonesia  
Tel.: (+62341) 571260; Fax: (+62341) 580801  
Email: [jels@ub.ac.id](mailto:jels@ub.ac.id)  
Web: [jels.ub.ac.id](http://jels.ub.ac.id)

